Publication No. 04-055-134

# CRUST FORMATION AND DESICCATION CHARACTERISTICS FOR PHOSPHATIC CLAYS

## *User's Manual for Computer Program CONDES0*

*Prepared by*
University of Colorado, Boulder

*under a grant sponsored by*

FIPR
Florida Institute of Phosphate Research

October 1997

The Florida Institute of Phosphate Research was created iin 1978 by the Florida Legislature (Chapter 378.101, Florida Statutes) and empowered to conduct research supportive to the responsible development of the state's phosphate resources. The Institute has targeted areas of research responsibility. These are: reclamation alternatives in mining and processing, including wetlands reclamation, phosphogypsum storage areas and phosphatic clay containment areas; methods for more efficient, economical and environmentally balanced phosphate recovery and processing; disposal and utilization of phosphatic clay; and environmental effects involving the health and welfare of the people, including those effects related to radiation and water consumption.

FIPR is located in Polk County, in the heart of the central Florida phosphate district. The Institute seeks to serve as an information center on phosphate-related topics and welcomes information requests made in person, by mail, or by telephone.

**Research Staff**

**Executive Director**
**Paul R. Clifford**

**Research Directors**

| | |
|---|---|
| **G. Michael Lloyd Jr.** | **-Chemical Processing** |
| **Jinrong P. Zhang** | **-Mining & Beneficiation** |
| **Steven G. Richardson** | **-Reclamation** |
| **Gordon D. Nifong** | **-Environmental Services** |

Florida Institute of Phosphate Research
1855 West Main Street
Bartow, Florida 33830
(863) 534-7160
Fax(863)534-7165
http://www.fipr.state.fl.us

# User's Manual for Computer Program CONDES0

Numerical Solution Guide
to
One-dimensional Large Strain Consolidation and Desiccation
by
the Finite Difference Implicit Method
(CONDES0)

**by**
Daniel T.C. Yao
Dobroslav Znidarcic

Prepared for
Florida Institute of Phosphate Research
1855 West Main Street, Bartow, Florida 33830

Department of Civil, Environmental and Architectural Engineering
University of Colorado, Boulder, CO 80309

October, 1997

# DISCLAIMER

The contents of this report are reproduced herein as received from the contractor.

The opinions, findings and conclusions expressed herein are not necessarily those of the Florida Institute of Phosphate Research, nor does mention of company names or products constitute endorsement by the Florida Institute of Phosphate Research.

# PERSPECTIVE

Patrick Zhang, Research Director - Beneficiation & Mining

Although, many new disposal/reclamation approaches for the phosphatic clays have been proposed and investigated, the conventional method still dominates. The traditional phosphatic clay disposal procedure is quite simple. Twenty- to sixty-foot high dikes are constructed around areas 300 to 800 acres in extent. The clay slurry (3 to 5 pct solids) is pumped into the impoundments at a rate of 20,000 to 80,000 gpm. During natural settling, most clays consolidate to a 12 to 15% solids level within 3 to 30 months. After the initial settling, surface water is drained from the settled material, which allows the solids to desiccate and form a crust. Frequently, sand tailings and/or overburden materials are used to cap the clays to promote further consolidation and compaction.

As a result of two decades of extensive research, several computer programs, based on the finite strain consolidation theory, have been introduced to the phosphate industry. Several mathematical models describing the consolidation behavior of the phosphatic clays are in routine use and have proved to be helpful tools for planning the size of required settling areas and as well as for predicting when reclamation is technically feasible. However, none of the existing models addresses the desiccation process which has a significant effect on the eventual volume of consolidated phosphatic clays.

Recently, a new theory for modeling desiccation of soft soil has been developed at the University of Colorado at Boulder. This new theory involves four components: (1) consolidation under one-dimensional compression, (2) desiccation under one-dimensional shrinkage, (3) propagation of desiccation vertical cracks with depth, and (4) desiccation under three-dimensional shrinkage.

This project was originally designed to overlay the new desiccation theory onto au existing phosphatic clay consolidation model. It consisted of three steps. First, existing literature as well as field and laboratory observations related to the desiccation of phosphatic clays will be thoroughly reviewed in the light of the new theory, to make sure that the numerical model will properly simulate field conditions and observations. The present theory will then be modified, if necessary, to reflect the desiccation characteristics specific to the behavior of phosphatic clays. Finally, the consolidation model SLURRY will be critically examined to correct its deficiencies, and a computer program will be formulated to incorporate the new theory into SLURRY.

As it turned out, a completely different model from the SLURRY was developed for two major reasons: 1) it was technically difficult to overlay the new clay desiccation and crusting theory onto SLURRY, and 2) the SLURRY was not very user friendly.

FIPR recently sponsored a workshop for a hands-on training on the model. The participants were impressed by the user friendliness of the new model. Those who had experience in the SLURRY agreed that the new model has many advantages over SLURRY. This product can be used as a stand-alone consolidation model. It could also model both consolidation and desiccation, if the required desiccation parameters are properly determined.

# CONTENTS

# Introduction

CONDES0 is a numerical algorithm for the analysis of the one-dimensional large strain consolidation and desiccation of soft fine-grained soils using implicit finite difference method. It solves a non-linear second order partial differential equation formulated for one-dimensional compression, three-dimensional shrinkage, and propagation of vertical cracks in soft fine-grained soils. It provides the one-dimensional time-dependent solutions of void ratio distribution (solid content distributions), layer thickness and gives information on propagation and volume of cracks.

CONDES0 is written in FORTRAN. It can be used on any IBM compatible system. A PC with at least 8MB RAM is required and a 486DX2-66 processor is recommended for better performance. The executable file “DOSXMF.EXE” is required for running CONDES0.

# Theory

## *Governing Equations*

The basic assumptions in the one-dimensional large strain consolidation and desiccation theory are (Abu-Heileh and Znidarcic, 1994, 1995):

1. the soft fine-grained soils remain fully saturated in one-dimensional compression and three-dimensional desiccation until the void ratio reaches the void ratio at shrinkage limit, where the soil shrinkage is terminated;
2. only one-dimensional vertical flow is considered, which results in vertical deformation during the one-dimensional compression and vertical as well as lateral deformations during three-dimensional desiccation;
3. the soil is horizontally homogeneous (one-dimensional assumption);
4. the soil skeleton exhibits no intrinsic time effects with incompressible water and solid phases (no creep);
5. the desiccation process leads to uniform crack depth and crack spacing;
6. the lateral and vertical planes are principal stress planes through any point in the cracked and the uncracked soil columns during the overall consolidation and desiccation processes.

Besides the assumptions stated above, the Darcy's Law is also used along with the conservation of mass in both one-dimensional compression and three-dimensional desiccation processes. The constitutive relationships used in this analysis are:

one-dimensional compression void ratio-effective stress relationship (Liu and Znidarcic, 1991):

$$e = A_1(\sigma' + Z_1)^{B_1} \qquad \textbf{(1)}$$

where $e$ and $\sigma'$ are the void ratio and the vertical effective stress respectively; $A_1$, $B_1$ and $Z_1$ are empirical constants;

three-dimensional desiccation void ratio-effective stress relationship (Abu-Hejleh and Znidarcic, 1995):

$$e = A_1 (\sigma' + Z_2)^{B_2} \tag{2}$$

where $A_2$, $B_2$ and $Z_2$ are empirical constants;

hydraulic conductivity-void ratio relationship in one-dimensional compression and three-dimensional desiccation (Somogyi, 1971):

$$K = Ce^D \tag{3}$$

where $K$ is the hydraulic conductivity, $C$ and $D$ are empirical constants;

The governing equations in one-dimensional compression and three-dimensional desiccation are formulated with the velocity functions and conservation of mass in Lagrangian coordinate system. The velocity functions and conservation of mass are presented as:

***one-dimensional compression***

velocity function:
$$v_u = \frac{K \cdot (Gs - 1)}{1 + e} + \frac{K \cdot (1 + e_0)}{\gamma_w \cdot (1 + e)} \frac{d\sigma_v'}{de} \frac{\partial e}{\partial a} \tag{4}$$

conservation of mass:
$$\frac{\partial v_u}{\partial a} = \frac{-1}{1 + e_0} \frac{\partial e}{\partial t} \tag{5}$$

***three-dimensional desiccation***

velocity function:
$$v_c = -K + \frac{K(e \cdot \gamma_w + \gamma_s)}{\gamma_w (1 + e)} \left(1 - \frac{\partial \sigma_v'}{\partial e_{cr}} \frac{de_{cr}}{d\sigma_v}\right) + \frac{K \cdot \alpha \cdot (1 + e_{cr})}{\gamma_w (1 + e)} \frac{\partial \sigma_v'}{\partial e} \frac{\partial e}{\partial a_1} \tag{6}$$

conservation of mass:
$$\frac{\partial (\alpha \cdot v_c)}{\partial a_1} + \eta E \frac{\partial \alpha}{\partial a_1} = \frac{-1}{(1 + e_i)} \frac{\partial e}{\partial t} \tag{7}$$

***interface node:***

conservation of mass: $$\frac{\partial(\alpha \cdot v)}{\partial \xi} = \frac{-1}{1+e}\frac{\partial e}{\partial t} \quad (8)$$

where $t$ : time

$a, a_1$ : Lagrangian coordinate systems

$\xi$ : Eulerian coordinate system

$e_{cr}$ : cracking void ratio (see the definition in the Cracking Function below)

$e_0$ : void ratio at zero effective stress

$Gs$ : specific gravity of soil particles

$v_c$ : velocity function in cracking soil

$v_u$ : velocity function in uncracked soil

$\alpha$ : ratio of the area of the element to its height

$\gamma_s, \gamma_w$ : unit weights of soil solids and water respectively

$E$ : evaporation rate from the top intact soil surface

$\eta$ : empirical parameter for determining evaporation from crack walls

The interface nodal conservation of mass is defined at the point of the crack tip. Above this point the three-dimensional desiccation mechanism prevails and below it the one-dimensional compression mechanism takes place. The interface formulation of conservation of mass is required between these two mechanisms.

## ***Special Functions***

*Cracking Function*

The crack is assumed developing from the top surface of the soil and propagating downward. Cracking function is defined as the relationship between total stress and cracking void ratio ($e_{cr}$). The cracking void ratio is defined as the void ratio where the three-dimensional shrinkage starts at a given total vertical stress. It is an empirical function and all the parameters *a*, *b*, *c*, and *d* should be determined experimentally.

$$e_{cr} = \frac{1}{d} + \frac{1}{(b \cdot \sigma + a)^c} \tag{9}$$

The development and propagation of the crack depend upon the desiccation history. Any prior crack with unknown desiccation history can not be analyzed properly with this theory.

### *α-Function*

α-function is defined to characterize the proportion of vertical and lateral deformations along the incremental isotropic effective stress paths from the beginning of three-dimensional shrinkage, where $e=e_{cr}$, to a current void ratio e. Simply, α-function is defined as the ratio of the area of the element to its height. The small strain theory and an isotropic material are assumed for the following α-function.

$$\alpha = \frac{1+e}{1+\frac{2}{3}e_{cr}+\frac{1}{3}e} \tag{10}$$

## ***Numerical Formulation***

### *Governing Equations*

The numerical descritization schemes for both 1D compression and three-dimensional desiccation are obtained as:

a) one-dimensional compression:

$$\frac{\{\frac{C\cdot(e_{i+\frac{1}{2}}^{j+\frac{1}{2}})^{D}(Gs-1)}{(1+e_{i+\frac{1}{2}}^{j+\frac{1}{2}})}+\frac{C\cdot(e_{i+\frac{1}{2}}^{j+\frac{1}{2}})^{D}(1+e_0)}{\gamma_w\cdot(1+e_{i+\frac{1}{2}}^{j+\frac{1}{2}})}[\frac{1}{A_1\cdot B_1}(\frac{e_{i+\frac{1}{2}}^{j+\frac{1}{2}}}{A_1})^{\frac{1}{B_1}-1}]\frac{e_{i+1}^{j+1}-e_i^{j+1}}{\Delta q_i}\}-\{\frac{C\cdot(e_{i-\frac{1}{2}}^{j+\frac{1}{2}})^{D}(Gs-1)}{(1+e_{i-\frac{1}{2}}^{j+\frac{1}{2}})}+\frac{C\cdot(e_{i-\frac{1}{2}}^{j+\frac{1}{2}})^{D}(1+e_0)}{\gamma_w\cdot(1+e_{i-\frac{1}{2}}^{j+\frac{1}{2}})}[\frac{1}{A_1\cdot B_1}(\frac{e_{i-\frac{1}{2}}^{j+\frac{1}{2}}}{A_1})^{\frac{1}{B_1}-1}]\frac{e_i^{j+1}-e_{i-1}^{j+1}}{\Delta q_{i-1}}\}}{\frac{1}{2}(\Delta q_i+\Delta q_{i-1})}$$

$$=\frac{-1}{(1+e_0)}\frac{e_i^{j+1}-e_i^{j}}{\Delta t_j} \tag{11}$$

b) three-dimensional desiccation:

$$\frac{\alpha_{i+\frac{1}{2}}\{-C\cdot(e_{i+\frac{1}{2}}^{j+\frac{1}{2}})^{D}+\frac{-C\cdot(e_{i+\frac{1}{2}}^{j+\frac{1}{2}})^{D}(e_{i+\frac{1}{2}}^{j+\frac{1}{2}}\cdot\gamma_w+\gamma_s)}{\gamma_w\cdot(1+e_{i+\frac{1}{2}}^{j+\frac{1}{2}})}[1-EVC_{i+\frac{1}{2}}\cdot TVC_{i+\frac{1}{2}}]+\frac{-C\cdot(e_{i+\frac{1}{2}}^{j+\frac{1}{2}})^{D}\cdot\alpha_{i+\frac{1}{2}}\cdot(1+e_i^{vc})}{\gamma_w\cdot(1+e_{i+\frac{1}{2}}^{j+\frac{1}{2}})}[\frac{1}{A_2\cdot B_2}(\frac{e_{\sigma i+\frac{1}{2}}^{j+\frac{1}{2}}}{A_2})^{\frac{1}{B2}-1}]\frac{e_{i+1}^{j+1}-e_i^{j+1}}{\Delta q_i}}{\frac{1}{2}(\Delta q_i+\Delta q_{i-1})}-$$

$$\frac{\alpha_{i+\frac{1}{2}}\{-C\cdot(e_{i+\frac{1}{2}}^{j+\frac{1}{2}})^{D}+\frac{-C\cdot(e_{i+\frac{1}{2}}^{j+\frac{1}{2}})^{D}(e_{i+\frac{1}{2}}^{j+\frac{1}{2}}\cdot\gamma_w+\gamma_s)}{\gamma_w\cdot(1+e_{i+\frac{1}{2}}^{j+\frac{1}{2}})}[1-EVC\cdot[\frac{-C^*\cdot B^*}{(B^*\cdot\sigma_v+A^*)^{C^*+1}}]]+\frac{-C\cdot(e_{i+\frac{1}{2}}^{j+\frac{1}{2}})^{D}\cdot\alpha_{i+\frac{1}{2}}\cdot(1+e_i^{vc})}{\gamma_w(1+e_{i+\frac{1}{2}}^{j+\frac{1}{2}})}[\frac{1}{A_2\cdot B_2}(\frac{e_{\sigma i+\frac{1}{2}}^{j+\frac{1}{2}}}{A_2})^{\frac{1}{B2}-1}]\frac{e_{i+1}^{j+1}-e_i^{j+1}}{\Delta q_i}}{\frac{1}{2}(\Delta q_i+\Delta q_{i-1})}$$

$$=\frac{-1}{1+e_i^{vc}}\frac{e_i^{j+1}-e_i^{j}}{\Delta t_j} \tag{12}$$

where

$$EVC_{i=\frac{1}{2}}=\frac{1}{A_1\cdot B_1}(\frac{e_{cr\,i+\frac{1}{2}}^{j+\frac{1}{2}}}{A_1})^{\frac{1}{B_1}-1}-\frac{1}{A_2\cdot B_2}(\frac{e_{cr\,i+\frac{1}{2}}^{j+\frac{1}{2}}}{A_2})^{\frac{1}{B2}-1} \tag{13}$$

$$VCT_{i+\frac{1}{2}}=\frac{-c\cdot b}{(b\cdot\sigma_v{}^{i+\frac{1}{2}}+a)^{c+1}} \tag{14}$$

c) interface node:

$$\alpha_{i+\frac{1}{2}}\{-C\cdot(e_{i+\frac{1}{2}}^{j+\frac{1}{2}})^{D}+\frac{-C\cdot(e_{i+\frac{1}{2}}^{j+\frac{1}{2}})^{D}(e_{i+\frac{1}{2}}^{j+\frac{1}{2}}\cdot\gamma_w+\gamma_s)}{\gamma_w\cdot(1+e_{i+\frac{1}{2}}^{j+\frac{1}{2}})}[1-EVC_{i+\frac{1}{2}}\cdot TVC_{i+\frac{1}{2}}]+\frac{-C\cdot(e_{i+\frac{1}{2}}^{j+\frac{1}{2}})^{D}\cdot\alpha_{i+\frac{1}{2}}\cdot(1+e_i^{vc})}{\gamma_w\cdot(1+e_{i+\frac{1}{2}}^{j+\frac{1}{2}})}[\frac{1}{A_2\cdot B_2}(\frac{e_{\sigma_{i+\frac{1}{2}}}^{j+\frac{1}{2}}}{A_2})^{\frac{1}{B_2}-1}]\frac{e_{i+1}^{j+1}-e_i^{j+1}}{\Delta a_i}}{\frac{1}{2}(\Delta a_i+\Delta a_{i-1})}-$$

$$\frac{\{\frac{C\cdot(e_{i+\frac{1}{2}}^{j+\frac{1}{2}})^{D}(Gs-1)}{(1+e_{i+\frac{1}{2}}^{j+\frac{1}{2}})}+\frac{C\cdot(e_{i+\frac{1}{2}}^{j+\frac{1}{2}})^{D}(1+e_0)}{\gamma_w\cdot(1+e_{i+\frac{1}{2}}^{j+\frac{1}{2}})}[\frac{1}{A_1\cdot B_1}(\frac{e_{i+\frac{1}{2}}^{j+\frac{1}{2}}}{A_1})^{\frac{1}{B_1}-1}]\frac{e_{i+1}^{j+1}-e_i^{j+1}}{\Delta a_i}\}-\{\frac{C\cdot(e_{i-\frac{1}{2}}^{j+\frac{1}{2}})^{D}(Gs-1)}{(1+e_{i-\frac{1}{2}}^{j+\frac{1}{2}})}+\frac{C\cdot(e_{i-\frac{1}{2}}^{j+\frac{1}{2}})^{D}(1+e_0)}{\gamma_w\cdot(1+e_{i-\frac{1}{2}}^{j+\frac{1}{2}})}[\frac{1}{A_1\cdot B_1}(\frac{e_{i-\frac{1}{2}}^{j+\frac{1}{2}}}{A_1})^{\frac{1}{B_1}-1}]\frac{e_i^{j+1}-e_{i-1}^{j+1}}{\Delta a_{i-1}}\}}{\frac{1}{2}(\Delta a_i+\Delta a_{i-1})}$$

$$=\frac{-1}{(1+e_0)}\frac{e_i^{j+1}-e_i^{j}}{\Delta t_j}$$

*Boundary Conditions*

a) Neuman's type:

A derivative of void ratio with respect to Lagrangian coordinate system is formulated from the velocity functions:

one-dimensional compression

$$e_{i+1}^{j+1}-e_i^{j+1}=\Delta a_i\cdot\{\frac{\gamma_w\cdot(1+e_{i+\frac{1}{2}}^{j=\frac{1}{2}})\cdot A_1\cdot B_1}{K\cdot(1+e_0)\cdot(\frac{e_{i+\frac{1}{2}}^{j+\frac{1}{2}}}{A_1})^{\frac{1}{B_2}-1}}\cdot[v-\frac{K\cdot(Gs-1)}{(1+e_{i+\frac{1}{2}}^{j+\frac{1}{2}})}]\} \tag{16}$$

three-dimensional desiccation

$$e_{i+1}^{j+1}-e_i^{j+1}=\Delta a_i\cdot\{\frac{\gamma_w\cdot(1+e_{i+\frac{1}{2}}^{j=\frac{1}{2}})\cdot A_2\cdot B_2}{K\cdot\alpha_{i+\frac{1}{2}}\cdot(1+e_i^{vc})\cdot(\frac{e_{i+\frac{1}{2}}^{j+\frac{1}{2}}}{A_2})^{\frac{1}{B_2}-1}}\cdot[v+K-\frac{K\cdot(Gs+e_{i+\frac{1}{2}}^{j+\frac{1}{2}})}{(1+e_{i+\frac{1}{2}}^{j+\frac{1}{2}})}\cdot(1-EVC_{i=\frac{1}{2}}\cdot VCT_{i+\frac{1}{2}}]\} \tag{17}$$

b) Dirichilet’s type

The void ratios at boundary are calculated using the void ratio-effective stress equations and then imposed on the boundary. Both the applied loads and heads are converted into stresses using the effective stress principle.

# Input and Output

## *Input*

The program requires the information of all the parameters in the constitutive relationships as well as the information on the geometry, filling history and boundary conditions. These can be accepted by the program in two ways: 1) the interactive mode under DOS command by following the instruction step by step; or 2) constructed input file in advance. The detail of these two types of input format is addressed in the CONDESO Input Instructions section of this manual.

CONDESO is capable of providing solutions to a single soil-with initially uniformly or non-uniformly distributed void ratios (solid contents) in one-dimensional compression and three-dimensional desiccation cases. Only processes in which monotonically increasing loading is encountered can be analyzed by the program. Cases in which light expansion of soil may be encountered could be analyzed, but for such cases the solution will be only approximate and the users should be capable of properly interpreting the results. Analyzing the processes with large expansion in CONDESO will lead to pre-mature termination of the program or wrong results.

The three-dimensional desiccation analysis must start with a non-crack condition. The case with pre-existing cracks and unknown cracking history can not be analyzed with the current theory because the cracking void ratio is required in the three-dimensional desiccation void ratio-effective stress relationship. For the same reason a smaller maximum time step is needed in the three-dimensional desiccation analysis. If a too large maximum time step is selected an error may accumulate through out the process to unknown level.

### *Material Characteristics*

- One-dimensional Compression (A1, B1, and Z1)

The one-dimensional compressibility and permeability characteristics of the material are required to model the consolidation process. The compressibility is usually presented in the form of void ratio-effective stress

relationship. The extended power function in the form of Eq.(1) proposed by Liu and Znidarcic (1991) having three parameters Al, B1, and Z1 is implemented in CONDES0. Z1 has the unit of stress but A1 and B1 are dimensionless and depend upon the unit used for Z1.

- Three-dimensional Compression (A2 and B2)

Similar to the one-dimensional compressibility characteristics, the three-dimensional shrinkage characteristics are also presented in a form of power function Eq.(2) (Abu-Hejleh, 1993). TWO parameters, A2 and B2, are needed in the void ratio-effective stress relationship to model the three-dimensional shrinkage process. In Eq.(2) the Z2 will be automatically calculated from the cracking function by CONDES0 with the same unit used for Z1 in one-dimensional compressibility characteristics.

- Hydraulic Conductivity (C and D)

The other power function in the form of Eq.(3) is used for the void ratio-permeability relationship (Somogyi, 1979). Two parameters, C and D, in which C has the unit of hydraulic conductivity (length/time) and D is dimensionless, are used in this relationship.

- Cracking Function (a, b, c, and d)

In three-dimensional shrinkage process the lateral stress induced by the horizontal shrinkage will exceed the lateral tensile strength of the soil at certain time during the shrinkage process. At that time the crack starts to develop. The lateral tensile strength of the soil can be related to the undrained shear strength (Abu-Hejleh, 1993) which is half of the unconfined compressive strength. By equating the tensile strength to tensile stress at the crack tip, and by applying the effective stress principle, a cracking function, relating cracking void ratio to the vertical stress, is obtained. The cracking function can be approximated with an analytical expression using four parameters a, b, c, and d in the form of Eq.(9). These four parameters have to be experimentally determined.

- Crust Void Ratio (CV)

The crust void ratio is defined as the void ratio at which the soil becomes strong enough to be considered a part of the “crust”. This number needs to be experimentally determined.

- Specific Gravity of Solid (Gs)

The specific gravity of solid is defined as the ratio of the density of soil solid particles to the density of the water. It is a dimensionless number.

- Unit Weight of Water (Gw)

The unit weight of water can be input in any system of units. However, the unit has to be consistent with the unit used in Z1 in the void ratio-effective stress relationship.

- Minimum Void Ratio (ME)

The minimum void ratio is the void ratio which can not be reduced any further by any means. It must be a positive number.

*Filling Data*

- Height at Time 0 (H0)

The initial height of soil is the actual height of the soil at the beginning of the analysis. This value could be zero at the beginning of the stage filling process.

- Number of Filling Stages (NS)

The number of the filling stages should cover the time from the start to the end of the simulation in the current run. All the filling stages, such as zero filling rate, instantaneous tilling, and continuous filling should be counted as separate stages. The plot of the nominal heights verses time is useful in the process of determining the number of filling stages. Every segment in such a plot is considered as one stage. (Fig. 1)

- Beginning Filling Time (TBF), End Filling Time (TEF), and Filling Rate or Height (FRH)

The staged loading information should cover all the times in the current run. The instantaneous loading at the starting time is not acceptable. The instantaneous loading at beginning should be included in the initial height. If the initial condition of an instantaneous loading of a layer of uniformly distributed void ratio is placed on top of a layer with non-uniformly distributed void ratio, the initial condition with uniform and

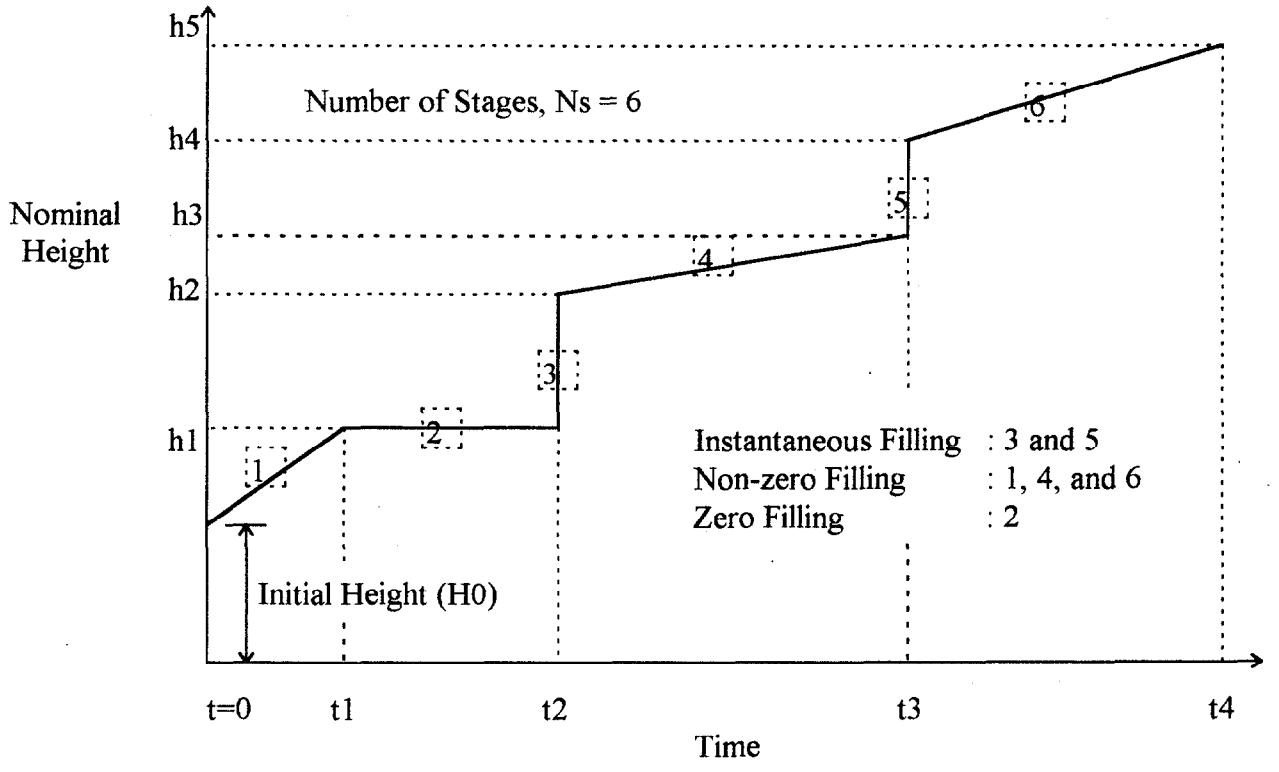


Figure 1. Illustration of Nominal Height Plot in Stage Filling Analysis

| Stage number | TBF | TEF | FRH | Filling Type |
|---|---|---|---|---|
| 1 | 0 | t1 | (h1-H)/t1 | Non-zero Filling |
| 2 | t1 | t2 | 0 | Zero Filling |
| 3 | t2 | t2 | (h2-h1) | Instantaneous Filling |
| 4 | t2 | t3 | (h3-h2))/(t3-t2) | Non-zero Filling |
| 5 | t3 | t3 | (h4-h3) | Instantaneous Filling |
| 6 | t3 | t4 | (h5-h4)/(t4-t3) | Non-zero Filling |

Table 1. Input Table for Stage Filling

non-uniform void ratios must be manually input. For each stage, the beginning time (TBF) and ending time (TEF) should be input as well as the nominal filling rate (FRH) as shown in Table 1. For the case of an instantaneous filling the beginning and ending times are identical and the filling rate (FTH) is replaced by the nominal height difference.

*Boundary Conditions*

- Boundary Condition at Top (BCT)

The boundary on top has two options: 1) the evaporation type, which is defined in a unit of velocity, and 2) the surcharge type, which is in a unit of stress. The evaporation type is to simulate the situation with constant water withdrawn from the top of the soil. The surcharge type simulates the condition with an additional loading and a pervious layer on top. In the staged loading process only the zero surcharge condition is acceptable for the top boundary condition. The desiccation analysis must be performed by restarting the analysis from the end of consolidation process, In this case the analysis should be performed in two steps, The first step is to perform the analysis to the end of the consolidation stage and then take the soil condition (void ratio distribution) at the end as the initial condition of the desiccation analysis and impose the evaporation rate on top boundary in the second step. Desiccation stages can start at anytime during consolidation as long as the upward water velocity during consolidation is lower than the evaporation rate. In the case that the desiccation analysis is started before the consolidation upward flow is reduced below the evaporation rate, the program will continue the consolidation analysis until the time at which consolidation flow at top soil surface becomes equal to the evaporation rate. At that time the desiccation analysis will automatically start with the imposed evaporation rate.

- Boundary Condition at Bottom (BCB)

There are four options available for the bottom condition

1) The impervious boundary presents a no-flow boundary, for which a zero velocity is automatically imposed by the program.
2) The velocity type is a more general case for the flow boundary, which gives the user more power to simulate the field situation like dewatering scheme with a constant flow rate at the bottom of the slurry. However, this option should be used with extreme care and requires a knowledgeable user capable of interpreting the results.
3) The pervious boundary simulates a self-adjusting drained bottom boundary with a water head at bottom always coinciding with the water level at top of the soil layer.
4) The pore pressure head boundary on the other hand features the boundary condition with a fixed but arbitrary water head at bottom. Both positive and negative heads are acceptable. The user should be

aware of the possible instability caused by the high pore pressure at bottom when the pore pressure assigned exceeds the total stress at the bottom resulting from the soil weight. In all the cases when the pore pressure head boundary condition is imposed at the bottom, it is assumed that the water level at the top boundary coincides with the soil top surface. Different ponding depth could be simulated by modifying the bottom head value, However, the user should be careful when assigning such values and when interpreting the results.

- Velocity at Top (VT), Velocity at Bottom (VB), Load at Top (LT), and Head at Bottom (HB)

The coordinate system in CONDES0 is chosen as positive upwards and negative downwards. The imposed dewatering flow rate on top (VT) is therefore positive and is negative at the bottom (VB). Imposing flow rates with opposite signs will cause soil expansion and while the program will give the approximate results, they should be interpreted with great care.

The additional loading (LT) on top is always positive. The pore pressure head imposed at bottom (HB) is a relative height respective to the bottom elevation. Both positive (above bottom level) and negative (below bottom level) values for head are acceptable.

- Side-wall loss parameter ($\eta$-parameter)

The parameter $\eta$ is used for controlling the evaporation during the desiccation process through the side of the crack. It is a factor by which the input evaporation rate is multiplied in order to get the evaporation rate from the crack walls. This parameter needs to be experimentally determined. In general cases, a positive number of $\eta$ is used for evaporation from the side of crack.

*Output*

CONDES0 will provide the continuous time-settlement curve as well as the void ratio distributions (solid content distributions) at each selected time for output in one-dimensional compression and three-dimensional desiccation analyses. In addition to the void ratio distributions (solid content distributions),

the steady state void ratio distributions will also be provided in one-dimensional compression analysis if it exists. In the three-dimensional desiccation analysis, a continuous record of crack depths, soil heights, total soil volumes, crack volumes, fluid loss volumes, side-wall loss, and simulated evaporation rates is given.

The detailed information about the output format for the three output files is given in General Information about Using CONDES0.

## Crack Wall Loss

The fluid extracted from the soil sample in the one-dimensional compression with flow type of boundary condition is either from the top or the bottom surfaces, which are intact soil surfaces. However, the fluid extracted in the three-dimensional desiccation from the soil layer consists of two sources, 1) from the intact top soil surface, and 2) the side-walls of the crack. The fluid loss from the intact top soil surface is dominated by the evaporation rate, which is the top velocity assigned in the flow type boundary condition. The fluid loss from the crack, which is from the side-wall of the crack, however has a very complicated mechanism. The factors such as the crack depth, crack width, evaporation rate, wind speed on top of the soil surface, temperature gradient in the soil, and humidity, affect the fluid loss from the crack. It is not only very difficult to incorporate those factors into a simple model but determining the relevant model parameters would also require a significant effort, Incorporating these factors would make the model much more complicated and less attractive. The CONDES0 therefore incorporates a lump-sum parameter $\eta$ which simplifies the imposed evaporation rate to simulate the loss from the crack. The governing equation of three-dimensional desiccation is modified as:

conservation of mass:
$$\frac{\partial(\alpha \cdot v_c)}{\partial a_1} + \eta E \frac{\partial \alpha}{\partial a_1} = \frac{-1}{(1+e_i)} \frac{\partial e}{\partial t} \qquad (7)$$

With the Eq.(7) , we are able to better simulate the mechanism of three-dimensional desiccation and more closely monitor the development of the crack. The parameter $\eta$ is assumed a constant at this time and could be expanded to a function for further study.

Eq.(7) is constructed based upon the conservation of mass in unit element. The fluid loss from the side-wall of cracks in the unit element is proportional to the area of the side-wall, the evaporation rate, and inversely proportional to the slope of crack side wall.

## Staged Filling Scheme

In the mining processes, the mine tailings are deposited into the sediment pond for sedimentation and consolidation. The height of the deposited material is accumulated with time, which is different from the one-time filling scenario. The stage filling scheme is therefore designed to simulate this time dependent filling scenario.

The staged filling scheme has two major categories, First of all, the continuous filling, in which the additional height of soil is added on top continuously with time, is simulating the case in which the mine tailing is pumped into the sediment pond continuously at a more or less constant rate. A zero filling rate is acceptable in CONDES0, which represents a period of no deposition activity. The second one is instantaneous loading, which simulates certain amount of slurry being deposited during a very short period of time or at a specific time.

A deposition chart of nominal height vs. time (Fig. 1) is recommended to simulate staged loading process using CONDES0. The chart should cover all the activities from the beginning to the end of simulating process. The non-constant rate deposition scenario should be approximated with several periods of constant rates. The maximum of 50 periods including the constant rate depositions and instantaneous depositions is acceptable. The following issues should be noticed before using staged loading function.

1. An instantaneous deposition at beginning of the current simulation is not allowed if the current simulation is a continuation from previous analysis. The instantaneous filling should be incorporated into the initial void ratio distribution (solid content distribution) to start with for the current simulation.
2. During the staged filling process, the top boundary condition is automatically assigned zero effective stress. No desiccation analysis can be performed as a continuation of the filling process. At the end of filling, a new analysis for desiccation is needed.
3. The time frame of staged filling scheme in input format should cover the complete analysis from beginning to the end.

## CONDES0 Steady State Analysis

CONDES0 will provide the steady state solution whenever it exits. The steady state does not exist when flow type boundary condition is used both on top and bottom boundaries, for example when a constant evaporation rate is imposed at top boundary of a soil layer that is undrained at the bottom boundary. In the cases with flow type boundary condition on top and at bottom of soil layer, the program will stop when the minimum void ratio is reached at any point in the soil layer.

The steady state calculation is using the algorithm developed by Abu-Hejleh and Znidarcic (1992 and 1994). The steady state is calculated independently of transient state of the process, The calculation is performed using the water level at initial height of soil layer for instantaneous filling or the final nominal height of soil layer for stage filling. Therefore, the soil heights and void ratio distributions obtained from the steady state analyses may be different from those calculated through the transient process in the cases for which the head type boundary conditions are used at the bottom boundary. By changing the bottom head boundary condition one can simulate various ponding depth above the soil layer. A good understanding of the overall process is needed to conduct and interpret such analysis.

The steady state analysis will not be performed in the desiccation processes. The steady state analysis results should always be interpreted with great care.

## Structure of CONDES0

**Reading Input Data and Values Initialization**

- reading input data
- calculating and assigning initial values
- normalizing void ratios, heights, and times
- determining initial time step and initial height for staged loading scheme

**Steady State Calculation** (Subroutine SSC)

- calculate steady state void ratio distribution (solid content distribution) if it exists

**Boundary Mesh Modification** (Subroutine BOUNDMOD)

- check the Neuman type (flow type) of boundary condition
  - add additional nodes if it is necessary at top and bottom
  - assigning the initial values of void ratio and intervals to the additional nodes using linear interpolation
  - reassigning the sequence of nodes
  - warning sign will pop out and the program will stop if the number of additional nodes exceeds the allowable total number of nodes
  - calculate and assign the effective stresses to the nodes

**Calculation Start**

- output initial condition including void ratio distribution (solid content distribution)
- calculating marching time
- redistributing nodal information of current void ratio distribution (solid content distribution) (subroutine NODREDIS)
  - distributing current number of nodes evenly to current height of sample for staged loading scheme, monitoring and recalculating additional nodes needed at bottom and top boundaries
  - will not be activated during three-dimensional desiccation analysis
- recording current nodal information
- performing staged loading analysis (subroutine STEP)
  - adding incremental height to top of current deposition in accordance with marching time increment

- redistributing nodal information evenly along the height after new deposition

- reevaluating the necessity to modify the boundary mesh (subroutine BOUNDMOD)
- recording current nodal information
- assemble matrix coefficients (subroutine MATCOE)
  - assemble the matrix coefficients in consolidation and desiccation cases using the normalized and discretized governing equations
  - interface element is added between the cracked and uncracking elements (if both exist)
  - central difference is used for spatial discretization
- impose boundary conditions (subroutine BOUNDCON)
  - Neuman's type
  - Dirichlet's type
    - the pore water pressure types of boundary condition are checked for piping or heave problems; program stops and message is displayed if a problem is detected
    - the piping or heave problems are checked by inspecting the stress condition at bottom of the soil column (the bottom pore pressure should not be greater than the total stress at bottom)
- solve u-i-diagonal matrix (subroutine TRTDAG, from Numerical Recipes (Press et al., 1992))
- reassigning nodal sequence due to the rearrangement of nodal sequence in tri-diagonal solver
- impose dilation restriction criterion
  - the void ratio can not exceed the original initial void ratio $e_0$ for all nodes and the void ratios on top and bottom boundaries can not exceed the one obtained from previous time step in consolidation analysis
  - the void ratio can not exceed the one from the previous time step in three-dimensional desiccation analysis for internal nodes
- calculate the void ratio difference for the stopping criterion and the error for the corrector method
  - the void ratio difference is calculated from the square of difference between the void ratios from the current iteration and the previous time step
  - the maximum difference among all pairs of void ratios (the current ones and the previous ones) is selected to represent the marching difference for current iteration, which means by satisfying the marching difference criterion every nodal void ratio has been changed at a rate lower than the selected value of $10^{-20}$

- the error level is calculated from the difference square of the void ratios between two consecutive iterations
- again, like the marching difference criterion, the maximum nodal difference is selected as the representative error, which means by satisfying the error criterion every nodal void ratio difference between two consecutive iterations is less than the value of error criterion of $10^{-20}$
- calculate new total stresses for each node

- check for cracking (if desiccation is considered)
  - check the propagation of the crack by comparing the current void ratios with cracking void ratios obtained from the cracking function
- Corrector Method
  - use the average void ratios from the previous time step and current iteration to characterize the governing equation and calculate the matrix coefficients (MATCOE) for next iteration
  - if number of iterations exceeds 600, the void ratios at the current iteration is used to characterize the governing equation
  - reduce the marching time interval by half if an instability occurs during the iteration in current time step and restart the iteration with a half marching time interval from the previous time step
  - the instability is defined when the current error level is greater than the previous error level

**End of Iteration Loop**

- for the Neuman type boundary condition check if the self-weight consolidation induced flow rate is larger than the imposed velocity; if it is, the analysis will follow the self-weight analysis until the velocity becomes less than the imposed velocity
- in three-dimensional desiccation problem, calculate the crack depth, soil height, total soil volume, total crack volume, fluid volume, side-wall loss, and current evaporation rate
- calculate the new time by using the new time interval as 1.5 times of the current one and if the new time interval is greater than the pre-assigned maximum time step, use the maximum time step
- continue marching to the next time step if the error criterion between two consecutive iteration is satisfied, otherwise go back to the MATCOE and continue the iteration within the current time step
- stopping criteria
  - check the time to either continue the process or stop for output (refer to the marching difference criterion stated above)

**Main Program Stops**

Subroutine POSTPRO

> process the output data

- calculate secondary variables such as pore water pressures, solid contents, and alpha values
- write out the required information at each assigned output time

Subroutine CONPRO

> write out the void ratio distribution file as an input file for subsequent analysis

Subroutine BOUNDCON

> impose Neuman's and Dirichlet's types of boundary conditions

Subroutine TRIDAG

> solve the tri-diagnol matrix constructed using the governing equations

Subroutine BOUNDMOD

> check the boundary condition for the need of boundary mesh refinement and perform the mesh refinement process if the condition calls for it in the Neuman's type of boundary condition

- calculate the maximum allowable Lagrangian nodal interval with the boundary condition
- refine the first boundary nodal interval with the maximum allowable Lagrangian nodal interval
- reassign the nodal and interval sequences, linearly interpolate the void ratios, calculate the effective stresses for additional nodes

Subroutine MATCOE

> calculate the coefficients of the tri-diagnol matrix to be used in the TRIDAG

- compose the tri-diagnol matrix using the discretized governing equations from one-dimensional compression, interface, and three-dimensional desiccation.

Subroutine SSC

> calculate the steady state void ratio distribution (solid content distribution) if it exists in one-dimensional compression analysis

- calculate the void ratio distribution (solid content distribution) using effective stress principle
- four basic scenarios are used to analyze the void ratio distribution (solid content distribution) at the steady state, no flow, velocity is constant and known, velocity is constant but unknown and iteration is needed, and impervious top boundary and pressure head at bottom.

Subroutine NODINT

> convert the existing or given void ratio distribution (solid content distribution) to a distribution with finer mesh

> linear interpolation is used between two given nodes

Subroutine STEP

> perform staged loading processes

- placing additional height of soil on top of the soil column to simulate the continuous and instantaneous types of loading
- minimum 20 steps of loading within one continuous loading period, which is controlled by the number of time steps
- the additional height of soil is product of deposition rate and time interval in continuous loading
- nodal information is rearranged according to the new height of soil into a new distribution with same nodal height differences but at least two nodes are assigned to the top when additional height is added

Subroutine NODREDIS

> reassign the sequence of nodal information such as void ratios, elevations, and Lagrangian nodal intervals evenly along the current height of soil sample according to the current number of nodes

Functions - contain all the functions required in the main program and all the subroutines

# General Information about Using CONDES0

## *Input*

The input data for program CONDES0 can be entered in the interactive mode. After starting the program, CONDES0 will ask for all the necessary parameters one after another. Simply by following the instructions appearing on the screen, the user can easily perform the analysis interactively with CONDES0. After the last necessary input data is entered, the calculation starts immediately.

Alternatively, an input file can be created using an editor and the program is then executed by typing *CONDES0<filename.* This mode of program execution is more convenient when modifying an existing input file, but it is also recommended as the preferred mode of program execution. The procedure of execution using this mode is introduced as follows:

Step 1: Construct an input file

1. Construct an input file following the format in the *CONDES0 Input Instruction* and name the input file (for example: in1)
2. The parameters in the same line can be separated by comma or one space
3. The input tile can have any name except CONDES0.EXE, INPUT, TS.OUT, TC.OUT and VD.OUT. These names are reserved for program generated files.

Step 2: Run the program

1. Under the DOS command, type *CONDES0 < INI*

## *Output*

CONDES0 will automatically generate four output files, TS.OUT, TC.OUT, VD.OUT and INPUT.

VD.OUT - General output file containing:

1. Output information including node numbers, elevations, corresponding void ratios, solid contents and pore water pressures at each requested time. In addition to the requested times the file will contain the same information for those times that are crucial to the analysis.
2. Steady state void ratio distribution (solid content distribution) if it is available.
3. a-value for each node for the desiccation analysis.

INPUT- all input information and void ratio distribution at the end of analysis

Part 1: General input information

- Containing the input information used for the current run

Part 2: Void ratio distribution (solid content distribution)

- Containing the void ratios and elevations at program stopping time

1. This file is designed for continuing the process with different boundary condition. For this case the file name must be changed.
2. The parameters needed to be changed are Boundary Conditions, Initial Status, Number of Output Times, Times of the Output , starting time, sample height, and three-dimensional Desiccation Status if desiccation will be considered in the next run
3. If the three-dimensional desiccation will be considered in the next run, all the information needed in the three-dimensional shrinkage analysis must be added according to the format in the *CONDES0 Input Instruction*

*Warning!* Desiccation analyses must always be conducted in a single run. Continuing the desiccation analysis from an already cracked profile will produce erroneous results.

TS.OUT - Time-settlement information

1. Containing complete time-settlement curves
2. At specified times, sample heights, average dry densities, accumulated flow volumes from top and bottom boundaries, and crust thickness are given.

TC.OUT - Detail result from three-dimensional Analysis

1. Containing complete three-dimensional desiccation information

2. The information includes times, crack depths, layer height, total intact soil volume, crack volume, fluid loss from top intact soil surface, and fluid loss as well as the simulated evaporation rate.

***On the screen***

CONDES0 will show the current running situation on the screen. The information includes:

1. Current time, which refers to the elapsed time in the field CONDES0 is simulating.
2. The marching difference, which refers to the maximum difference between the void ratios from the current time step and previous time step.
3. Iteration information, which includes the iteration number and error level
4. Height difference in percentage between steady state and current state if the steady state is available
5. Boundary mesh modification, which includes the additional numbers of nodes needed on top and bottom boundaries
6. Total number of nodes at current time step
7. Crack depth and node number where the crack tip is
8. Warning signs:
    - numerical instability
    - failure to converge
    - inappropriate combination of soil parameters and boundary conditions
    - high pressure at bottom causing instability
9. Informative messages
    - Boundary condition change from self-weight consolidation to imposed velocity when the imposed velocity is initially less than the velocity induced by the self-weight consolidation
    - Reaching the minimum void ratio
    - Availability of the steady state

# CONDES0 Input Instruction

## *General Instruction*

CONDES0 operates in DOS environment. An interactive input as well as a data file input are acceptable to CONDES0. However, the interactive input is recommended for the first time users.

### The Interactive Input

This is the most direct way of input. The users can simply type *CONDES0* under the DOS command and follow the instructions on the screen. Multiple numbers requested in the same line should be separated by either a comma or a space. The CONDES0 will request all the necessary information and lead the users through the input process. All the input information will be automatically stored in a data file called *INPUT* after the conclusion of calculation. The users can inspect the input data in *INPUT* to verify that the proper parameters were used in the analysis.

### The Data File Input

This is the most efficient way of input. The users can simply construct an input data file with the file name of users' choice; and type *CONDES0<filename* under DOS command to start the calculation process. The input data should have the format shown in the following section, Input Data File Format. Any multiple numbers in the same line should be separated using either comma or space.

The file names, INPUT, TS.OUT, TC.OUT, VD.OUT as well as CONDES0.EXE must not be used as the file name of the input data file.

***Input Data File Format***

**Line 1:** A, B, C, D, Z

The material parameters for the void ratio-effective stress equation in one-dimensional compression and hydraulic conductivity functions

**Line 2:** 1 for Yes, 2 for No

(Answer the following question: )

Is three-dimensional Desiccation considered in this case?

*Line 2-1 to 2-4 are required if 1 is selected in Line 2*

***Line 2-1:*** *A2, B2*

*The material parameters in three-dimensional shrinkage equation*

***Line 2-2:*** *a, b, c, d*

*The material parameters of the cracking function*

***Line 2-3:*** *η-value*

*The side-wall evaporation factor, positive for losing, negative for gaining water from the side-wall.*

***Line 2-4:*** *CV*

*Crust void ratio*

**Line 3:** Gs

Specific gravity of solids

**Line 4:** Gw

Unit weight of water

**Line 5:** H0

Initial height of slurry

**Line 6:** 1 for Yes, 2 for No

(Answer the following question: )

Is stage filling considered in this case?

*Line 6-1 to 6-2 are rewired if 1 is selected for Line 6*

***Line 6-1:*** *NS*

*Number of filling stages*

*The number of filling stages should consider the time frame from the starting time to the ending time of the simulation in the current run. Ail the loading schemes, such as zero loading, instantaneous loading, and continuous filling should be counted The plot of the nominal loading in soil height verses time is recommended. Every segment in this plot will be considered as one stage. (see Fig. 1)*

***Line 6-2-1~Line 6-2-NS:*** *TBF(i), TEF(i), FRH(i)*

*Stage filling information:*

*TBF(i) - beginning time of filling stage i*

*TEF(i) - ending time of filling stage i*

*FRH(i) - rate of filling height of soil at initial void ratio E0*

*~ filling rate (height/time) for continuous filling*

*~ height for one-lime loading*

*Note: for instantaneous loading, TBF and TEF should be the same and specify the time when this loading is applied. The FRH is the added height of the soil.*

**Line 7:** BCT

Boundary condition at top

1 - Velocity type (Neuman type)

2 - Surcharge (Dirichelet type)

**Line 8:** VT or LT

The values corresponding to the types of boundary condition in Line 8

VT - the velocity when BCT=1, and a **POSITIVE** number for extracting water from the soil layer, the unit has to be consistent with C in Line 1

LT - surcharge, the unit has to be consistent with Z in Line 1

**Line 9:** BCB

Boundary condition at bottom

1 - Impervious Boundary (Velocity = 0.0) (skip Line 9-1)

2 - Pressure Head at Bottom (Line 9-1 is needed)

3 - Pervious Boundary (skip Line 9-1). The head is assumed to be equal to the water level on top of the layer.

4 - Neuman Type (Velocity ≠ 0.0) (Line 9-1 is needed)

*Line 9-1 is required if 2 or 4 is selected in Line 9*

***Line 9-1:*** *VB or HB*

*The values corresponding to the types of boundary condition in Line 9*

*VB - the velocity when BCB = 4, and a* ***NEGATIVE*** *number for extracting water from the soil layer, the unit has to be consistent with C in Line 1*

*HB - the pressure head with respect to the elevation at bottom, the unit has to be consistent with H0 in Line 5*

**Line 10:** ME

The minimum void ratio, the program will stop when it reaches this value in any one of the nodes.

**Line 11:** TO

The starting time (It has to be consistent with the ending time of the last run if 1 is selected in Line 15.)

**Line 12:** NO

Number of requested output times

**Line 13-1~Line 13-NO:** T(i)

The times where the output information is required (They have to be larger than the starting time T0 in Line 11 if 1 is selected in Line 15.)

**Line 14:** MAXDT

The maximum time interval for performing calculation

The choice for MAXDT will depend on how precise the desiccation analysis needs to be and how much time the user is willing to spend on performing calculation. MAXDT of 1 day is a good starting value for desiccation analysis.

**Line 15:** 1 for Yes, 2 for No

(Answer the following question: )

Do you want to specify the initial void ratio distribution?

*Line 15-1 to 15-2 are required if 1 is selected for Line 15*

***Line 15-1:*** *ND*

*Number of the pairs of initial void ratio-elevation information*

***Line 15-2-1~15-2-ND*** *E(i), ELV(i)*

- *The void ratios E(j), the elevations ELV(j)*
- *The void ratio distribution (solid content distribution ) in terms of void ratios and elevations should be input in the descending order for elevations (i.e. from top to bottom of the layer). The origin of the coordinate system is always assumed to be at the bottom of the layer.*
- *Starting from the void ratio and elevation at node ND, which is at the fop of the soil.*

## Problem Shootings

When using CONDES0, numerical difficulties and faults may be encountered owing to unrealistic values, erroneous input format, or inappropriate types of analyses. Warning signs and informative messages will be displayed on the screen when these numerical difficulties and faults are encountered. The users must be familiar with these difficulties and faults to correct the errors or enhance the power of analyses using CONDES0.

The users also have to be aware that this theory is developed for fine grain materials with relatively high compressibility and low permeability. Any attempts to analyze the coarse material with relatively low compressibility or relatively high permeability is expected to result in numerical problems and possibly give erroneous results. The problem shooting techniques and resolutions will be provided here.

*- Numerical Instability*

The numerical instability occurs when the error level between two iterations begins to increase. The numerical instability will increase program running time and likely lead to higher error level in analyses. CONDES0 will reduce the marching time to half of the current value and continue the calculation when numerical instability is encountered. The solution will still be obtained, but prolonged execution time should be expected.

The numerical instability usually occurs when velocity type (desiccation) boundary conditions are used for extremely high evaporation rates. The users should check the imposed velocity values, material characteristics and initial void ratio distributions for possible modification to eliminate the numerical instabilities.

*- Failure to Converge*

The convergence problem occurs when the number of iteration is greater then 600. It means, the analysis converges either at a very slow rate or does not converge at all (when accompanied by numerical

instabilities). CONDESO will continue the analysis with the result at the 600th iteration and inevitably generate greater error, The users should be alerted when the convergence problem message appears more than 10 times at an error level higher than $10^{-12}$. This may cause unpredictable error in the results,

The users should first inspect the material characteristics and boundary conditions (types and values) for possible modification to reduce the convergence problems.

*- Inappropriate Combination of Soil Parameters and Boundary Conditions*

This message will be displayed on the screen when the number of total nodes needed for analysis exceeds 20,000. It usually happens when a relatively high velocity is imposed on the boundary of a stiff soil with low permeability. The remedy is to reduce the imposed velocity or possibly modify the material characteristics including the compressibility and permeability. However, even with these modifications the minimum void ratio could be reached very soon on the boundary after the process is started.

*- Material Instability Due to High Pressure at Bottom*

This message will be displayed on the screen when a pressure head type boundary condition is used at bottom and the water pressure exceeds the total stress of soil at bottom. The users should immediately reduce the value of water pressure head at bottom to be able to perform the analysis.

A positive non-zero pressure head boundary condition at bottom should be used with extreme care especially when a very small or zero initial height is used.

*- Reaching Minimum Void Ratio*

CONDES0 will terminate the analysis when the minimum void ratio is reached at any node in soil. This is a normal termination of program. However, if it appears that the minimum void ratio is reached too soon, the users should inspect the boundary conditions and values. Usually the minimum void ratio will be reached sooner when a high velocity is imposed on the boundary of a stiff soil with low permeability.

*- Domain Error or Divided by Zero*

These messages will be displayed on the screen usually when the input number format, structure, or the data generated by CONDES0 is not acceptable to the operation system of computers. The users should always go back to the input data and inspect the data format and structure. The consistency of units should also be checked. However, for certain sets of correct input data it is possible to generate singularities in calculation. The resolution would be to change one or more numbers by a very small amount to avoid the singularities. This message is usually a strong indication that the analysis of a physically impossible situation is being attempted.

*- Please Specify Initial Height Instead of Instantaneous Filling*

At beginning of stage filling process, an instantaneous filling is not acceptable when a non-zero initial height is used. In other words, when a pre-existing layer of soil prior to filling is included in the analysis and an instantaneous filling is imposed at beginning of the process, this message will be displayed on the screen and program stops.

The remedy is to incorporate the instantaneous filling at beginning into the initial void ratio distribution with which to start the analysis.

*- Calculation Terminates for Unstable Situation*

The consolidation and desiccation are diffusive processes. The numerical oscillation within calculation is very likely but it should attenuate with time. If the number of numerical oscillation between two iterations within a time step is higher than 5 and with the amplitude greater than the initial void ratio, CONDES0 will display this message on the screen and stop the analysis.

The users should check the input data for any inconsistency of units, incompatible material characteristics such as a relatively high permeability, or a much too large time step.

# References


1. Abu-Hejleh, A.N., and Znidarcic, D., (1992). User Manual for Computer Program SICTA, *Report for Florida Institute of Phosphate Research*, University of Colorado, Boulder, CO. 80309-0428.

2. Abu-Hejleh, A.N., and Znidarcic, D., (1994). Estimation of the Consolidation Constitutive Relations, *Computer Method and Advances in Geomechanics*, Proceedings of the Eighth International Conference on Computer Methods and Advances in Geomechanics, Morgantown, West Virginia, 22-*28* May, 1994.

3. Abu-Hejleh, A.N., and Znidarcic, D., (1995). Desiccation Theory for Soft Cohesive Soils, *J. of Geotechnical Engineering,* ASCE, Vol. 121, No. 6, pp.493-502.

4. Abu-Hejleh, A.N., Znidarcic, D., and Barnes, B.L., (1996). Consolidation Characteristic of Phosphatic Clays, *J. of Geotechnical Engineering,* ASCE, Vol. 122, No. 4, pp.295-301.

5. Liu, J.C. and Znidarcic, D., (1991), Modeling One-Dimensional Compression Characteristics of Soils, *J. of GeotechnicaI Eng.* ASCE, Vol. 117(1), pp162-169.

6. Press, W .H., Teukolsky, S. A., Vetterling, W .T., and Flannery, B.P., (1992). Numerical Recipes, Cambridge University Press,

7. Somogyi, F. (1979). Analysis and Prediction of Phosphatic Clay Consolidation: Implementation Package, *Technical Report, Florida Phosphatic Clay Research Project,* Lakeland, Florida.

# APPENDICES

# Examples

**Material Characteristics of Example Problems**
**Void Ratio - Effective Stress Curve**

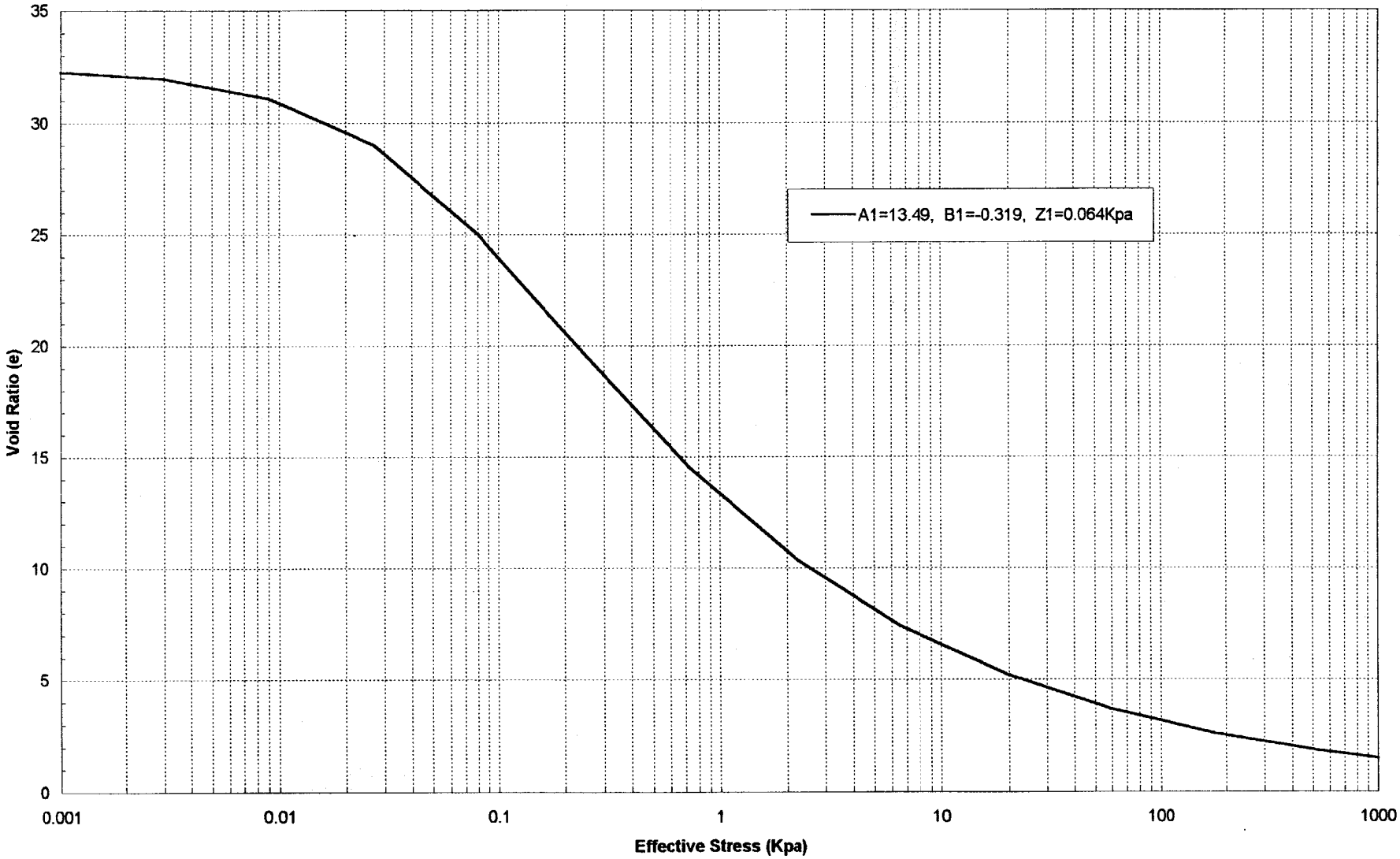

**Material Characteristics for Example Problems**
**Void Ratio - Permeability Curve**

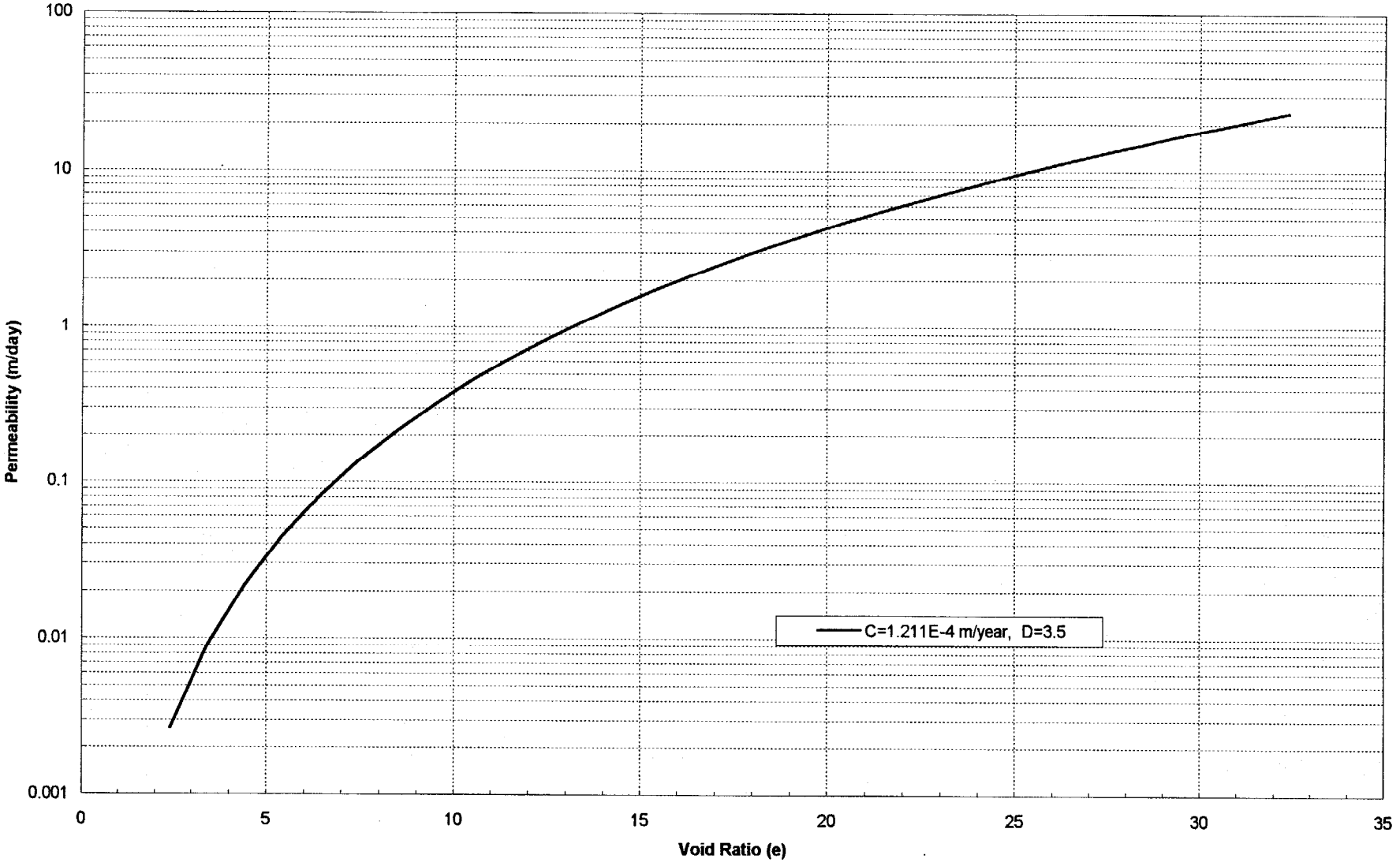

**Example 1** - Instantaneous Filling Consolidation Analysis

*Case Description*

The slurried soil with the following compression and permeability characteristics is deposited into a confined facility in a very short period of time with a height of 17.85 meters, The shrinkage limit of this material is 0.5. The specific gravity of soil solids is 2.71. An impervious layer exists at bottom of the confined facility. A layer of ponding water is always on top of the soil. The consolidation analysis is requested for 60 years.

*Required Data*

A1 = 13.49
B1 = -0.319
Z1 = 0.064 kpa
C = 1.211E-4 m/year
D = 3.5

Gs = 2.71
H0 = 17.85 m
Gw = 9.81 $kN/m^3$
$e_{(min)}$ = 0.5
T0 = 0.0
T = 0.5, 1, 2, 3, 5, 7, 10, 12.5, 15, 17.5, 20, 22.5, 25, 30, 35, 40, 45, 50, 55, 60
MAXDT = 0.5 year (arbitrary number, approximately 1/100 of time span)

Boundary Conditions: Top - zero surcharge
Bottom - impervious
Analysis Status: Consolidation (No desiccation)
No stage filling
New analysis

*Input and Output*

The complete input file, output files such as TS.OUT and INPUT, and part of the VD.OUT are provided in following pages. The time-settlement curve (Fig. EX1-1) and solid content distribution curve (Fig. EX1-2) are also plotted.

Example 1 - **Input File**

```
13.490 -.3190 .12110E-03 3.5000 .64000E-01     A1,B1,C,D,Z1
 2                                             3-D DESSICATION STATUS
 2.7100                                        SPECIFIC GRAVITY OF SOLIDS
 9.8100                                        UNIT WEIGHT OF WATER
 17.850                                        INITIAL HEIGHT OF SOIL
 2                                             STAGE FILLING STATUS
 2                                             TOP BOUNDARY CONDITION
 .00000                                        TOP BOUNDARY CONDITION VALUES
 1                                             BOTTOM BOUNDARY CONDITION
.50000                                         MINIMUM VOID RATIO
 .00000                                        STARTING TIME
  20                                           NUMBER OF OUTPUT FILES
 .50000                                        SPECIFIED TIME FOR OUTPUT
 1.0000                                        SPECIFIED TIME FOR OUTPUT
 2.0000                                        SPECIFIED TIME FOR OUTPUT
 3.0000                                        SPECIFIED TIME FOR OUTPUT
 5.0000                                        SPECIFIED TIME FOR OUTPUT
 7.0000                                        SPECIFIED TIME FOR OUTPUT
 10.000                                        SPECIFIED TIME FOR OUTPUT
 12.500                                        SPECIFIED TIME FOR OUTPUT
 15.000                                        SPECIFIED TIME FOR OUTPUT
 17.500                                        SPECIFIED TIME FOR OUTPUT
 20.000                                        SPECIFIED TIME FOR OUTPUT
 22.500                                        SPECIFIED TIME FOR OUTPUT
 25.000                                        SPECIFIED TIME FOR OUTPUT
 30.000                                        SPECIFIED TIME FOR OUTPUT
 35.000                                        SPECIFIED TIME FOR OUTPUT
 40.000                                        SPECIFIED TIME FOR OUTPUT
 45.000                                        SPECIFIED TIME FOR OUTPUT
 50.000                                        SPECIFIED TIME FOR OUTPUT
 55.000                                        SPECIFIED TIME FOR OUTPUT
 60.000                                        SPECIFIED TIME FOR OUTPUT
 .50000                                        MAXIMUM TIME INTERVAL
 2                                             INITIAL STATUS
```

Example 1 - **TS.OUT**

| -TIME- | SOIL -HEIGHT- | AVERAGE DRY -DENSITY- | CUMULATED OUTFLOW -TOP- | CUMULATED OUTFLOW -BOTTOM- | CRUST -THINKNESS- |
|---|---|---|---|---|---|
| .0000E+00 | .1785E+02 | .7954E+00 | .0000E+00 | .0000E+00 | .0000E+00 |
| .5000E+00 | .1724E+02 | .8236E+00 | .6005E+00 | .0000E+00 | .0000E+00 |
| .1000E+01 | .1664E+02 | .8534E+00 | .1202E+01 | .0000E+00 | .0000E+00 |
| .2000E+01 | .1543E+02 | .9199E+00 | .2404E+01 | .0000E+00 | .0000E+00 |
| .3000E+01 | .1423E+02 | .9976E+00 | .3606E+01 | .0000E+00 | .0000E+00 |
| .5000E+01 | .1191E+02 | .1192E+01 | .5975E+01 | .0000E+00 | .0000E+00 |
| .7000E+01 | .1009E+02 | .1407E+01 | .8052E+01 | .0000E+00 | .0000E+00 |
| .1000E+02 | .8496E+01 | .1671E+01 | .1004E+02 | .0000E+00 | .0000E+00 |
| .1250E+02 | .7732E+01 | .1836E+01 | .1095E+02 | .0000E+00 | .0000E+00 |
| .1313E+02 | .7585E+01 | .1872E+01 | .1112E+02 | .0000E+00 | .0000E+00 |
| .1500E+02 | .7226E+01 | .1965E+01 | .1152E+02 | .0000E+00 | .0000E+00 |
| .1750E+02 | .6870E+01 | .2067E+01 | .1192E+02 | .0000E+00 | .0000E+00 |
| .2000E+02 | .6610E+01 | .2148E+01 | .1221E+02 | .0000E+00 | .0000E+00 |
| .2250E+02 | .6413E+01 | .2214E+01 | .1243E+02 | .0000E+00 | .0000E+00 |
| .2500E+02 | .6262E+01 | .2267E+01 | .1259E+02 | .0000E+00 | .0000E+00 |
| .3000E+02 | .6049E+01 | .2347E+01 | .1282E+02 | .0000E+00 | .0000E+00 |
| .3500E+02 | .5912E+01 | .2402E+01 | .1297E+02 | .0000E+00 | .0000E+00 |
| .4000E+02 | .5821E+01 | .2439E+01 | .1307E+02 | .0000E+00 | .0000E+00 |
| .4500E+02 | .5761E+01 | .2465E+01 | .1313E+02 | .0000E+00 | .0000E+00 |
| .5000E+02 | .5720E+01 | .2482E+01 | .1318E+02 | .0000E+00 | .0000E+00 |
| .5500E+02 | .5692E+01 | .2494E+01 | .1320E+02 | .0000E+00 | .0000E+00 |

THE TOTAL HEIGHT OF SOIL SOLID IS 5.340784702856478E-001

Example 1 - **INPUT**

```
13.490 -.3190 .12110E-03 3.5000 .64000E-01      A,B,C,D,Z
 2           3-D DESSICATION STATUS
 2.7100      SPECIFIC GRAVITY OF SOLIDS
 9.8100      UNIT WEIGHT OF WATER
 17.850      INITIAL HEIGHT OF SOIL
 2           STAGE FILLING STATUS
 2           TOP BOUNDARY CONDITION
 .00000      TOP BOUNDARY CONDITION VALUES
 1           BOTTOM BOUNDARY CONDITION
.50000       MINIMUM VOID RATIO
 .00000      STARTING TIME
  20         NUMBER OF OUTPUT FILES
 .50000      SPECIFIED TIME FOR OUTPUT
 1.0000      SPECIFIED TIME FOR OUTPUT
 2.0000      SPECIFIED TIME FOR OUTPUT
 3.0000      SPECIFIED TIME FOR OUTPUT
 5.0000      SPECIFIED TIME FOR OUTPUT
 7.0000      SPECIFIED TIME FOR OUTPUT
 10.000      SPECIFIED TIME FOR OUTPUT
 12.500      SPECIFIED TIME FOR OUTPUT
 15.000      SPECIFIED TIME FOR OUTPUT
 17.500      SPECIFIED TIME FOR OUTPUT
 20.000      SPECIFIED TIME FOR OUTPUT
 22.500      SPECIFIED TIME FOR OUTPUT
 25.000      SPECIFIED TIME FOR OUTPUT
 30.000      SPECIFIED TIME FOR OUTPUT
 35.000      SPECIFIED TIME FOR OUTPUT
 40.000      SPECIFIED TIME FOR OUTPUT
 45.000      SPECIFIED TIME FOR OUTPUT
 50.000      SPECIFIED TIME FOR OUTPUT
 55.000      SPECIFIED TIME FOR OUTPUT
 60.000      SPECIFIED TIME FOR OUTPUT
 .50000      MAXIMUM TIME INTERVAL
 2           INITIAL STATUS
  51         NUMBER OF NODE
       32.422054984641240        5.674487541744587
       21.195470817042390        5.394340260488300
       17.789860290638950        5.177620559522043
       15.904399020643510        4.987759400716409
       14.645206686338720        4.814300774633645
       13.719711308169720        4.652350851757830
       12.998360723847950        4.499117567358582
       12.413304491796910        4.352817303964338
       11.924925707195880        4.212222966220039
       11.508248263002960        4.076444685785501
       11.146598875512050        3.944811185747430
       10.828341529437350        3.816800304977005
       10.545062134813940        3.691995767896046
       10.290497030039960        3.570058962003451
       10.059869047796950        3.450709779884724
        9.849459229503648        3.333713186443708
        9.656321024578595        3.218869539609180
        9.478083966686841        3.106007450803481
        9.312815393254837        2.994978411171858
        9.158920892778477        2.885652674709757
        9.015071237694038        2.777916054741753
        8.880147829726495        2.671667396339986
```

Input Data

| | | |
|---|---|---|
| 8.753201338432236 | 2.566816557186957 | |
| 8.633419907057558 | 2.463282776512300 | |
| 8.520104405987143 | 2.360993344152627 | Void Ratio Distribution at |
| 8.412648951972463 | 2.259882504501205 | the end of current analysis |
| 8.310525413055075 | 2.159890546301076 | and informative messages such |
| 8.213270966189473 | 2.060963040944921 | as final height and stopping |
| 8.120478018505622 | 1.963050200534038 | time |
| 8.031785977095080 | 1.866106333329373 | |
| 7.946874477900224 | 1.770089379023290 | |
| 7.865457776245909 | 1.674960509904422 | |
| 7.787280069599235 | 1.580683786784226 | |
| 7.712111574034014 | 1.487225860719750 | |
| 7.639745214312526 | 1.394555713259438 | |
| 7.569993816796147 | 1.302644429271791 | |
| 7.502687716924221 | 1.211464997474651 | |
| 7.437672710462387 | 1.120992134628521 | |
| 7.374808291359117 | 1.031202130037820 | |
| 7.313966129779025 | 9.420727075550041E-001 | |
| 7.255028752378028 | 8.535829027313504E-001 | |
| 7.197888393658171 | 7.657129531258965E-001 | |
| 7.142445992671273 | 6.784442000868419E-001 | |
| 7.088610313720155 | 5.917590005703519E-001 | |
| 7.036297173259166 | 5.056406477701512E-001 | |
| 6.985428758089641 | 4.200732995054321E-001 | |
| 6.935933022318205 | 3.350419134607279E-001 | |
| 6.887743152497059 | 2.505321884945074E-001 | |
| 6.840797091979013 | 1.665305113373851E-001 | |
| 6.795037116859221 | 8.302390808925575E-002 | |
| 6.750409456991932 | 0.000000000000000E+000 | |
| 5.6745 | FINAL HEIGHT OF SOIL | |
| 60.000 | STOPPING TIME | |

Example 1 - **VD.OUT**

TIME = .0000

| | INITIAL STATE | | | | STEADY STATE | |
|---|---|---|---|---|---|---|
| -NODE- | -ELEVATION- | VOID -RATIO- | SOLID -CONTENT- | WATER -PRESSURE- | -ELEVATION- | VOID -RATIO- |
| 51 | .1785E+02 | .3242E+02 | .7714E-01 | .0000E+00 | .5635E+01 | .3242E+02 |
| 50 | .1749E+02 | .3242E+02 | .7714E-01 | .3681E+01 | .5355E+01 | .2118E+02 |
| 49 | .1714E+02 | .3242E+02 | .7714E-01 | .7363E+01 | .5138E+01 | .1776E+02 |
| 48 | .1678E+02 | .3242E+02 | .7714E-01 | .1104E+02 | .4949E+01 | .1586E+02 |
| 47 | .1642E+02 | .3242E+02 | .7714E-01 | .1473E+02 | .4776E+01 | .1460E+02 |
| 46 | .1607E+02 | .3242E+02 | .7714E-01 | .1841E+02 | .4614E+01 | .1367E+02 |
| 45 | .1571E+02 | .3242E+02 | .7714E-01 | .2209E+02 | .4462E+01 | .1294E+02 |
| 44 | .1535E+02 | .3242E+02 | .7714E-01 | .2577E+02 | .4316E+01 | .1235E+02 |
| 43 | .1499E+02 | .3242E+02 | .7714E-01 | .2945E+02 | .4176E+01 | .1186E+02 |
| 42 | .1464E+02 | .3242E+02 | .7714E-01 | .3313E+02 | .4041E+01 | .1144E+02 |
| 41 | .1428E+02 | .3242E+02 | .7714E-01 | .3681E+02 | .3910E+01 | .1108E+02 |
| 40 | .1392E+02 | .3242E+02 | .7714E-01 | .4049E+02 | .3783E+01 | .1075E+02 |
| 39 | .1357E+02 | .3242E+02 | .7714E-01 | .4418E+02 | .3659E+01 | .1047E+02 |
| 38 | .1321E+02 | .3242E+02 | .7714E-01 | .4786E+02 | .3538E+01 | .1021E+02 |
| 37 | .1285E+02 | .3242E+02 | .7714E-01 | .5154E+02 | .3419E+01 | .9979E+01 |
| 36 | .1250E+02 | .3242E+02 | .7714E-01 | .5522E+02 | .3303E+01 | .9767E+01 |
| 35 | .1214E+02 | .3242E+02 | .7714E-01 | .5890E+02 | .3189E+01 | .9573E+01 |
| 34 | .1178E+02 | .3242E+02 | .7714E-01 | .6258E+02 | .3077E+01 | .9393E+01 |
| 33 | .1142E+02 | .3242E+02 | .7714E-01 | .6626E+02 | .2967E+01 | .9227E+01 |
| 32 | .1107E+02 | .3242E+02 | .7714E-01 | .6995E+02 | .2859E+01 | .9072E+01 |
| 31 | .1071E+02 | .3242E+02 | .7714E-01 | .7363E+02 | .2752E+01 | .8927E+01 |
| 30 | .1035E+02 | .3242E+02 | .7714E-01 | .7731E+02 | .2647E+01 | .8792E+01 |
| 29 | .9996E+01 | .3242E+02 | .7714E-01 | .8099E+02 | .2543E+01 | .8665E+01 |
| 28 | .9639E+01 | .3242E+02 | .7714E-01 | .8467E+02 | .2440E+01 | .8544E+01 |
| 27 | .9282E+01 | .3242E+02 | .7714E-01 | .8835E+02 | .2339E+01 | .8431E+01 |
| 26 | .8925E+01 | .3242E+02 | .7714E-01 | .9203E+02 | .2239E+01 | .8323E+01 |
| 25 | .8568E+01 | .3242E+02 | .7714E-01 | .9572E+02 | .2140E+01 | .8221E+01 |
| 24 | .8211E+01 | .3242E+02 | .7714E-01 | .9940E+02 | .2042E+01 | .8124E+01 |
| 23 | .7854E+01 | .3242E+02 | .7714E-01 | .1031E+03 | .1945E+01 | .8032E+01 |
| 22 | .7497E+01 | .3242E+02 | .7714E-01 | .1068E+03 | .1849E+01 | .7943E+01 |
| 21 | .7140E+01 | .3242E+02 | .7714E-01 | .1104E+03 | .1754E+01 | .7859E+01 |
| 20 | .6783E+01 | .3242E+02 | .7714E-01 | .1141E+03 | .1659E+01 | .7778E+01 |
| 19 | .6426E+01 | .3242E+02 | .7714E-01 | .1178E+03 | .1566E+01 | .7701E+01 |
| 18 | .6069E+01 | .3242E+02 | .7714E-01 | .1215E+03 | .1473E+01 | .7626E+01 |
| 17 | .5712E+01 | .3242E+02 | .7714E-01 | .1252E+03 | .1382E+01 | .7555E+01 |
| 16 | .5355E+01 | .3242E+02 | .7714E-01 | .1288E+03 | .1291E+01 | .7486E+01 |
| 15 | .4998E+01 | .3242E+02 | .7714E-01 | .1325E+03 | .1200E+01 | .7420E+01 |
| 14 | .4641E+01 | .3242E+02 | .7714E-01 | .1362E+03 | .1111E+01 | .7356E+01 |
| 13 | .4284E+01 | .3242E+02 | .7714E-01 | .1399E+03 | .1022E+01 | .7294E+01 |
| 12 | .3927E+01 | .3242E+02 | .7714E-01 | .1436E+03 | .9336E+00 | .7234E+01 |
| 11 | .3570E+01 | .3242E+02 | .7714E-01 | .1473E+03 | .8460E+00 | .7177E+01 |
| 10 | .3213E+01 | .3242E+02 | .7714E-01 | .1509E+03 | .7589E+00 | .7121E+01 |
| 9 | .2856E+01 | .3242E+02 | .7714E-01 | .1546E+03 | .6725E+00 | .7067E+01 |
| 8 | .2499E+01 | .3242E+02 | .7714E-01 | .1583E+03 | .5866E+00 | .7014E+01 |
| 7 | .2142E+01 | .3242E+02 | .7714E-01 | .1620E+03 | .5013E+00 | .6964E+01 |
| 6 | .1785E+01 | .3242E+02 | .7714E-01 | .1657E+03 | .4165E+00 | .6914E+01 |
| 5 | .1428E+01 | .3242E+02 | .7714E-01 | .1693E+03 | .3322E+00 | .6866E+01 |
| 4 | .1071E+01 | .3242E+02 | .7714E-01 | .1730E+03 | .2484E+00 | .6820E+01 |
| 3 | .7140E+00 | .3242E+02 | .7714E-01 | .1767E+03 | .1651E+00 | .6774E+01 |
| 2 | .3570E+00 | .3242E+02 | .7714E-01 | .1804E+03 | .8234E-01 | .6730E+01 |
| 1 | .0000E+00 | .3242E+02 | .7714E-01 | .1841E+03 | .0000E+00 | .6687E+01 |

TIME = .5000

| -NODE- | -ELEVATION- | VOID -RATIO- | SOLID -CONTENT- | WATER -PRESSURE- | ALPHA -VALUES- |
|---|---|---|---|---|---|
| 51 | .1724E+02 | .3242E+02 | .7714E-01 | .0000E+00 | .1000E+01 |
| 50 | .1688E+02 | .3242E+02 | .7714E-01 | .3681E+01 | .1000E+01 |
| 49 | .1653E+02 | .3242E+02 | .7714E-01 | .7363E+01 | .1000E+01 |
| 48 | .1617E+02 | .3242E+02 | .7714E-01 | .1104E+02 | .1000E+01 |
| 47 | .1581E+02 | .3242E+02 | .7714E-01 | .1473E+02 | .1000E+01 |
| 46 | .1546E+02 | .3242E+02 | .7714E-01 | .1841E+02 | .1000E+01 |
| 45 | .1510E+02 | .3242E+02 | .7714E-01 | .2209E+02 | .1000E+01 |
| 44 | .1474E+02 | .3242E+02 | .7714E-01 | .2577E+02 | .1000E+01 |
| 43 | .1438E+02 | .3242E+02 | .7714E-01 | .2945E+02 | .1000E+01 |
| 42 | .1403E+02 | .3242E+02 | .7714E-01 | .3313E+02 | .1000E+01 |
| 41 | .1367E+02 | .3242E+02 | .7714E-01 | .3681E+02 | .1000E+01 |
| 40 | .1331E+02 | .3242E+02 | .7714E-01 | .4049E+02 | .1000E+01 |
| 39 | .1296E+02 | .3242E+02 | .7714E-01 | .4418E+02 | .1000E+01 |
| 38 | .1260E+02 | .3242E+02 | .7714E-01 | .4786E+02 | .1000E+01 |
| 37 | .1224E+02 | .3242E+02 | .7714E-01 | .5154E+02 | .1000E+01 |
| 36 | .1189E+02 | .3242E+02 | .7714E-01 | .5522E+02 | .1000E+01 |
| 35 | .1153E+02 | .3242E+02 | .7714E-01 | .5890E+02 | .1000E+01 |
| 34 | .1117E+02 | .3242E+02 | .7714E-01 | .6258E+02 | .1000E+01 |
| 33 | .1081E+02 | .3242E+02 | .7714E-01 | .6626E+02 | .1000E+01 |
| 32 | .1046E+02 | .3242E+02 | .7714E-01 | .6995E+02 | .1000E+01 |
| 31 | .1010E+02 | .3242E+02 | .7714E-01 | .7363E+02 | .1000E+01 |
| 30 | .9743E+01 | .3242E+02 | .7714E-01 | .7731E+02 | .1000E+01 |
| 29 | .9386E+01 | .3242E+02 | .7714E-01 | .8099E+02 | .1000E+01 |
| 28 | .9029E+01 | .3242E+02 | .7714E-01 | .8467E+02 | .1000E+01 |
| 27 | .8672E+01 | .3242E+02 | .7714E-01 | .8835E+02 | .1000E+01 |
| 26 | .8315E+01 | .3242E+02 | .7714E-01 | .9203E+02 | .1000E+01 |
| 25 | .7958E+01 | .3242E+02 | .7714E-01 | .9572E+02 | .1000E+01 |
| 24 | .7601E+01 | .3242E+02 | .7714E-01 | .9940E+02 | .1000E+01 |
| 23 | .7244E+01 | .3242E+02 | .7714E-01 | .1031E+03 | .1000E+01 |
| 22 | .6887E+01 | .3242E+02 | .7714E-01 | .1068E+03 | .1000E+01 |
| 21 | .6530E+01 | .3242E+02 | .7714E-01 | .1104E+03 | .1000E+01 |
| 20 | .6173E+01 | .3242E+02 | .7714E-01 | .1141E+03 | .1000E+01 |
| 19 | .5816E+01 | .3242E+02 | .7714E-01 | .1178E+03 | .1000E+01 |
| 18 | .5459E+01 | .3242E+02 | .7714E-01 | .1215E+03 | .1000E+01 |
| 17 | .5102E+01 | .3242E+02 | .7714E-01 | .1252E+03 | .1000E+01 |
| 16 | .4745E+01 | .3242E+02 | .7714E-01 | .1288E+03 | .1000E+01 |
| 15 | .4388E+01 | .3242E+02 | .7715E-01 | .1325E+03 | .1000E+01 |
| 14 | .4031E+01 | .3241E+02 | .7716E-01 | .1362E+03 | .1000E+01 |
| 13 | .3675E+01 | .3240E+02 | .7720E-01 | .1399E+03 | .1000E+01 |
| 12 | .3318E+01 | .3236E+02 | .7727E-01 | .1436E+03 | .1000E+01 |
| 11 | .2962E+01 | .3229E+02 | .7743E-01 | .1472E+03 | .1000E+01 |
| 10 | .2607E+01 | .3213E+02 | .7777E-01 | .1509E+03 | .1000E+01 |
| 9 | .2255E+01 | .3182E+02 | .7847E-01 | .1545E+03 | .1000E+01 |
| 8 | .1907E+01 | .3123E+02 | .7985E-01 | .1581E+03 | .1000E+01 |
| 7 | .1568E+01 | .3019E+02 | .8238E-01 | .1616E+03 | .1000E+01 |
| 6 | .1243E+01 | .2853E+02 | .8674E-01 | .1650E+03 | .1000E+01 |
| 5 | .9391E+00 | .2625E+02 | .9357E-01 | .1681E+03 | .1000E+01 |
| 4 | .6622E+00 | .2355E+02 | .1032E+00 | .1709E+03 | .1000E+01 |
| 3 | .4147E+00 | .2081E+02 | .1152E+00 | .1735E+03 | .1000E+01 |
| 2 | .1953E+00 | .1834E+02 | .1288E+00 | .1757E+03 | .1000E+01 |
| 1 | .0000E+00 | .1632E+02 | .1424E+00 | .1776E+03 | .1000E+01 |

**Figure EX1-1 Time-Settlement Curve**

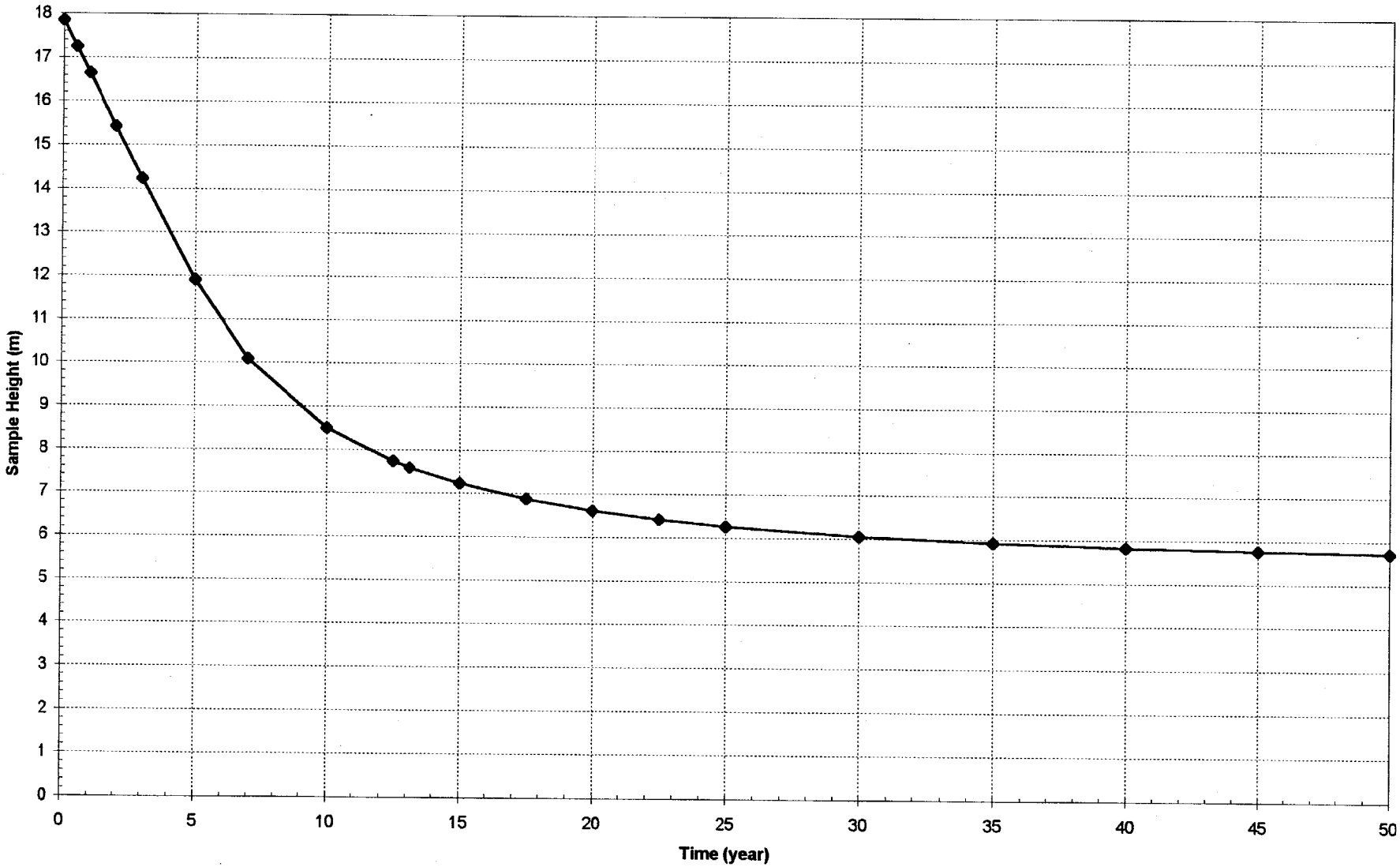

**Figure EX1-2 Solid Content Distribution**

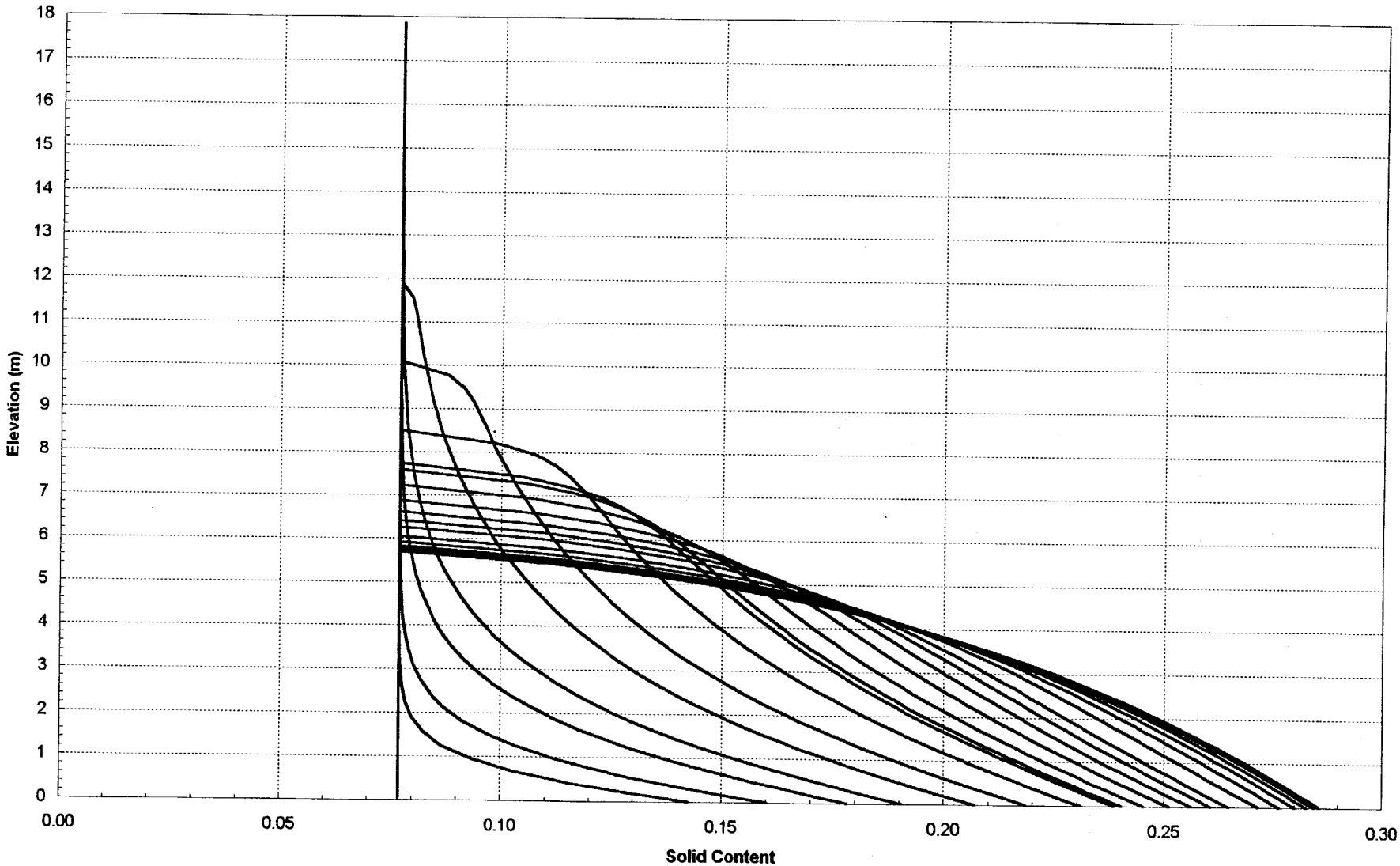

**Example 2** - Stage Filling Consolidation Analysis with Impervious Bottom Boundary

*Case Description*

The slurried soil with the following compression and permeability characteristics is deposited into a confined facility with the stage filling schedule showing in Fig. EX2-1 (the nominal height - time plot). The detailed filling information is in Table EX2-1. The shrinkage limit of this material is 0.5. The specific gravity of soil solids is 2.71. An impervious layer exists at bottom of the confined facility. A layer of ponding water is always on top of the soil. The consolidation analysis is requested and information is needed for 55 years.

*Required Data*

Table EX2-1

| Stage Number | Starting Time (year) | Ending Time (year) | Filling Rate (m/year) |
|---|---|---|---|
| 1 | 0.0 | 4.0 | 2.4 |
| 2 | 4.0 | 9.13 | 0.0 |
| 3 | 9.13 | 13.13 | 2.0625 |
| 4 | 13.13 | 55 | 0.0 |

(total height : 18.75 m)

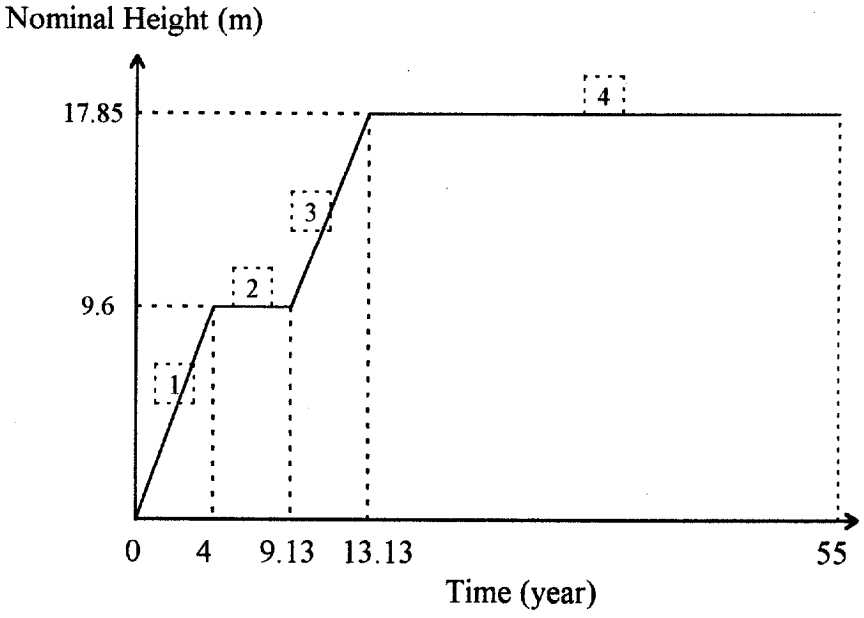


Figure EX2-1

A1 =13.49
B1 = -0.319
Z1 = 0.064 kpa
C = 1.211E-4 m/year
D = 3.5

Gs = 2.71
H0 = 0.0 m
Gw = 9.81 kN/m$^3$
$e_{(min)}$ = 0.5
T0 = 0.0

T = 0.5, 1, 2, 4, 4.3, 4.7, 5.5, 6.5, 7.5, 8.5, 9.13, 10, 10.5, 11.5, 12.5, 13.13, 14, 15, 17, 20, 25, 30, 35, 50, 55
MAXDT = 1.0 year (arbitrary number, approximately 1/50 of time span)

Boundary Conditions: Top - zero surcharge
Bottom - impervious
Analysis Status: Consolidation (No desiccation)
Stage filling
New analysis

*Input and Output*

The complete input file, output files such as TS.OUT and INPUT, and part of the VD.OUT are provided in following pages. The time-settlement curve (Fig. EX2-2) and solid content curve (Fig. EX2-3) are also plotted.

Example 2 - **Input File**

```
13.490 -.3190 .12110E-03 3.5000 .64000E-01      A1,B1,C,D,Z1
 2                                              3-D DESSICATION STATUS
 2.7100                                         SPECIFIC GRAVITY OF SOLIDS
 9.8100                                         UNIT WEIGHT OF WATER
 .00000                                         INITIAL HEIGHT OF SOIL
 1                                              STAGE FILLING STATUS
 4                                              NUMBER OF FILLING STAGES
.00000    4.0000    2.4000          BEGINNING TIME,ENDING TIME,HEIGHTS OR RATES
4.0000    9.1300    .00000          BEGINNING TIME,ENDING TIME,HEIGHTS OR RATES
9.1300    13.130    2.0625          BEGINNING TIME,ENDING TIME,HEIGHTS OR RATES
13.130    55.000    .00000          BEGINNING TIME,ENDING TIME,HEIGHTS OR RATES
 2                                              TOP BOUNDARY CONDITION
 .00000                                         TOP BOUNDARY CONDITION VALUES
 1                                              BOTTOM BOUNDARY CONDITION
.50000                                          MINIMUM VOID RATIO
 .00000                                         STARTING TIME
  25                                            NUMBER OF OUTPUT FILES
 .50000                                         SPECIFIED TIME FOR OUTPUT
 1.0000                                         SPECIFIED TIME FOR OUTPUT
 2.0000                                         SPECIFIED TIME FOR OUTPUT
 4.0000                                         SPECIFIED TIME FOR OUTPUT
 4.3000                                         SPECIFIED TIME FOR OUTPUT
 4.7000                                         SPECIFIED TIME FOR OUTPUT
 5.5000                                         SPECIFIED TIME FOR OUTPUT
 6.5000                                         SPECIFIED TIME FOR OUTPUT
 7.5000                                         SPECIFIED TIME FOR OUTPUT
 8.5000                                         SPECIFIED TIME FOR OUTPUT
 9.1300                                         SPECIFIED TIME FOR OUTPUT
 10.000                                         SPECIFIED TIME FOR OUTPUT
 10.500                                         SPECIFIED TIME FOR OUTPUT
 11.500                                         SPECIFIED TIME FOR OUTPUT
 12.500                                         SPECIFIED TIME FOR OUTPUT
 13.130                                         SPECIFIED TIME FOR OUTPUT
 14.000                                         SPECIFIED TIME FOR OUTPUT
 15.000                                         SPECIFIED TIME FOR OUTPUT
 17.000                                         SPECIFIED TIME FOR OUTPUT
 20.000                                         SPECIFIED TIME FOR OUTPUT
 25.000                                         SPECIFIED TIME FOR OUTPUT
 30.000                                         SPECIFIED TIME FOR OUTPUT
 35.000                                         SPECIFIED TIME FOR OUTPUT
 50.000                                         SPECIFIED TIME FOR OUTPUT
 55.000                                         SPECIFIED TIME FOR OUTPUT
 1.0000                                         MAXIMUM TIME INTERVAL
 2                                              INITIAL STATUS
```

Example 2 - **TS.OUT**

| -TIME- | SOIL -HEIGHT- | AVERAGE DRY -DENSITY- | CUMULATED OUTFLOW -TOP- | CUMULATED OUTFLOW -BOTTOM- | CRUST -THINKNESS- |
|---|---|---|---|---|---|
| .0000E+00 | .1375E-03 | .7954E+00 | .0000E+00 | .0000E+00 | .0000E+00 |
| .5000E+00 | .8372E+00 | .1076E+01 | .4354E+00 | .0000E+00 | .0000E+00 |
| .1000E+01 | .1552E+01 | .1168E+01 | .9516E+00 | .0000E+00 | .0000E+00 |
| .2000E+01 | .3098E+01 | .1233E+01 | .2039E+01 | .0000E+00 | .0000E+00 |
| .4000E+01 | .5556E+01 | .1340E+01 | .4296E+01 | .0000E+00 | .0000E+00 |
| .4300E+01 | .5309E+01 | .1402E+01 | .4608E+01 | .0000E+00 | .0000E+00 |
| .4700E+01 | .5065E+01 | .1470E+01 | .4923E+01 | .0000E+00 | .0000E+00 |
| .5500E+01 | .4722E+01 | .1577E+01 | .5331E+01 | .0000E+00 | .0000E+00 |
| .6500E+01 | .4427E+01 | .1682E+01 | .5694E+01 | .0000E+00 | .0000E+00 |
| .7500E+01 | .4223E+01 | .1763E+01 | .5952E+01 | .0000E+00 | .0000E+00 |
| .8500E+01 | .4070E+01 | .1829E+01 | .6156E+01 | .0000E+00 | .0000E+00 |
| .9130E+01 | .3994E+01 | .1864E+01 | .6247E+01 | .0000E+00 | .0000E+00 |
| .1000E+02 | .5513E+01 | .1693E+01 | .7098E+01 | .0000E+00 | .0000E+00 |
| .1050E+02 | .6030E+01 | .1679E+01 | .7643E+01 | .0000E+00 | .0000E+00 |
| .1150E+02 | .7014E+01 | .1666E+01 | .8731E+01 | .0000E+00 | .0000E+00 |
| .1250E+02 | .8282E+01 | .1629E+01 | .9829E+01 | .0000E+00 | .0000E+00 |
| .1313E+02 | .8738E+01 | .1643E+01 | .1053E+02 | .0000E+00 | .0000E+00 |
| .1400E+02 | .8223E+01 | .1746E+01 | .1123E+02 | .0000E+00 | .0000E+00 |
| .1500E+02 | .7850E+01 | .1829E+01 | .1167E+02 | .0000E+00 | .0000E+00 |
| .1700E+02 | .7351E+01 | .1954E+01 | .1228E+02 | .0000E+00 | .0000E+00 |
| .2000E+02 | .6886E+01 | .2086E+01 | .1283E+02 | .0000E+00 | .0000E+00 |
| .2500E+02 | .6437E+01 | .2231E+01 | .1334E+02 | .0000E+00 | .0000E+00 |
| .3000E+02 | .6177E+01 | .2325E+01 | .1362E+02 | .0000E+00 | .0000E+00 |
| .3500E+02 | .6013E+01 | .2388E+01 | .1380E+02 | .0000E+00 | .0000E+00 |
| .5000E+02 | .5785E+01 | .2482E+01 | .1404E+02 | .0000E+00 | .0000E+00 |
| .5500E+02 | .5752E+01 | .2497E+01 | .1408E+02 | .0000E+00 | .0000E+00 |

THE TOTAL HEIGHT OF SOIL SOLID IS 5.340784702856478E-001

Example 2 - **INPUT**

```
13.490 -.3190 .12110E-03 3.5000 .64000E-01      A,B,C,D,Z
 2          3-D DESSICATION STATUS
 2.7100     SPECIFIC GRAVITY OF SOLIDS
 9.8100     UNIT WEIGHT OF WATER
 .00000     INITIAL HEIGHT OF SOIL
 1          STAGE FILLING STATUS
   4        NUMBER OF FILLING STAGES
.00000    4.0000    2.4000          BEGINNING TIME,ENDING TIME,HEIGHTS OR RATES
4.0000    9.1300    .00000          BEGINNING TIME,ENDING TIME,HEIGHTS OR RATES
9.1300    13.130    2.0625          BEGINNING TIME,ENDING TIME,HEIGHTS OR RATES
13.130    55.000    .00000          BEGINNING TIME,ENDING TIME,HEIGHTS OR RATES
 2          TOP BOUNDARY CONDITION
 .00000     TOP BOUNDARY CONDITION VALUES
 1          BOTTOM BOUNDARY CONDITION
.50000      MINIMUM VOID RATIO
 .00000     STARTING TIME
  25        NUMBER OF OUTPUT FILES
 .50000     SPECIFIED TIME FOR OUTPUT
 1.0000     SPECIFIED TIME FOR OUTPUT                                  Input Data
 2.0000     SPECIFIED TIME FOR OUTPUT
 4.0000     SPECIFIED TIME FOR OUTPUT
 4.3000     SPECIFIED TIME FOR OUTPUT
 4.7000     SPECIFIED TIME FOR OUTPUT
 5.5000     SPECIFIED TIME FOR OUTPUT
 6.5000     SPECIFIED TIME FOR OUTPUT
 7.5000     SPECIFIED TIME FOR OUTPUT
 8.5000     SPECIFIED TIME FOR OUTPUT
 9.1300     SPECIFIED TIME FOR OUTPUT
 10.000     SPECIFIED TIME FOR OUTPUT
 10.500     SPECIFIED TIME FOR OUTPUT
 11.500     SPECIFIED TIME FOR OUTPUT
 12.500     SPECIFIED TIME FOR OUTPUT
 13.130     SPECIFIED TIME FOR OUTPUT
 14.000     SPECIFIED TIME FOR OUTPUT
 15.000     SPECIFIED TIME FOR OUTPUT
 17.000     SPECIFIED TIME FOR OUTPUT
 20.000     SPECIFIED TIME FOR OUTPUT
 25.000     SPECIFIED TIME FOR OUTPUT
 30.000     SPECIFIED TIME FOR OUTPUT
 35.000     SPECIFIED TIME FOR OUTPUT
 50.000     SPECIFIED TIME FOR OUTPUT
 55.000     SPECIFIED TIME FOR OUTPUT
 1.0000     MAXIMUM TIME INTERVAL
 2          INITIAL STATUS
  51        NUMBER OF NODE
      32.422054984641240        5.752027357154709
      24.334014261187130        5.591902449054009
      20.986737235158430        5.460347429909175
      18.896553739764630        5.337223501678341
      17.408540499199900        5.218770412075667
      16.275079069269160        5.103856519878152
      15.372948636459350        4.991893503692096
      14.631531372107840        4.882405887942356
      14.006848242941650        4.774958330964521
      13.469968595317250        4.669161398700991
      13.001067111543070        4.564681253986252
      12.586073950565550        4.461234932378257
```

| | |
|---|---|
| 12.214697650394350 | 4.358581313350121 |
| 11.879212505407360 | 4.256512401976116 |
| 11.573688262035760 | 4.154846240688936 |
| 11.293484816533000 | 4.053421511615261 |
| 11.034910788788520 | 3.952093461620046 |
| 10.794986854208680 | 3.850730884320503 |
| 10.571277789075730 | 3.749213867380634 |
| 10.361770711496220 | 3.647432065959234 |
| 10.164785271645320 | 3.545283415578417 |
| 9.978906223580150 | 3.442673130930264 |
| 9.802932114623751 | 3.339512959257551 |
| 9.635835632309695 | 3.235720579493376 |
| 9.476732650208088 | 3.131219151507700 |
| 9.324857715253774 | 3.025936926176617 |
| 9.179544491823192 | 2.919806934352653 |
| 9.040209973122389 | 2.812766702979162 |
| 8.906341616348273 | 2.704757977679066 |
| 8.777486814428118 | 2.595726473154327 |
| 8.653244149377562 | 2.485621579941438 |
| 8.533256143844179 | 2.374396084638676 |
| 8.417203193183878 | 2.262005873074222 |
| 8.304798444073574 | 2.148409598323453 |
| 8.195783512842185 | 2.033568378248417 |
| 8.089924786799781 | 1.917445403529108 |
| 7.987010343159509 | 1.800005603475873 |
| 7.886847353428014 | 1.681215341300123 |
| 7.789259869790741 | 1.561042111584872 |
| 7.694086936233466 | 1.439454245055905 |
| 7.601181030044783 | 1.316420697439354 |
| 7.510406746582693 | 1.191910879013696 |
| 7.421639673852521 | 1.065894503385271 |
| 7.334765493053377 | 9.383415521267187E-001 |
| 7.249679234483943 | 8.092223057750302E-001 |
| 7.166284561485262 | 6.785072777828557E-001 |
| 7.084493272023701 | 5.461673606028537E-001 |
| 7.004224870474969 | 4.121740011812467E-001 |
| 6.925406187548409 | 2.764993854431538E-001 |
| 6.847971037484180 | 1.391166243638678E-001 |
| 6.771859938627181 | 0.000000000000000E+000 |
| 5.7520 FINAL HEIGHT OF SOIL | |
| 55.000 STOPPING TIME | |

Void Ratio Distribution at the end of current analysis and informative messages such as final height and stopping time

Example 2 - **VD.OUT**

TIME = .0000

| | INITIAL STATE | | | | STEADY STATE | |
|---|---|---|---|---|---|---|
| | | VOID | SOLID | WATER | | VOID |
| -NODE- | -ELEVATION- | -RATIO- | -CONTENT- | -PRESSURE- | -ELEVATION- | -RATIO- |
| 51 | .1375E-03 | .3242E+02 | .7714E-01 | .0000E+00 | .5635E+01 | .3242E+02 |
| 50 | .1347E-03 | .3242E+02 | .7714E-01 | .2836E-04 | .5355E+01 | .2118E+02 |
| 49 | .1320E-03 | .3242E+02 | .7714E-01 | .5671E-04 | .5138E+01 | .1776E+02 |
| 48 | .1292E-03 | .3242E+02 | .7714E-01 | .8507E-04 | .4949E+01 | .1586E+02 |
| 47 | .1265E-03 | .3242E+02 | .7714E-01 | .1134E-03 | .4776E+01 | .1460E+02 |
| 46 | .1237E-03 | .3242E+02 | .7714E-01 | .1418E-03 | .4614E+01 | .1367E+02 |
| 45 | .1210E-03 | .3242E+02 | .7714E-01 | .1701E-03 | .4462E+01 | .1294E+02 |
| 44 | .1182E-03 | .3242E+02 | .7714E-01 | .1985E-03 | .4316E+01 | .1235E+02 |
| 43 | .1155E-03 | .3242E+02 | .7714E-01 | .2268E-03 | .4176E+01 | .1186E+02 |
| 42 | .1127E-03 | .3242E+02 | .7714E-01 | .2552E-03 | .4041E+01 | .1144E+02 |
| 41 | .1100E-03 | .3242E+02 | .7714E-01 | .2836E-03 | .3910E+01 | .1108E+02 |
| 40 | .1072E-03 | .3242E+02 | .7714E-01 | .3119E-03 | .3783E+01 | .1075E+02 |
| 39 | .1045E-03 | .3242E+02 | .7714E-01 | .3403E-03 | .3659E+01 | .1047E+02 |
| 38 | .1017E-03 | .3242E+02 | .7714E-01 | .3686E-03 | .3538E+01 | .1021E+02 |
| 37 | .9899E-04 | .3242E+02 | .7714E-01 | .3970E-03 | .3419E+01 | .9979E+01 |
| 36 | .9624E-04 | .3242E+02 | .7714E-01 | .4253E-03 | .3303E+01 | .9767E+01 |
| 35 | .9349E-04 | .3242E+02 | .7714E-01 | .4537E-03 | .3189E+01 | .9573E+01 |
| 34 | .9074E-04 | .3242E+02 | .7714E-01 | .4820E-03 | .3077E+01 | .9393E+01 |
| 33 | .8799E-04 | .3242E+02 | .7714E-01 | .5104E-03 | .2967E+01 | .9227E+01 |
| 32 | .8524E-04 | .3242E+02 | .7714E-01 | .5387E-03 | .2859E+01 | .9072E+01 |
| 31 | .8249E-04 | .3242E+02 | .7714E-01 | .5671E-03 | .2752E+01 | .8927E+01 |
| 30 | .7974E-04 | .3242E+02 | .7714E-01 | .5955E-03 | .2647E+01 | .8792E+01 |
| 29 | .7699E-04 | .3242E+02 | .7714E-01 | .6238E-03 | .2543E+01 | .8665E+01 |
| 28 | .7424E-04 | .3242E+02 | .7714E-01 | .6522E-03 | .2440E+01 | .8544E+01 |
| 27 | .7149E-04 | .3242E+02 | .7714E-01 | .6805E-03 | .2339E+01 | .8431E+01 |
| 26 | .6874E-04 | .3242E+02 | .7714E-01 | .7089E-03 | .2239E+01 | .8323E+01 |
| 25 | .6599E-04 | .3242E+02 | .7714E-01 | .7372E-03 | .2140E+01 | .8221E+01 |
| 24 | .6324E-04 | .3242E+02 | .7714E-01 | .7656E-03 | .2042E+01 | .8124E+01 |
| 23 | .6049E-04 | .3242E+02 | .7714E-01 | .7939E-03 | .1945E+01 | .8032E+01 |
| 22 | .5774E-04 | .3242E+02 | .7714E-01 | .8223E-03 | .1849E+01 | .7943E+01 |
| 21 | .5500E-04 | .3242E+02 | .7714E-01 | .8507E-03 | .1754E+01 | .7859E+01 |
| 20 | .5225E-04 | .3242E+02 | .7714E-01 | .8790E-03 | .1659E+01 | .7778E+01 |
| 19 | .4950E-04 | .3242E+02 | .7714E-01 | .9074E-03 | .1566E+01 | .7701E+01 |
| 18 | .4675E-04 | .3242E+02 | .7714E-01 | .9357E-03 | .1473E+01 | .7626E+01 |
| 17 | .4400E-04 | .3242E+02 | .7714E-01 | .9641E-03 | .1382E+01 | .7555E+01 |
| 16 | .4125E-04 | .3242E+02 | .7714E-01 | .9924E-03 | .1291E+01 | .7486E+01 |
| 15 | .3850E-04 | .3242E+02 | .7714E-01 | .1021E-02 | .1200E+01 | .7420E+01 |
| 14 | .3575E-04 | .3242E+02 | .7714E-01 | .1049E-02 | .1111E+01 | .7356E+01 |
| 13 | .3300E-04 | .3242E+02 | .7714E-01 | .1077E-02 | .1022E+01 | .7294E+01 |
| 12 | .3025E-04 | .3242E+02 | .7714E-01 | .1106E-02 | .9336E+00 | .7234E+01 |
| 11 | .2750E-04 | .3242E+02 | .7714E-01 | .1134E-02 | .8460E+00 | .7177E+01 |
| 10 | .2475E-04 | .3242E+02 | .7714E-01 | .1163E-02 | .7589E+00 | .7121E+01 |
| 9 | .2200E-04 | .3242E+02 | .7714E-01 | .1191E-02 | .6725E+00 | .7067E+01 |
| 8 | .1925E-04 | .3242E+02 | .7714E-01 | .1219E-02 | .5866E+00 | .7014E+01 |
| 7 | .1650E-04 | .3242E+02 | .7714E-01 | .1248E-02 | .5013E+00 | .6964E+01 |
| 6 | .1375E-04 | .3242E+02 | .7714E-01 | .1276E-02 | .4165E+00 | .6914E+01 |
| 5 | .1100E-04 | .3242E+02 | .7714E-01 | .1304E-02 | .3322E+00 | .6866E+01 |
| 4 | .8249E-05 | .3242E+02 | .7714E-01 | .1333E-02 | .2484E+00 | .6820E+01 |
| 3 | .5500E-05 | .3242E+02 | .7714E-01 | .1361E-02 | .1651E+00 | .6774E+01 |
| 2 | .2750E-05 | .3242E+02 | .7714E-01 | .1389E-02 | .8234E-01 | .6730E+01 |
| 1 | .0000E+00 | .3242E+02 | .7714E-01 | .1418E-02 | .0000E+00 | .6687E+01 |

TIME = .5000

| -NODE- | -ELEVATION- | VOID -RATIO- | SOLID -CONTENT- | WATER -PRESSURE- | ALPHA -VALUES- |
|---|---|---|---|---|---|
| 51 | .8372E+00 | .3242E+02 | .7714E-01 | .0000E+00 | .1000E+01 |
| 50 | .8195E+00 | .3211E+02 | .7782E-01 | .1810E+00 | .1000E+01 |
| 49 | .8019E+00 | .3182E+02 | .7848E-01 | .3605E+00 | .1000E+01 |
| 48 | .7845E+00 | .3154E+02 | .7913E-01 | .5385E+00 | .1000E+01 |
| 47 | .7672E+00 | .3126E+02 | .7977E-01 | .7150E+00 | .1000E+01 |
| 46 | .7501E+00 | .3099E+02 | .8041E-01 | .8901E+00 | .1000E+01 |
| 45 | .7331E+00 | .3072E+02 | .8106E-01 | .1064E+01 | .1000E+01 |
| 44 | .7162E+00 | .3045E+02 | .8173E-01 | .1236E+01 | .1000E+01 |
| 43 | .6996E+00 | .3017E+02 | .8243E-01 | .1406E+01 | .1000E+01 |
| 42 | .6830E+00 | .2988E+02 | .8315E-01 | .1575E+01 | .1000E+01 |
| 41 | .6666E+00 | .2958E+02 | .8392E-01 | .1742E+01 | .1000E+01 |
| 40 | .6504E+00 | .2927E+02 | .8473E-01 | .1907E+01 | .1000E+01 |
| 39 | .6343E+00 | .2895E+02 | .8560E-01 | .2071E+01 | .1000E+01 |
| 38 | .6184E+00 | .2861E+02 | .8654E-01 | .2232E+01 | .1000E+01 |
| 37 | .6027E+00 | .2824E+02 | .8755E-01 | .2391E+01 | .1000E+01 |
| 36 | .5871E+00 | .2788E+02 | .8859E-01 | .2550E+01 | .1000E+01 |
| 35 | .5713E+00 | .2752E+02 | .8965E-01 | .2709E+01 | .1000E+01 |
| 34 | .5555E+00 | .2716E+02 | .9072E-01 | .2869E+01 | .1000E+01 |
| 33 | .5397E+00 | .2681E+02 | .9181E-01 | .3029E+01 | .1000E+01 |
| 32 | .5238E+00 | .2645E+02 | .9292E-01 | .3190E+01 | .1000E+01 |
| 31 | .5078E+00 | .2610E+02 | .9405E-01 | .3352E+01 | .1000E+01 |
| 30 | .4918E+00 | .2575E+02 | .9521E-01 | .3513E+01 | .1000E+01 |
| 29 | .4757E+00 | .2541E+02 | .9639E-01 | .3675E+01 | .1000E+01 |
| 28 | .4596E+00 | .2506E+02 | .9759E-01 | .3838E+01 | .1000E+01 |
| 27 | .4434E+00 | .2471E+02 | .9882E-01 | .4000E+01 | .1000E+01 |
| 26 | .4272E+00 | .2437E+02 | .1001E+00 | .4163E+01 | .1000E+01 |
| 25 | .4109E+00 | .2403E+02 | .1014E+00 | .4327E+01 | .1000E+01 |
| 24 | .3946E+00 | .2369E+02 | .1027E+00 | .4491E+01 | .1000E+01 |
| 23 | .3782E+00 | .2336E+02 | .1040E+00 | .4655E+01 | .1000E+01 |
| 22 | .3616E+00 | .2303E+02 | .1053E+00 | .4821E+01 | .1000E+01 |
| 21 | .3450E+00 | .2270E+02 | .1066E+00 | .4987E+01 | .1000E+01 |
| 20 | .3283E+00 | .2239E+02 | .1080E+00 | .5154E+01 | .1000E+01 |
| 19 | .3114E+00 | .2207E+02 | .1093E+00 | .5322E+01 | .1000E+01 |
| 18 | .2945E+00 | .2177E+02 | .1107E+00 | .5491E+01 | .1000E+01 |
| 17 | .2776E+00 | .2147E+02 | .1121E+00 | .5660E+01 | .1000E+01 |
| 16 | .2606E+00 | .2117E+02 | .1135E+00 | .5829E+01 | .1000E+01 |
| 15 | .2435E+00 | .2089E+02 | .1148E+00 | .5999E+01 | .1000E+01 |
| 14 | .2263E+00 | .2060E+02 | .1162E+00 | .6170E+01 | .1000E+01 |
| 13 | .2092E+00 | .2033E+02 | .1176E+00 | .6340E+01 | .1000E+01 |
| 12 | .1919E+00 | .2006E+02 | .1190E+00 | .6511E+01 | .1000E+01 |
| 11 | .1747E+00 | .1979E+02 | .1204E+00 | .6682E+01 | .1000E+01 |
| 10 | .1574E+00 | .1954E+02 | .1218E+00 | .6853E+01 | .1000E+01 |
| 9 | .1400E+00 | .1928E+02 | .1232E+00 | .7024E+01 | .1000E+01 |
| 8 | .1226E+00 | .1904E+02 | .1246E+00 | .7196E+01 | .1000E+01 |
| 7 | .1052E+00 | .1879E+02 | .1260E+00 | .7367E+01 | .1000E+01 |
| 6 | .8779E-01 | .1856E+02 | .1274E+00 | .7539E+01 | .1000E+01 |
| 5 | .7031E-01 | .1833E+02 | .1288E+00 | .7711E+01 | .1000E+01 |
| 4 | .5279E-01 | .1810E+02 | .1302E+00 | .7883E+01 | .1000E+01 |
| 3 | .3524E-01 | .1788E+02 | .1316E+00 | .8055E+01 | .1000E+01 |
| 2 | .1764E-01 | .1767E+02 | .1330E+00 | .8228E+01 | .1000E+01 |
| 1 | .0000E+00 | .1746E+02 | .1343E+00 | .8401E+01 | .1000E+01 |

**Figure EX2-2 Time-Settlement Curve**

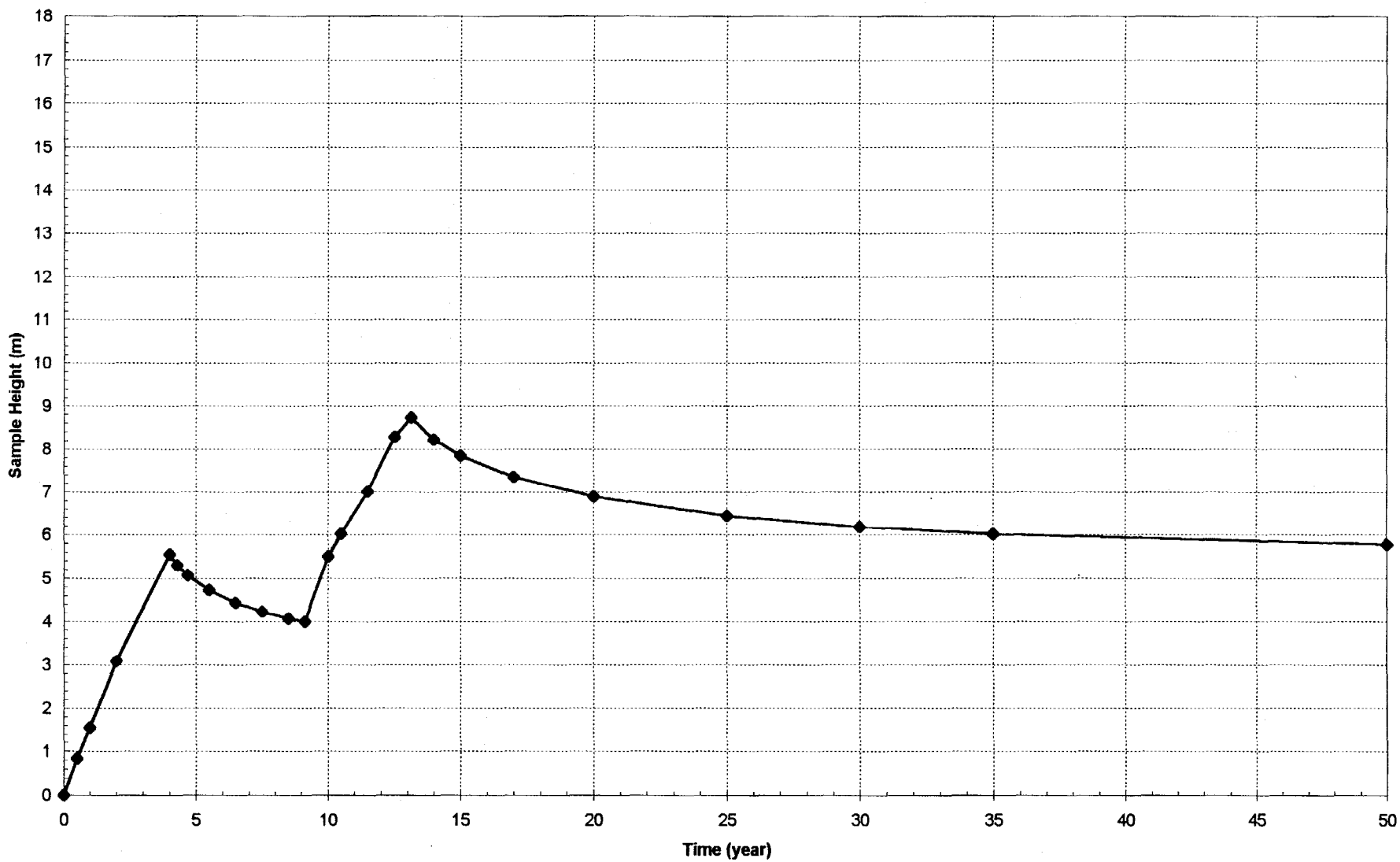

**Figure EX2-3 Solid Content Curve**

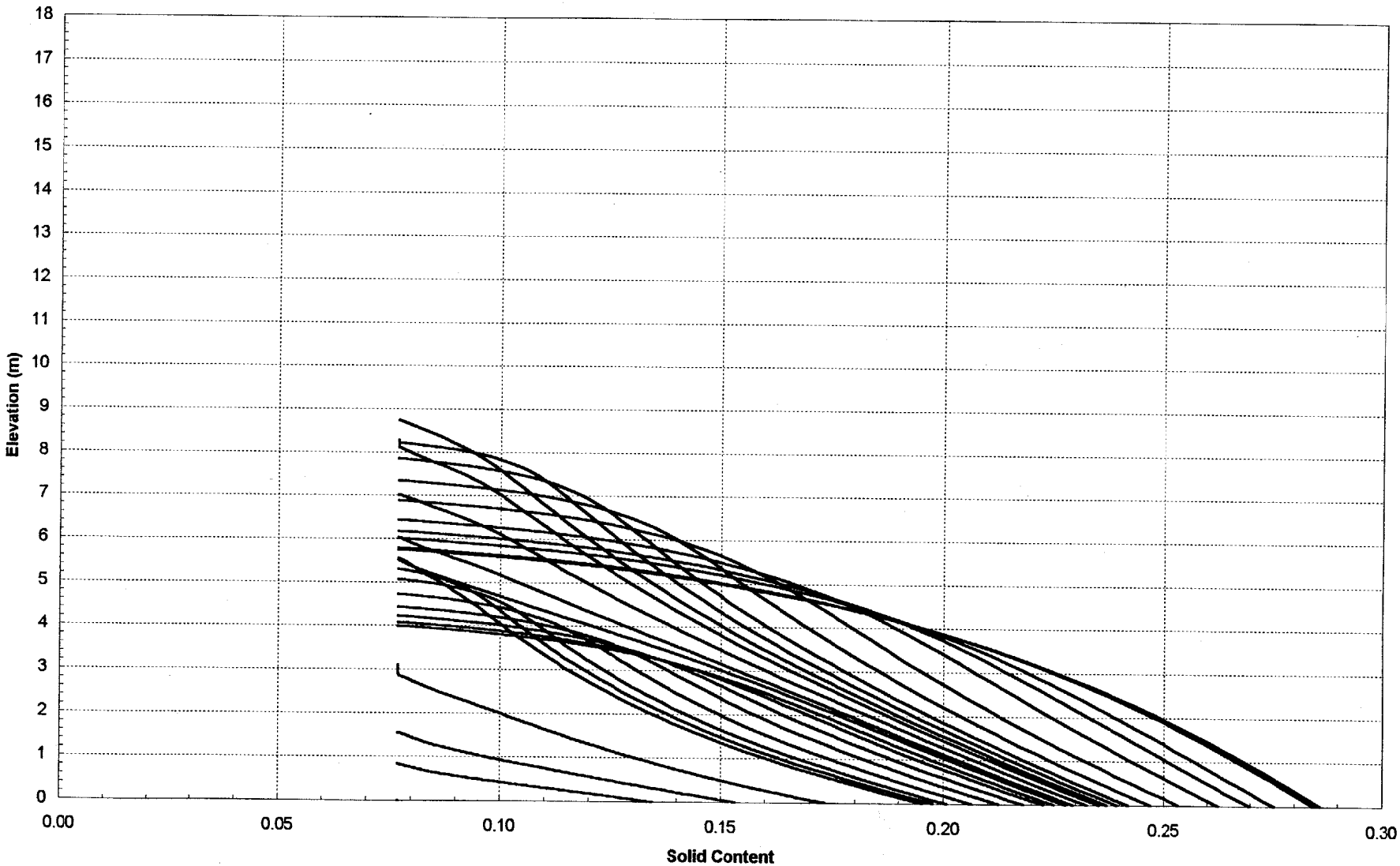

**Example 3** - Stage Filling Consolidation Analysis with Pervious Bottom Boundary

*Case Description*

The slurried soil with the following compression and permeability characteristics is deposited into a confined facility with the stage filling schedule showing in Fig. EX3-1 (the nominal height - time plot). The detailed filling information is in Table EX3-1. The shrinkage limit of this material is 0.5. The specific gravity of soil solids is 2.71. An pervious layer exists at bottom of the confined facility. A layer of ponding water is always on top of the soil. The consolidation analysis is requested and information is needed for 55 years.

*Required Data*

Table EX3-1

| Stage Number | Starting Time (year) | Ending Time (year) | Filling Rate (m/year) |
|---|---|---|---|
| 1 | 0.0 | 4.0 | 2.4 |
| 2 | 4.0 | 9.13 | 0.0 |
| 3 | 9.13 | 13.13 | 2.0625 |
| 4 | 13.13 | 55 | 0.0 |

(total height : 18.75 m)

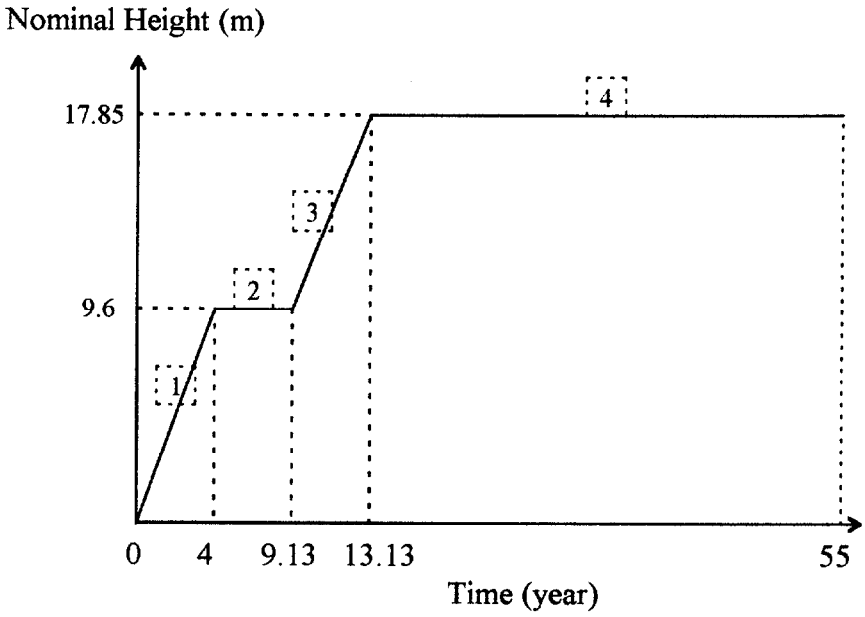


Figure EX3-1

A1 =13.49
B1 = -0.319
Z1 = 0.064 kpa
C = 1.211E-4 m/year
D = 3.5

Gs = 2.71
H0 = 0.0 m
Gw = 9.81 kN/m$^3$
$e_{(min)}$ = 0.5
T0 = 0.0
T = 0.5, 1, 2, 4, 4.3, 4.7, 5.5, 6.5, 7.5, 8.5, 9.13, 10, 10.5, 11.5, 12.5, 13.13, 14, 15, 17, 20, 25, 30, 35, 50, 55

MAXDT = 1.0 year (arbitrary number, approximately l/50 of time span)

Boundary Conditions: Top - zero surcharge
Bottom - pervious
Analysis Status: Consolidation (No desiccation)
Stage filling
New analysis

*Input and Output*

The complete input file, output files such as TS.OUT and INPUT, and part of the VD.OUT are provided in following pages. The time-settlement curve (Fig. EX3-2) and solid content curve (Fig. EX3-3) are also plotted.

Example 3 - **Input File**

```
13.490 -.3190 .12110E-03 3.5000 .64000E-01      A1,B1,C,D,Z1
 2                                              3-D DESSICATION STATUS
 2.7100                                         SPECIFIC GRAVITY OF SOLIDS
 9.8100                                         UNIT WEIGHT OF WATER
 .00000                                         INITIAL HEIGHT OF SOIL
 1                                              STAGE FILLING STATUS
 4                                              NUMBER OF FILLING STAGES
.00000    4.0000    2.4000              BEGINNING TIME,ENDING TIME,HEIGHTS OR RATES
4.0000    9.1300    .00000              BEGINNING TIME,ENDING TIME,HEIGHTS OR RATES
9.1300    13.130    2.0625              BEGINNING TIME,ENDING TIME,HEIGHTS OR RATES
13.130    55.000    .00000              BEGINNING TIME,ENDING TIME,HEIGHTS OR RATES
 2                                              TOP BOUNDARY CONDITION
 .00000                                         TOP BOUNDARY CONDITION VALUES
 3                                              BOTTOM BOUNDARY CONDITION
.50000                                          MINIMUM VOID RATIO
 .00000                                         STARTING TIME
  25                                            NUMBER OF OUTPUT FILES
 .50000                                         SPECIFIED TIME FOR OUTPUT
 1.0000                                         SPECIFIED TIME FOR OUTPUT
 2.0000                                         SPECIFIED TIME FOR OUTPUT
 4.0000                                         SPECIFIED TIME FOR OUTPUT
 4.3000                                         SPECIFIED TIME FOR OUTPUT
 4.7000                                         SPECIFIED TIME FOR OUTPUT
 5.5000                                         SPECIFIED TIME FOR OUTPUT
 6.5000                                         SPECIFIED TIME FOR OUTPUT
 7.5000                                         SPECIFIED TIME FOR OUTPUT
 8.5000                                         SPECIFIED TIME FOR OUTPUT
 9.1300                                         SPECIFIED TIME FOR OUTPUT
 10.000                                         SPECIFIED TIME FOR OUTPUT
 10.500                                         SPECIFIED TIME FOR OUTPUT
 11.500                                         SPECIFIED TIME FOR OUTPUT
 12.500                                         SPECIFIED TIME FOR OUTPUT
 13.130                                         SPECIFIED TIME FOR OUTPUT
 14.000                                         SPECIFIED TIME FOR OUTPUT
 15.000                                         SPECIFIED TIME FOR OUTPUT
 17.000                                         SPECIFIED TIME FOR OUTPUT
 20.000                                         SPECIFIED TIME FOR OUTPUT
 25.000                                         SPECIFIED TIME FOR OUTPUT
 30.000                                         SPECIFIED TIME FOR OUTPUT
 35.000                                         SPECIFIED TIME FOR OUTPUT
 50.000                                         SPECIFIED TIME FOR OUTPUT
 55.000                                         SPECIFIED TIME FOR OUTPUT
 1.0000                                         MAXIMUM TIME INTERVAL
 2                                              INITIAL STATUS
```

Example 3 - **TS.OUT**

| -TIME- | SOIL -HEIGHT- | AVERAGE DRY -DENSITY- | CUMULATED OUTFLOW -TOP- | CUMULATED OUTFLOW -BOTTOM- | CRUST -THINKNESS- |
|---|---|---|---|---|---|
| .0000E+00 | .1375E-03 | .7954E+00 | .0000E+00 | .0000E+00 | .0000E+00 |
| .5000E+00 | .8117E+00 | .1110E+01 | .4284E+00 | -.7155E-01 | .0000E+00 |
| .1000E+01 | .1478E+01 | .1227E+01 | .9376E+00 | -.1638E+00 | .0000E+00 |
| .2000E+01 | .2905E+01 | .1315E+01 | .2015E+01 | -.3238E+00 | .0000E+00 |
| .4000E+01 | .5134E+01 | .1450E+01 | .4262E+01 | -.7121E+00 | .0000E+00 |
| .4300E+01 | .4866E+01 | .1530E+01 | .4572E+01 | -.7458E+00 | .0000E+00 |
| .4700E+01 | .4604E+01 | .1617E+01 | .4878E+01 | -.7820E+00 | .0000E+00 |
| .5500E+01 | .4251E+01 | .1751E+01 | .5256E+01 | -.8352E+00 | .0000E+00 |
| .6500E+01 | .3976E+01 | .1873E+01 | .5568E+01 | -.8828E+00 | .0000E+00 |
| .7500E+01 | .3811E+01 | .1954E+01 | .5767E+01 | -.9160E+00 | .0000E+00 |
| .8500E+01 | .3705E+01 | .2009E+01 | .5909E+01 | -.9404E+00 | .0000E+00 |
| .9130E+01 | .3658E+01 | .2035E+01 | .5961E+01 | -.9500E+00 | .0000E+00 |
| .1000E+02 | .5146E+01 | .1813E+01 | .6803E+01 | -.9835E+00 | .0000E+00 |
| .1050E+02 | .5642E+01 | .1795E+01 | .7345E+01 | -.1010E+01 | .0000E+00 |
| .1150E+02 | .6575E+01 | .1777E+01 | .8430E+01 | -.1068E+01 | .0000E+00 |
| .1250E+02 | .7786E+01 | .1733E+01 | .9526E+01 | -.1129E+01 | .0000E+00 |
| .1313E+02 | .8205E+01 | .1750E+01 | .1023E+02 | -.1180E+01 | .0000E+00 |
| .1400E+02 | .7657E+01 | .1876E+01 | .1092E+02 | -.1229E+01 | .0000E+00 |
| .1500E+02 | .7261E+01 | .1978E+01 | .1134E+02 | -.1273E+01 | .0000E+00 |
| .1700E+02 | .6746E+01 | .2129E+01 | .1191E+02 | -.1343E+01 | .0000E+00 |
| .2000E+02 | .6298E+01 | .2280E+01 | .1238E+02 | -.1415E+01 | .0000E+00 |
| .2500E+02 | .5941E+01 | .2417E+01 | .1275E+02 | -.1484E+01 | .0000E+00 |
| .3000E+02 | .5793E+01 | .2479E+01 | .1289E+02 | -.1517E+01 | .0000E+00 |
| .3500E+02 | .5729E+01 | .2506E+01 | .1295E+02 | -.1533E+01 | .0000E+00 |
| .5000E+02 | .5685E+01 | .2526E+01 | .1299E+02 | -.1544E+01 | .0000E+00 |
| .5500E+02 | .5683E+01 | .2527E+01 | .1299E+02 | -.1544E+01 | .0000E+00 |

THE TOTAL HEIGHT OF SOIL SOLID IS 5.340784702856478E-001

Example 3 - **INPUT**

```
13.490 -.3190 .12110E-03 3.5000 .64000E-01      A,B,C,D,Z
 2           3-D DESSICATION STATUS
 2.7100      SPECIFIC GRAVITY OF SOLIDS
 9.8100      UNIT WEIGHT OF WATER
 .00000      INITIAL HEIGHT OF SOIL
 1           STAGE FILLING STATUS
   4         NUMBER OF FILLING STAGES
.00000    4.0000    2.4000          BEGINNING TIME,ENDING TIME,HEIGHTS OR RATES
4.0000    9.1300    .00000          BEGINNING TIME,ENDING TIME,HEIGHTS OR RATES
9.1300    13.130    2.0625          BEGINNING TIME,ENDING TIME,HEIGHTS OR RATES
13.130    55.000    .00000          BEGINNING TIME,ENDING TIME,HEIGHTS OR RATES
 2           TOP BOUNDARY CONDITION
 .00000      TOP BOUNDARY CONDITION VALUES
 3           BOTTOM BOUNDARY CONDITION
.50000       MINIMUM VOID RATIO
 .00000      STARTING TIME
  25         NUMBER OF OUTPUT FILES
 .50000      SPECIFIED TIME FOR OUTPUT
 1.0000      SPECIFIED TIME FOR OUTPUT
 2.0000      SPECIFIED TIME FOR OUTPUT
 4.0000      SPECIFIED TIME FOR OUTPUT                          Input Data
 4.3000      SPECIFIED TIME FOR OUTPUT
 4.7000      SPECIFIED TIME FOR OUTPUT
 5.5000      SPECIFIED TIME FOR OUTPUT
 6.5000      SPECIFIED TIME FOR OUTPUT
 7.5000      SPECIFIED TIME FOR OUTPUT
 8.5000      SPECIFIED TIME FOR OUTPUT
 9.1300      SPECIFIED TIME FOR OUTPUT
 10.000      SPECIFIED TIME FOR OUTPUT
 10.500      SPECIFIED TIME FOR OUTPUT
 11.500      SPECIFIED TIME FOR OUTPUT
 12.500      SPECIFIED TIME FOR OUTPUT
 13.130      SPECIFIED TIME FOR OUTPUT
 14.000      SPECIFIED TIME FOR OUTPUT
 15.000      SPECIFIED TIME FOR OUTPUT
 17.000      SPECIFIED TIME FOR OUTPUT
 20.000      SPECIFIED TIME FOR OUTPUT
 25.000      SPECIFIED TIME FOR OUTPUT
 30.000      SPECIFIED TIME FOR OUTPUT
 35.000      SPECIFIED TIME FOR OUTPUT
 50.000      SPECIFIED TIME FOR OUTPUT
 55.000      SPECIFIED TIME FOR OUTPUT
 1.0000      MAXIMUM TIME INTERVAL
 2           INITIAL STATUS
  51         NUMBER OF NODE
      32.422054984641240        5.682814109268166
      24.496674738763940        5.528687089002062
      21.209895416737060        5.404409399594580
      19.130759542624870        5.288101201631341
      17.637590899944020        5.176114604634348
      16.493136091794770        5.067399108893608
      15.577715154644750        4.961383219018271
      14.822629567404460        4.857667932365626
      14.184653809015170        4.755873173840262
      13.635131769444460        4.655649470282872
      13.154304612980940        4.556690084679289
      12.728082911231160        4.458729788744641
```

| | |
|---|---|
| 12.346127077314980 | 4.361539593589464 |
| 12.000656055752080 | 4.264919779098419 |
| 11.685685113243620 | 4.168693690230822 |
| 11.396523488032420 | 4.072702810884292 |
| 11.129433798983610 | 3.976802936360070 |
| 10.881395302375820 | 3.880861249079868 |
| 10.649935529809480 | 3.784754067922193 |
| 10.433008103963080 | 3.688365101439075 |
| 10.228902443799690 | 3.591584078227295 |
| 10.036175978322690 | 3.494305680605121 |
| 9.853602463122069 | 3.396428687942703 |
| 9.680132053187444 | 3.297855282790680 |
| 9.514860063347040 | 3.198490470024837 |
| 9.357002258751290 | 3.098241583771947 |
| 9.205875065894238 | 2.997017829253217 |
| 9.060879599194308 | 2.894729860881658 |
| 8.921488590566597 | 2.791289333874973 |
| 8.787235628098573 | 2.686608435340607 |
| 8.657706195244028 | 2.580599357099507 |
| 8.532530129003877 | 2.473173677490923 |
| 8.411375214216639 | 2.364241628705536 |
| 8.293941713145292 | 2.253711244362600 |
| 8.179957643527834 | 2.141487354225257 |
| 8.069174691338391 | 2.027470425931387 |
| 7.961364617129897 | 1.911555199788267 |
| 7.856316113237273 | 1.793629137036179 |
| 7.753832053686150 | 1.673570677879037 |
| 7.653727064207407 | 1.551247274108676 |
| 7.555825405507233 | 1.426513224524766 |
| 7.459959152175511 | 1.299207329502191 |
| 7.365966637133159 | 1.169150361201888 |
| 7.273691153185606 | 1.036142368894518 |
| 7.182979920716410 | 8.999598654511560E-001 |
| 7.093683338965257 | 7.603529628654631E-001 |
| 7.005654496861318 | 6.170424700557684E-001 |
| 6.918748966647099 | 4.697170424158975E-001 |
| 6.832824885989846 | 3.180304621685386E-001 |
| 6.747743336143766 | 1.615991481870680E-001 |
| 6.663369015311635 | 0.000000000000000E+000 |

Void Ratio Distribution at the end of current analysis and informative messages such as final height and stopping time

5.6828 FINAL HEIGHT OF SOIL
55.000 STOPPING TIME

Example 3 - **VD.OUT**

TIME = .0000

| | INITIAL STATE | | | | STEADY STATE | |
|---|---|---|---|---|---|---|
| -NODE- | -ELEVATION- | VOID -RATIO- | SOLID -CONTENT- | WATER -PRESSURE- | -ELEVATION- | VOID -RATIO- |
| 51 | .1375E-03 | .3242E+02 | .7714E-01 | .0000E+00 | .5635E+01 | .3242E+02 |
| 50 | .1347E-03 | .3242E+02 | .7714E-01 | .2836E-04 | .5355E+01 | .2118E+02 |
| 49 | .1320E-03 | .3242E+02 | .7714E-01 | .5671E-04 | .5138E+01 | .1776E+02 |
| 48 | .1292E-03 | .3242E+02 | .7714E-01 | .8507E-04 | .4949E+01 | .1586E+02 |
| 47 | .1265E-03 | .3242E+02 | .7714E-01 | .1134E-03 | .4776E+01 | .1460E+02 |
| 46 | .1237E-03 | .3242E+02 | .7714E-01 | .1418E-03 | .4614E+01 | .1367E+02 |
| 45 | .1210E-03 | .3242E+02 | .7714E-01 | .1701E-03 | .4462E+01 | .1294E+02 |
| 44 | .1182E-03 | .3242E+02 | .7714E-01 | .1985E-03 | .4316E+01 | .1235E+02 |
| 43 | .1155E-03 | .3242E+02 | .7714E-01 | .2268E-03 | .4176E+01 | .1186E+02 |
| 42 | .1127E-03 | .3242E+02 | .7714E-01 | .2552E-03 | .4041E+01 | .1144E+02 |
| 41 | .1100E-03 | .3242E+02 | .7714E-01 | .2836E-03 | .3910E+01 | .1108E+02 |
| 40 | .1072E-03 | .3242E+02 | .7714E-01 | .3119E-03 | .3783E+01 | .1075E+02 |
| 39 | .1045E-03 | .3242E+02 | .7714E-01 | .3403E-03 | .3659E+01 | .1047E+02 |
| 38 | .1017E-03 | .3242E+02 | .7714E-01 | .3686E-03 | .3538E+01 | .1021E+02 |
| 37 | .9899E-04 | .3242E+02 | .7714E-01 | .3970E-03 | .3419E+01 | .9979E+01 |
| 36 | .9624E-04 | .3242E+02 | .7714E-01 | .4253E-03 | .3303E+01 | .9767E+01 |
| 35 | .9349E-04 | .3242E+02 | .7714E-01 | .4537E-03 | .3189E+01 | .9573E+01 |
| 34 | .9074E-04 | .3242E+02 | .7714E-01 | .4820E-03 | .3077E+01 | .9393E+01 |
| 33 | .8799E-04 | .3242E+02 | .7714E-01 | .5104E-03 | .2967E+01 | .9227E+01 |
| 32 | .8524E-04 | .3242E+02 | .7714E-01 | .5387E-03 | .2859E+01 | .9072E+01 |
| 31 | .8249E-04 | .3242E+02 | .7714E-01 | .5671E-03 | .2752E+01 | .8927E+01 |
| 30 | .7974E-04 | .3242E+02 | .7714E-01 | .5955E-03 | .2647E+01 | .8792E+01 |
| 29 | .7699E-04 | .3242E+02 | .7714E-01 | .6238E-03 | .2543E+01 | .8665E+01 |
| 28 | .7424E-04 | .3242E+02 | .7714E-01 | .6522E-03 | .2440E+01 | .8544E+01 |
| 27 | .7149E-04 | .3242E+02 | .7714E-01 | .6805E-03 | .2339E+01 | .8431E+01 |
| 26 | .6874E-04 | .3242E+02 | .7714E-01 | .7089E-03 | .2239E+01 | .8323E+01 |
| 25 | .6599E-04 | .3242E+02 | .7714E-01 | .7372E-03 | .2140E+01 | .8221E+01 |
| 24 | .6324E-04 | .3242E+02 | .7714E-01 | .7656E-03 | .2042E+01 | .8124E+01 |
| 23 | .6049E-04 | .3242E+02 | .7714E-01 | .7939E-03 | .1945E+01 | .8032E+01 |
| 22 | .5774E-04 | .3242E+02 | .7714E-01 | .8223E-03 | .1849E+01 | .7943E+01 |
| 21 | .5500E-04 | .3242E+02 | .7714E-01 | .8507E-03 | .1754E+01 | .7859E+01 |
| 20 | .5225E-04 | .3242E+02 | .7714E-01 | .8790E-03 | .1659E+01 | .7778E+01 |
| 19 | .4950E-04 | .3242E+02 | .7714E-01 | .9074E-03 | .1566E+01 | .7701E+01 |
| 18 | .4675E-04 | .3242E+02 | .7714E-01 | .9357E-03 | .1473E+01 | .7626E+01 |
| 17 | .4400E-04 | .3242E+02 | .7714E-01 | .9641E-03 | .1382E+01 | .7555E+01 |
| 16 | .4125E-04 | .3242E+02 | .7714E-01 | .9924E-03 | .1291E+01 | .7486E+01 |
| 15 | .3850E-04 | .3242E+02 | .7714E-01 | .1021E-02 | .1200E+01 | .7420E+01 |
| 14 | .3575E-04 | .3242E+02 | .7714E-01 | .1049E-02 | .1111E+01 | .7356E+01 |
| 13 | .3300E-04 | .3242E+02 | .7714E-01 | .1077E-02 | .1022E+01 | .7294E+01 |
| 12 | .3025E-04 | .3242E+02 | .7714E-01 | .1106E-02 | .9336E+00 | .7234E+01 |
| 11 | .2750E-04 | .3242E+02 | .7714E-01 | .1134E-02 | .8460E+00 | .7177E+01 |
| 10 | .2475E-04 | .3242E+02 | .7714E-01 | .1163E-02 | .7589E+00 | .7121E+01 |
| 9 | .2200E-04 | .3242E+02 | .7714E-01 | .1191E-02 | .6725E+00 | .7067E+01 |
| 8 | .1925E-04 | .3242E+02 | .7714E-01 | .1219E-02 | .5866E+00 | .7014E+01 |
| 7 | .1650E-04 | .3242E+02 | .7714E-01 | .1248E-02 | .5013E+00 | .6964E+01 |
| 6 | .1375E-04 | .3242E+02 | .7714E-01 | .1276E-02 | .4165E+00 | .6914E+01 |
| 5 | .1100E-04 | .3242E+02 | .7714E-01 | .1304E-02 | .3322E+00 | .6866E+01 |
| 4 | .8249E-05 | .3242E+02 | .7714E-01 | .1333E-02 | .2484E+00 | .6820E+01 |
| 3 | .5500E-05 | .3242E+02 | .7714E-01 | .1361E-02 | .1651E+00 | .6774E+01 |
| 2 | .2750E-05 | .3242E+02 | .7714E-01 | .1389E-02 | .8234E-01 | .6730E+01 |
| 1 | .0000E+00 | .3242E+02 | .7714E-01 | .1418E-02 | .0000E+00 | .6687E+01 |

TIME = .5000

| -NODE- | -ELEVATION- | VOID -RATIO- | SOLID -CONTENT- | WATER -PRESSURE- | ALPHA -VALUES- |
|---|---|---|---|---|---|
| 51 | .8117E+00 | .3242E+02 | .7714E-01 | .0000E+00 | .1000E+01 |
| 50 | .7942E+00 | .3210E+02 | .7786E-01 | .1783E+00 | .1000E+01 |
| 49 | .7769E+00 | .3179E+02 | .7856E-01 | .3549E+00 | .1000E+01 |
| 48 | .7597E+00 | .3149E+02 | .7924E-01 | .5300E+00 | .1000E+01 |
| 47 | .7427E+00 | .3120E+02 | .7992E-01 | .7036E+00 | .1000E+01 |
| 46 | .7259E+00 | .3091E+02 | .8060E-01 | .8756E+00 | .1000E+01 |
| 45 | .7092E+00 | .3063E+02 | .8129E-01 | .1046E+01 | .1000E+01 |
| 44 | .6926E+00 | .3034E+02 | .8200E-01 | .1215E+01 | .1000E+01 |
| 43 | .6762E+00 | .3005E+02 | .8273E-01 | .1382E+01 | .1000E+01 |
| 42 | .6600E+00 | .2974E+02 | .8350E-01 | .1548E+01 | .1000E+01 |
| 41 | .6439E+00 | .2943E+02 | .8431E-01 | .1711E+01 | .1000E+01 |
| 40 | .6280E+00 | .2911E+02 | .8517E-01 | .1873E+01 | .1000E+01 |
| 39 | .6123E+00 | .2877E+02 | .8608E-01 | .2033E+01 | .1000E+01 |
| 38 | .5967E+00 | .2841E+02 | .8707E-01 | .2191E+01 | .1000E+01 |
| 37 | .5813E+00 | .2804E+02 | .8814E-01 | .2346E+01 | .1000E+01 |
| 36 | .5661E+00 | .2765E+02 | .8925E-01 | .2500E+01 | .1000E+01 |
| 35 | .5508E+00 | .2727E+02 | .9038E-01 | .2655E+01 | .1000E+01 |
| 34 | .5354E+00 | .2690E+02 | .9153E-01 | .2811E+01 | .1000E+01 |
| 33 | .5199E+00 | .2652E+02 | .9270E-01 | .2966E+01 | .1000E+01 |
| 32 | .5044E+00 | .2615E+02 | .9390E-01 | .3122E+01 | .1000E+01 |
| 31 | .4888E+00 | .2578E+02 | .9513E-01 | .3279E+01 | .1000E+01 |
| 30 | .4732E+00 | .2541E+02 | .9638E-01 | .3436E+01 | .1000E+01 |
| 29 | .4576E+00 | .2504E+02 | .9767E-01 | .3593E+01 | .1000E+01 |
| 28 | .4419E+00 | .2467E+02 | .9899E-01 | .3750E+01 | .1000E+01 |
| 27 | .4262E+00 | .2430E+02 | .1003E+00 | .3907E+01 | .1000E+01 |
| 26 | .4104E+00 | .2393E+02 | .1017E+00 | .4065E+01 | .1000E+01 |
| 25 | .3946E+00 | .2356E+02 | .1032E+00 | .4223E+01 | .1000E+01 |
| 24 | .3787E+00 | .2319E+02 | .1046E+00 | .4381E+01 | .1000E+01 |
| 23 | .3627E+00 | .2283E+02 | .1061E+00 | .4539E+01 | .1000E+01 |
| 22 | .3467E+00 | .2247E+02 | .1076E+00 | .4698E+01 | .1000E+01 |
| 21 | .3305E+00 | .2212E+02 | .1092E+00 | .4858E+01 | .1000E+01 |
| 20 | .3143E+00 | .2176E+02 | .1107E+00 | .5018E+01 | .1000E+01 |
| 19 | .2979E+00 | .2142E+02 | .1123E+00 | .5179E+01 | .1000E+01 |
| 18 | .2816E+00 | .2107E+02 | .1139E+00 | .5340E+01 | .1000E+01 |
| 17 | .2651E+00 | .2073E+02 | .1156E+00 | .5501E+01 | .1000E+01 |
| 16 | .2486E+00 | .2040E+02 | .1173E+00 | .5662E+01 | .1000E+01 |
| 15 | .2321E+00 | .2007E+02 | .1190E+00 | .5823E+01 | .1000E+01 |
| 14 | .2155E+00 | .1974E+02 | .1207E+00 | .5983E+01 | .1000E+01 |
| 13 | .1989E+00 | .1941E+02 | .1225E+00 | .6143E+01 | .1000E+01 |
| 12 | .1823E+00 | .1909E+02 | .1243E+00 | .6303E+01 | .1000E+01 |
| 11 | .1657E+00 | .1877E+02 | .1262E+00 | .6462E+01 | .1000E+01 |
| 10 | .1490E+00 | .1845E+02 | .1281E+00 | .6620E+01 | .1000E+01 |
| 9 | .1324E+00 | .1814E+02 | .1300E+00 | .6776E+01 | .1000E+01 |
| 8 | .1158E+00 | .1782E+02 | .1320E+00 | .6932E+01 | .1000E+01 |
| 7 | .9917E-01 | .1751E+02 | .1340E+00 | .7086E+01 | .1000E+01 |
| 6 | .8257E-01 | .1719E+02 | .1362E+00 | .7238E+01 | .1000E+01 |
| 5 | .6599E-01 | .1688E+02 | .1383E+00 | .7388E+01 | .1000E+01 |
| 4 | .4943E-01 | .1656E+02 | .1406E+00 | .7536E+01 | .1000E+01 |
| 3 | .3291E-01 | .1625E+02 | .1429E+00 | .7682E+01 | .1000E+01 |
| 2 | .1643E-01 | .1593E+02 | .1454E+00 | .7824E+01 | .1000E+01 |
| 1 | .0000E+00 | .1561E+02 | .1479E+00 | .7963E+01 | .1000E+01 |

Figure EX3-2 Time - Settlement Curve

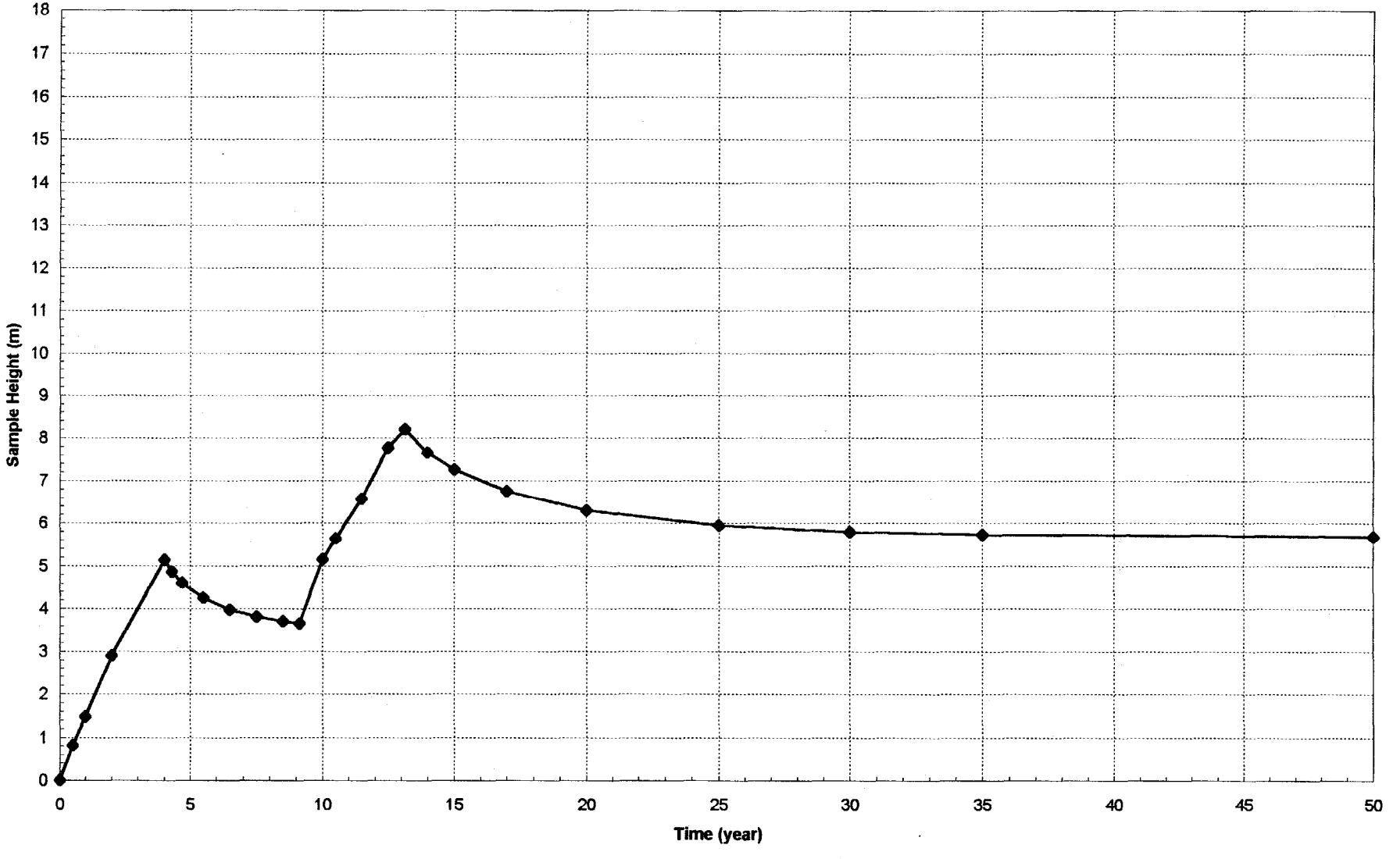

**Figure EX3-3 Solid Content Curve**

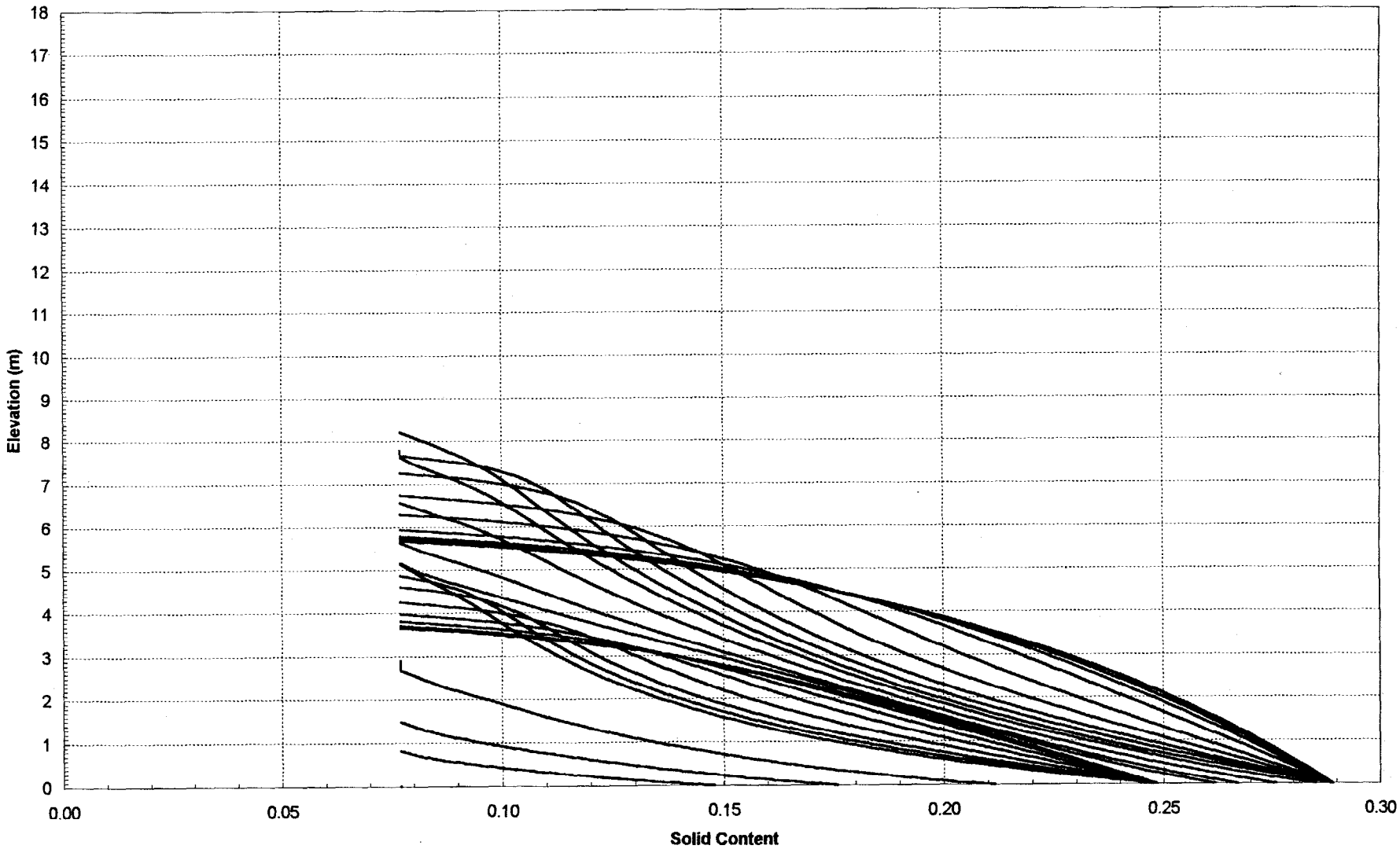

**Example 4** - Instantaneous Filling Consolidation Analysis with Dewatering Scheme at Bottom

*Case Description*

The slurried soil with the following compression and permeability characteristics is deposited into a confined facility in a very short period of time with a height of 17.85 meters. The shrinkage limit of this material is 0.5. The specific gravity of soil solids is 2.71. A dewatering scheme is estimated to withdraw 0.5 $m^3$/year from the deposited material bottom per meter square of the bottom area. A layer of ponding water is always on top of the soil. The consolidation analysis is requested and information is needed for 50 years.

*Required Data*

A1 = 13.49
B1 = -0.319
Z1 = 0.064 kpa
C = 1.211E-4 m/year
D = 3.5

Gs = 2.71
H0 = 17.85 m
Gw = 9.81 kN/$m^3$
$e_{(min)}$ = 0.5
T0 = 0.0
T=0.2, 0.5, 0.7, 1, 1.3, 1.6, 2, 2.5, 3, 4, 5, 7, 10, 13.13, 16, 20, 25, 30, 40, 50
MAXDT = 0.5 year (arbitrary number, approximately 1/100 of time span)

Boundary Conditions: Top - zero surcharge
Bottom - dewatering at the rate of 0.5m/year
Analysis Status: Consolidation and dewatering (No desiccation)
No stage filling
New analysis

The complete input file, output files such as TS.OUT and INPUT, and part of the VD.OUT are provided in following pages. The time-settlement curve (Fig. EX4-1) and solid content curve (Fig. EX4-2) are also plotted.

Example 4 - **Input File**

```
13.490 -.3190 .12110E-03 3.5000 .64000E-01      A1,B1,C,D,Z1
 2                                              3-D DESSICATION STATUS
 2.7100                                         SPECIFIC GRAVITY OF SOLIDS
 9.8100                                         UNIT WEIGHT OF WATER
 17.850                                         INITIAL HEIGHT OF SOIL
 2                                              STAGE FILLING STATUS
 2                                              TOP BOUNDARY CONDITION
 .00000                                         TOP BOUNDARY CONDITION VALUES
 4                                              BOTTOM BOUNDARY CONDITION
-0.5                                            BOTTOM BOUNDARY CONDITION VALUES
.10000                                          MINIMUM VOID RATIO
 .00000                                         STARTING TIME
  20                                            NUMBER OF OUTPUT FILES
 .20000                                         SPECIFIED TIME FOR OUTPUT
 .50000                                         SPECIFIED TIME FOR OUTPUT
 .70000                                         SPECIFIED TIME FOR OUTPUT
 1.0000                                         SPECIFIED TIME FOR OUTPUT
 1.3000                                         SPECIFIED TIME FOR OUTPUT
 1.6000                                         SPECIFIED TIME FOR OUTPUT
 2.0000                                         SPECIFIED TIME FOR OUTPUT
 2.5000                                         SPECIFIED TIME FOR OUTPUT
 3.0000                                         SPECIFIED TIME FOR OUTPUT
 4.0000                                         SPECIFIED TIME FOR OUTPUT
 5.0000                                         SPECIFIED TIME FOR OUTPUT
 7.0000                                         SPECIFIED TIME FOR OUTPUT
 10.000                                         SPECIFIED TIME FOR OUTPUT
 13.130                                         SPECIFIED TIME FOR OUTPUT
 16.000                                         SPECIFIED TIME FOR OUTPUT
 20.000                                         SPECIFIED TIME FOR OUTPUT
 25.000                                         SPECIFIED TIME FOR OUTPUT
 30.000                                         SPECIFIED TIME FOR OUTPUT
 40.000                                         SPECIFIED TIME FOR OUTPUT
 50.000                                         SPECIFIED TIME FOR OUTPUT
 .50000                                         MAXIMUM TIME INTERVAL
 2                                              INITIAL STATUS
```

Example 4 - **TS.OUT**

| -TIME- | SOIL -HEIGHT- | AVERAGE DRY -DENSITY- | CUMULATED OUTFLOW -TOP- | CUMULATED OUTFLOW -BOTTOM- | CRUST -THINKNESS- |
|---|---|---|---|---|---|
| .0000E+00 | .1785E+02 | .7954E+00 | .0000E+00 | .0000E+00 | .0000E+00 |
| .2000E+00 | .1717E+02 | .8272E+00 | .2398E+00 | -.5854E+00 | .0000E+00 |
| .5000E+00 | .1659E+02 | .8556E+00 | .6005E+00 | -.8542E+00 | .0000E+00 |
| .7000E+00 | .1626E+02 | .8732E+00 | .8410E+00 | -.9712E+00 | .0000E+00 |
| .1000E+01 | .1537E+02 | .9238E+00 | .1470E+01 | -.1235E+01 | .0000E+00 |
| .1300E+01 | .1486E+02 | .9556E+00 | .1831E+01 | -.1385E+01 | .0000E+00 |
| .1600E+01 | .1435E+02 | .9896E+00 | .2191E+01 | -.1535E+01 | .0000E+00 |
| .2000E+01 | .1367E+02 | .1039E+01 | .2672E+01 | -.1735E+01 | .0000E+00 |
| .2500E+01 | .1281E+02 | .1108E+01 | .3273E+01 | -.1985E+01 | .0000E+00 |
| .3000E+01 | .1196E+02 | .1187E+01 | .3874E+01 | -.2235E+01 | .0000E+00 |
| .4000E+01 | .1028E+02 | .1381E+01 | .5068E+01 | -.2735E+01 | .0000E+00 |
| .5000E+01 | .8699E+01 | .1632E+01 | .6202E+01 | -.3235E+01 | .0000E+00 |
| .7000E+01 | .6170E+01 | .2301E+01 | .7934E+01 | -.4235E+01 | .0000E+00 |
| .1000E+02 | .3670E+01 | .3869E+01 | .9130E+01 | -.5735E+01 | .0000E+00 |
| .1313E+02 | .2289E+01 | .6202E+01 | .9112E+01 | -.7300E+01 | .0000E+00 |
| .1600E+02 | .1956E+01 | .7261E+01 | .8046E+01 | -.8735E+01 | .0000E+00 |
| .2000E+02 | .1908E+01 | .7442E+01 | .6100E+01 | -.1074E+02 | .0000E+00 |
| .2050E+02 | .1907E+01 | .7445E+01 | .5851E+01 | -.1099E+02 | .0000E+00 |

THE TOTAL HEIGHT OF SOIL SOLID IS 5.340784702856478E-001
TIME WHEN THE SELF-WEIGHT CONSOLIDATION ENDS AT BOTTOM :
7.000000000000000E-001

Example 4 - **INPUT**

```
13.490 -.3190 .12110E-03 3.5000 .64000E-01      A,B,C,D,Z
 2          3-D DESSICATION STATUS
 2.7100     SPECIFIC GRAVITY OF SOLIDS
 9.8100     UNIT WEIGHT OF WATER
 17.850     INITIAL HEIGHT OF SOIL
 2          STAGE FILLING STATUS
 2          TOP BOUNDARY CONDITION
 .00000     TOP BOUNDARY CONDITION VALUES
 4          BOTTOM BOUNDARY CONDITION
-0.5        BOTTOM BOUNDARY CONDITION VALUES
.10000      MINIMUM VOID RATIO
 .00000     STARTING TIME
  20        NUMBER OF OUTPUT FILES
 .20000     SPECIFIED TIME FOR OUTPUT
 .50000     SPECIFIED TIME FOR OUTPUT
 .70000     SPECIFIED TIME FOR OUTPUT
 1.0000     SPECIFIED TIME FOR OUTPUT
 1.3000     SPECIFIED TIME FOR OUTPUT
 1.6000     SPECIFIED TIME FOR OUTPUT
 2.0000     SPECIFIED TIME FOR OUTPUT
 2.5000     SPECIFIED TIME FOR OUTPUT
 3.0000     SPECIFIED TIME FOR OUTPUT
 4.0000     SPECIFIED TIME FOR OUTPUT
 5.0000     SPECIFIED TIME FOR OUTPUT
 7.0000     SPECIFIED TIME FOR OUTPUT
 10.000     SPECIFIED TIME FOR OUTPUT
 13.130     SPECIFIED TIME FOR OUTPUT
 16.000     SPECIFIED TIME FOR OUTPUT
 20.000     SPECIFIED TIME FOR OUTPUT
 25.000     SPECIFIED TIME FOR OUTPUT
 30.000     SPECIFIED TIME FOR OUTPUT
 40.000     SPECIFIED TIME FOR OUTPUT
 50.000     SPECIFIED TIME FOR OUTPUT
 .50000     MAXIMUM TIME INTERVAL
 2          INITIAL STATUS
  51        NUMBER OF NODE
      32.422054984641240        1.907073298308393
      17.371242012859200        1.653687965670523
      12.724712851524990        1.485075645189317
      10.072608694427930        1.353684646212972
       8.284441429256891        1.245503436092247
       6.977997881883148        1.153636662255322
       5.976669398718620        1.073985081906903
       5.183972756794407        1.003850721381349
       4.541406929703762   9.413410806193000E-001
       4.010906065914185   8.850692285844041E-001
       3.566411843146337   8.339854963000487E-001
       3.189390932913684   7.872754642141052E-001
       2.866262087283071   7.442945022218754E-001
       2.586830063333967   7.045238844080785E-001
       2.343287152986987   6.675403302911547E-001
       2.129552313655678   6.329942615535981E-001
       1.940820058404616   6.005939136512537E-001
       1.773244471720533   5.700934940876393E-001
       1.623712955869560   5.412842054939151E-001
       1.489681123628028   5.139873389167987E-001
       1.369050297828272   4.880488900158455E-001
```

Input Data

```
      1.260075281785231   4.633353132316352E-001
      1.161294007485145   4.397301381734818E-001
      1.071473237923049   4.171312474641431E-001
  9.895662118826260E-001  3.954486677463206E-001
  9.146792825638893E-001  3.746027628777260E-001
  8.460454056793658E-001  3.545227452870206E-001
  7.830028975388232E-001  3.351454411795811E-001
  7.249782861481374E-001  3.164142598861275E-001
  6.714723688973769E-001  2.982783285857302E-001
  6.220488026591339E-001  2.806917619120070E-001
  5.763247088702919E-001  2.636130422743657E-001
  5.339628931156709E-001  2.470044915988558E-001
  4.946653668010703E-001  2.308318189789883E-001
  4.581679254085046E-001  2.150637316906766E-001
  4.242355890695059E-001  1.996715993623264E-001
  3.926587507406924E-001  1.846291629460437E-001
  3.632499080080482E-001  1.699122816176269E-001
  3.358408786052039E-001  1.554987119236276E-001
  3.102804186797097E-001  1.413679144558779E-001
  2.864321778554146E-001  1.275008841155021E-001
  2.641729371036727E-001  1.138800006666376E-001
  2.433910850222686E-001  1.004888968037135E-001
  2.239852958410824E-001  8.731234138772127E-002
  2.058633787213904E-001  7.433613586420571E-002
  1.889412729956274E-001  6.154702217272773E-002
  1.731421681431825E-001  4.893260070547690E-002
  1.583957307004290E-001  3.648125708044466E-002
  1.446374231051817E-001  2.418209666928250E-002
  1.318079017920784E-001  1.202488596743530E-002
  1.198525194323843E-001  0.000000000000000E+000
1.9071          FINAL HEIGHT OF SOIL
20.500          STOPPING TIME
```

Void Ratio Distribution at the end of current analysis and informative messages such as final height and stopping time

Example 4 - **VD.OUT**

TIME = .0000

| | INITIAL STATE | | | | STEADY STATE | |
|---|---|---|---|---|---|---|
| | | VOID | SOLID | WATER | | VOID |
| -NODE- | -ELEVATION- | -RATIO- | -CONTENT- | -PRESSURE- | -ELEVATION- | -RATIO- |
| 51 | .1785E+02 | .3242E+02 | .7714E-01 | .0000E+00 | .1907E+01 | .3242E+02 |
| 50 | .1749E+02 | .3242E+02 | .7714E-01 | .3681E+01 | .1654E+01 | .1739E+02 |
| 49 | .1714E+02 | .3242E+02 | .7714E-01 | .7363E+01 | .1485E+01 | .1273E+02 |
| 48 | .1678E+02 | .3242E+02 | .7714E-01 | .1104E+02 | .1353E+01 | .1007E+02 |
| 47 | .1642E+02 | .3242E+02 | .7714E-01 | .1473E+02 | .1245E+01 | .8284E+01 |
| 46 | .1607E+02 | .3242E+02 | .7714E-01 | .1841E+02 | .1153E+01 | .6976E+01 |
| 45 | .1571E+02 | .3242E+02 | .7714E-01 | .2209E+02 | .1074E+01 | .5975E+01 |
| 44 | .1535E+02 | .3242E+02 | .7714E-01 | .2577E+02 | .1004E+01 | .5182E+01 |
| 43 | .1499E+02 | .3242E+02 | .7714E-01 | .2945E+02 | .9411E+00 | .4539E+01 |
| 42 | .1464E+02 | .3242E+02 | .7714E-01 | .3313E+02 | .8848E+00 | .4009E+01 |
| 41 | .1428E+02 | .3242E+02 | .7714E-01 | .3681E+02 | .8338E+00 | .3564E+01 |
| 40 | .1392E+02 | .3242E+02 | .7714E-01 | .4049E+02 | .7871E+00 | .3188E+01 |
| 39 | .1357E+02 | .3242E+02 | .7714E-01 | .4418E+02 | .7441E+00 | .2865E+01 |
| 38 | .1321E+02 | .3242E+02 | .7714E-01 | .4786E+02 | .7044E+00 | .2585E+01 |
| 37 | .1285E+02 | .3242E+02 | .7714E-01 | .5154E+02 | .6674E+00 | .2342E+01 |
| 36 | .1250E+02 | .3242E+02 | .7714E-01 | .5522E+02 | .6329E+00 | .2128E+01 |
| 35 | .1214E+02 | .3242E+02 | .7714E-01 | .5890E+02 | .6005E+00 | .1940E+01 |
| 34 | .1178E+02 | .3242E+02 | .7714E-01 | .6258E+02 | .5700E+00 | .1772E+01 |
| 33 | .1142E+02 | .3242E+02 | .7714E-01 | .6626E+02 | .5412E+00 | .1623E+01 |
| 32 | .1107E+02 | .3242E+02 | .7714E-01 | .6995E+02 | .5139E+00 | .1489E+01 |
| 31 | .1071E+02 | .3242E+02 | .7714E-01 | .7363E+02 | .4880E+00 | .1368E+01 |
| 30 | .1035E+02 | .3242E+02 | .7714E-01 | .7731E+02 | .4633E+00 | .1259E+01 |
| 29 | .9996E+01 | .3242E+02 | .7714E-01 | .8099E+02 | .4397E+00 | .1161E+01 |
| 28 | .9639E+01 | .3242E+02 | .7714E-01 | .8467E+02 | .4171E+00 | .1071E+01 |
| 27 | .9282E+01 | .3242E+02 | .7714E-01 | .8835E+02 | .3954E+00 | .9891E+00 |
| 26 | .8925E+01 | .3242E+02 | .7714E-01 | .9203E+02 | .3746E+00 | .9142E+00 |
| 25 | .8568E+01 | .3242E+02 | .7714E-01 | .9572E+02 | .3545E+00 | .8456E+00 |
| 24 | .8211E+01 | .3242E+02 | .7714E-01 | .9940E+02 | .3351E+00 | .7826E+00 |
| 23 | .7854E+01 | .3242E+02 | .7714E-01 | .1031E+03 | .3164E+00 | .7247E+00 |
| 22 | .7497E+01 | .3242E+02 | .7714E-01 | .1068E+03 | .2983E+00 | .6712E+00 |
| 21 | .7140E+01 | .3242E+02 | .7714E-01 | .1104E+03 | .2807E+00 | .6218E+00 |
| 20 | .6783E+01 | .3242E+02 | .7714E-01 | .1141E+03 | .2636E+00 | .5761E+00 |
| 19 | .6426E+01 | .3242E+02 | .7714E-01 | .1178E+03 | .2470E+00 | .5338E+00 |
| 18 | .6069E+01 | .3242E+02 | .7714E-01 | .1215E+03 | .2308E+00 | .4945E+00 |
| 17 | .5712E+01 | .3242E+02 | .7714E-01 | .1252E+03 | .2151E+00 | .4580E+00 |
| 16 | .5355E+01 | .3242E+02 | .7714E-01 | .1288E+03 | .1997E+00 | .4241E+00 |
| 15 | .4998E+01 | .3242E+02 | .7714E-01 | .1325E+03 | .1846E+00 | .3925E+00 |
| 14 | .4641E+01 | .3242E+02 | .7714E-01 | .1362E+03 | .1699E+00 | .3631E+00 |
| 13 | .4284E+01 | .3242E+02 | .7714E-01 | .1399E+03 | .1555E+00 | .3357E+00 |
| 12 | .3927E+01 | .3242E+02 | .7714E-01 | .1436E+03 | .1414E+00 | .3102E+00 |
| 11 | .3570E+01 | .3242E+02 | .7714E-01 | .1473E+03 | .1275E+00 | .2864E+00 |
| 10 | .3213E+01 | .3242E+02 | .7714E-01 | .1509E+03 | .1139E+00 | .2641E+00 |
| 9 | .2856E+01 | .3242E+02 | .7714E-01 | .1546E+03 | .1005E+00 | .2433E+00 |
| 8 | .2499E+01 | .3242E+02 | .7714E-01 | .1583E+03 | .8731E-01 | .2239E+00 |
| 7 | .2142E+01 | .3242E+02 | .7714E-01 | .1620E+03 | .7434E-01 | .2058E+00 |
| 6 | .1785E+01 | .3242E+02 | .7714E-01 | .1657E+03 | .6155E-01 | .1889E+00 |
| 5 | .1428E+01 | .3242E+02 | .7714E-01 | .1693E+03 | .4893E-01 | .1731E+00 |
| 4 | .1071E+01 | .3242E+02 | .7714E-01 | .1730E+03 | .3648E-01 | .1584E+00 |
| 3 | .7140E+00 | .3242E+02 | .7714E-01 | .1767E+03 | .2418E-01 | .1446E+00 |
| 2 | .3570E+00 | .3242E+02 | .7714E-01 | .1804E+03 | .1202E-01 | .1318E+00 |
| 1 | .0000E+00 | .3242E+02 | .7714E-01 | .1841E+03 | .0000E+00 | .1199E+00 |

TIME = .2000

| -NODE- | -ELEVATION- | VOID -RATIO- | SOLID -CONTENT- | WATER -PRESSURE- | ALPHA -VALUES- |
|---|---|---|---|---|---|
| 51 | .1717E+02 | .3242E+02 | .7714E-01 | .0000E+00 | .1000E+01 |
| 50 | .1681E+02 | .3242E+02 | .7714E-01 | .3681E+01 | .1000E+01 |
| 49 | .1645E+02 | .3242E+02 | .7714E-01 | .7363E+01 | .1000E+01 |
| 48 | .1609E+02 | .3242E+02 | .7714E-01 | .1104E+02 | .1000E+01 |
| 47 | .1574E+02 | .3242E+02 | .7714E-01 | .1473E+02 | .1000E+01 |
| 46 | .1538E+02 | .3242E+02 | .7714E-01 | .1841E+02 | .1000E+01 |
| 45 | .1502E+02 | .3242E+02 | .7714E-01 | .2209E+02 | .1000E+01 |
| 44 | .1467E+02 | .3242E+02 | .7714E-01 | .2577E+02 | .1000E+01 |
| 43 | .1431E+02 | .3242E+02 | .7714E-01 | .2945E+02 | .1000E+01 |
| 42 | .1395E+02 | .3242E+02 | .7714E-01 | .3313E+02 | .1000E+01 |
| 41 | .1360E+02 | .3242E+02 | .7714E-01 | .3681E+02 | .1000E+01 |
| 40 | .1324E+02 | .3242E+02 | .7714E-01 | .4049E+02 | .1000E+01 |
| 39 | .1288E+02 | .3242E+02 | .7714E-01 | .4418E+02 | .1000E+01 |
| 38 | .1252E+02 | .3242E+02 | .7714E-01 | .4786E+02 | .1000E+01 |
| 37 | .1217E+02 | .3242E+02 | .7714E-01 | .5154E+02 | .1000E+01 |
| 36 | .1181E+02 | .3242E+02 | .7714E-01 | .5522E+02 | .1000E+01 |
| 35 | .1145E+02 | .3242E+02 | .7714E-01 | .5890E+02 | .1000E+01 |
| 34 | .1110E+02 | .3242E+02 | .7714E-01 | .6258E+02 | .1000E+01 |
| 33 | .1074E+02 | .3242E+02 | .7714E-01 | .6626E+02 | .1000E+01 |
| 32 | .1038E+02 | .3242E+02 | .7714E-01 | .6995E+02 | .1000E+01 |
| 31 | .1003E+02 | .3242E+02 | .7714E-01 | .7363E+02 | .1000E+01 |
| 30 | .9668E+01 | .3242E+02 | .7714E-01 | .7731E+02 | .1000E+01 |
| 29 | .9311E+01 | .3242E+02 | .7714E-01 | .8099E+02 | .1000E+01 |
| 28 | .8954E+01 | .3242E+02 | .7714E-01 | .8467E+02 | .1000E+01 |
| 27 | .8597E+01 | .3242E+02 | .7714E-01 | .8835E+02 | .1000E+01 |
| 26 | .8240E+01 | .3242E+02 | .7714E-01 | .9203E+02 | .1000E+01 |
| 25 | .7883E+01 | .3242E+02 | .7714E-01 | .9572E+02 | .1000E+01 |
| 24 | .7526E+01 | .3242E+02 | .7714E-01 | .9940E+02 | .1000E+01 |
| 23 | .7169E+01 | .3242E+02 | .7714E-01 | .1031E+03 | .1000E+01 |
| 22 | .6812E+01 | .3242E+02 | .7714E-01 | .1068E+03 | .1000E+01 |
| 21 | .6455E+01 | .3242E+02 | .7714E-01 | .1104E+03 | .1000E+01 |
| 20 | .6098E+01 | .3242E+02 | .7714E-01 | .1141E+03 | .1000E+01 |
| 19 | .5741E+01 | .3242E+02 | .7714E-01 | .1178E+03 | .1000E+01 |
| 18 | .5384E+01 | .3242E+02 | .7714E-01 | .1215E+03 | .1000E+01 |
| 17 | .5027E+01 | .3242E+02 | .7714E-01 | .1252E+03 | .1000E+01 |
| 16 | .4670E+01 | .3242E+02 | .7714E-01 | .1288E+03 | .1000E+01 |
| 15 | .4313E+01 | .3242E+02 | .7714E-01 | .1325E+03 | .1000E+01 |
| 14 | .3956E+01 | .3242E+02 | .7714E-01 | .1362E+03 | .1000E+01 |
| 13 | .3599E+01 | .3242E+02 | .7714E-01 | .1399E+03 | .1000E+01 |
| 12 | .3242E+01 | .3242E+02 | .7714E-01 | .1436E+03 | .1000E+01 |
| 11 | .2885E+01 | .3242E+02 | .7714E-01 | .1473E+03 | .1000E+01 |
| 10 | .2528E+01 | .3242E+02 | .7714E-01 | .1509E+03 | .1000E+01 |
| 9 | .2172E+01 | .3241E+02 | .7717E-01 | .1546E+03 | .1000E+01 |
| 8 | .1815E+01 | .3236E+02 | .7727E-01 | .1583E+03 | .1000E+01 |
| 7 | .1459E+01 | .3218E+02 | .7766E-01 | .1620E+03 | .1000E+01 |
| 6 | .1108E+01 | .3153E+02 | .7915E-01 | .1656E+03 | .1000E+01 |
| 5 | .7695E+00 | .2941E+02 | .8438E-01 | .1691E+03 | .1000E+01 |
| 4 | .4696E+00 | .2412E+02 | .1010E+00 | .1721E+03 | .1000E+01 |
| 3 | .2437E+00 | .1605E+02 | .1444E+00 | .1741E+03 | .1000E+01 |
| 2 | .9753E-01 | .9910E+01 | .2147E+00 | .1737E+03 | .1000E+01 |
| 1 | .0000E+00 | .6687E+01 | .2884E+00 | .1684E+03 | .1000E+01 |

**Figure EX4-1 Time - Settlement Curve**

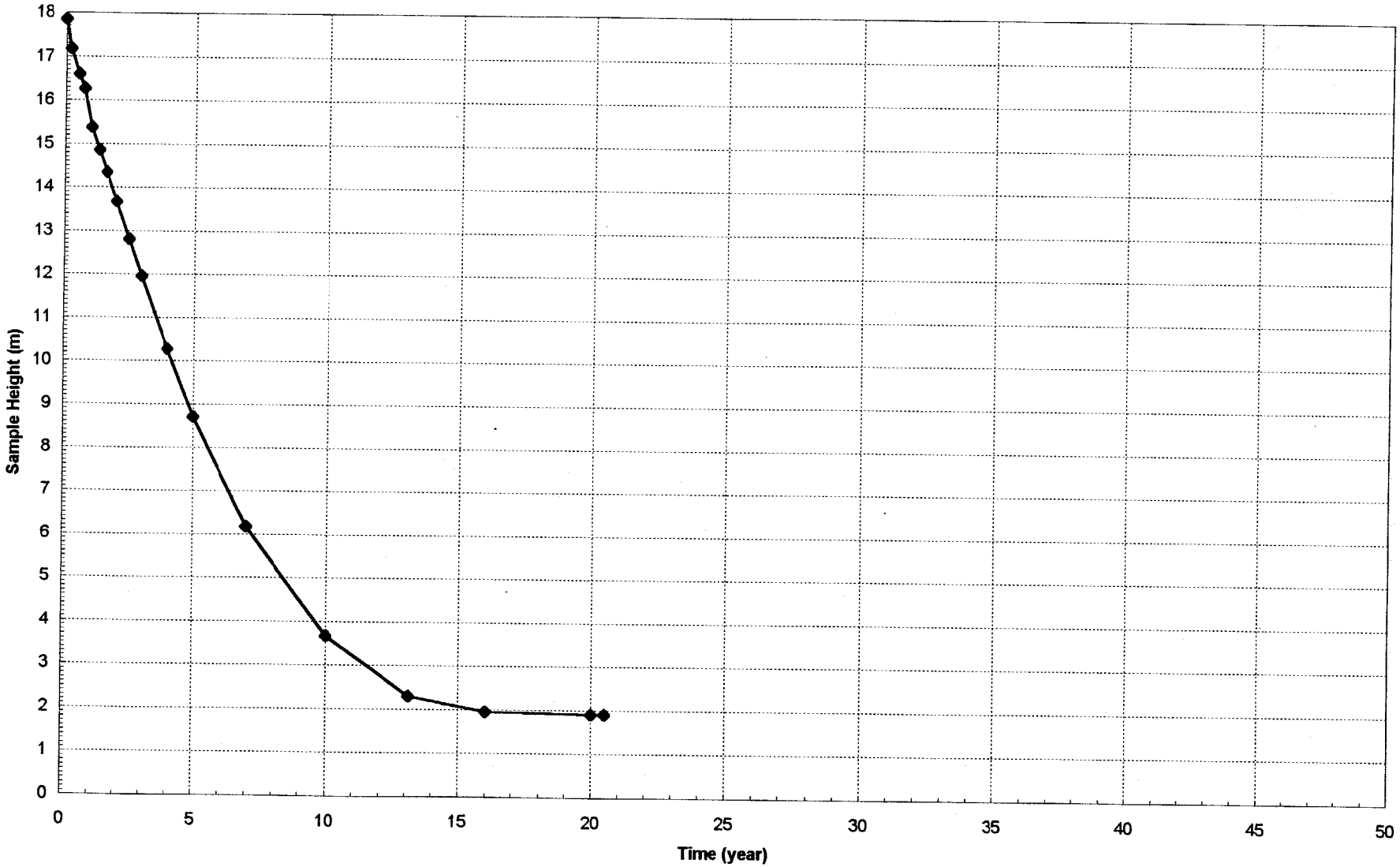

**Figure EX4-2 Solid Content Curve**

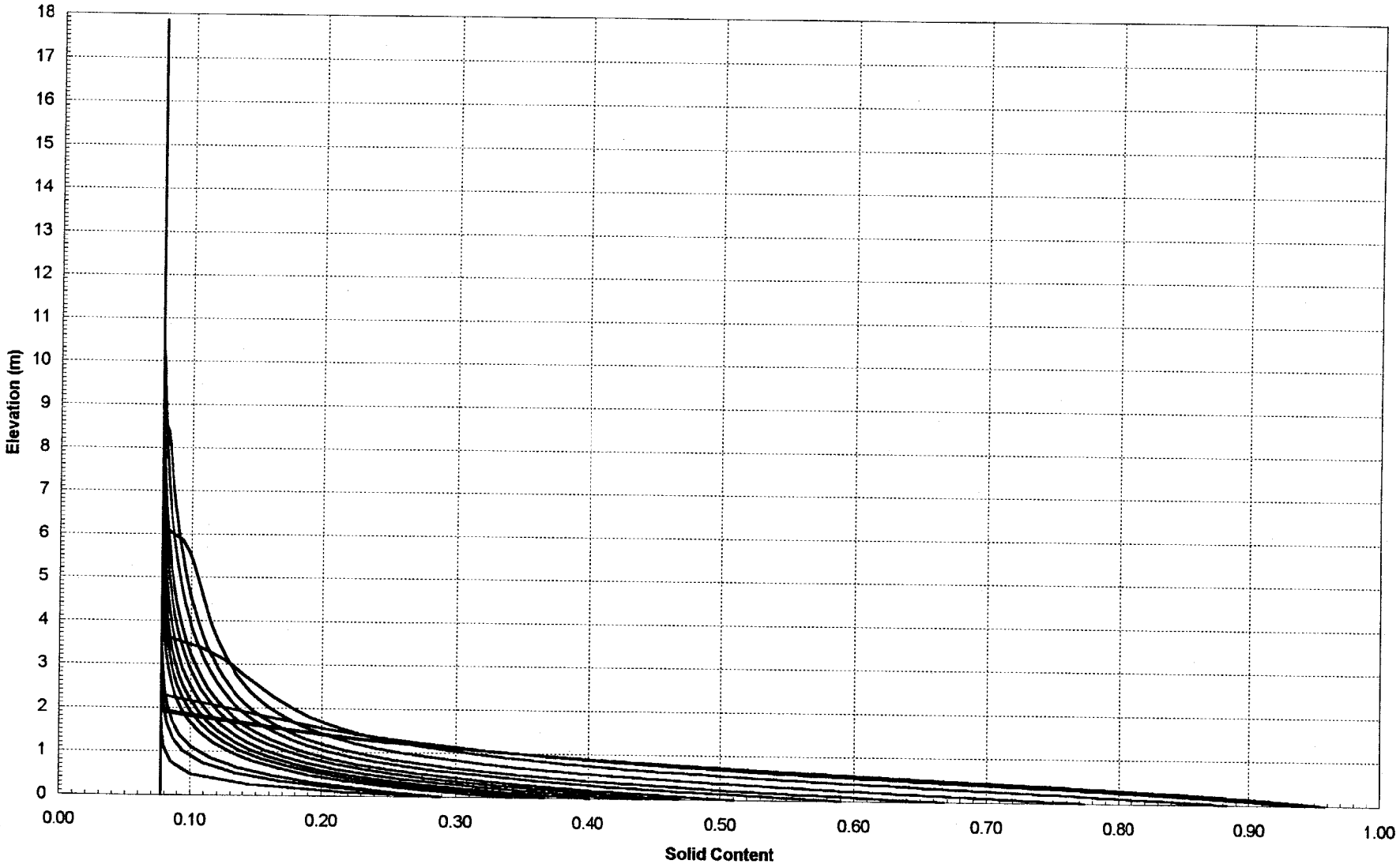

Example 5 - Stage Filling Consolidation and Desiccation Analysis

*Case Description*

The slurried soil with the following compression and permeability characteristics is deposited into a confined facility with the stage filling schedule showing in Fig. EX5-1 (the nominal height - time plot). The detailed filling information is in Table EX5-1. The shrinkage limit of this material is 0.5. The specific gravity of soil solids is 2.71. An impervious layer exists at bottom of the confined facility.

During the filling period (0.0 to 13.13 years, consolidation process), a layer of ponding water is always on top of the soil. Starting from the end of 13.13 year, the ponding water on top of soil is removed and the desiccation process starts. The average evaporation rate in Florida (1.05 m/year) is used in this example for the desiccation process.

The consolidation analysis is requested and information is needed for 13.13 year. The information about the desiccation process is needed to year 55.

*Required Data*

Table EX5-1

| Stage Number | Starting Time (year) | Ending Time (year) | Filling Rate (m/year) |
|---|---|---|---|
| 1 | 0.0 | 4.0 | 2.4 |
| 2 | 4.0 | 9.13 | 0.0 |
| 3 | 9.13 | 13.13 | 2.0625 |

(total height : 18.75 m)

A1 =13.49
B1 = -0.319
Z1 = 0.064 kpa
C = 1.211E-4 m/year

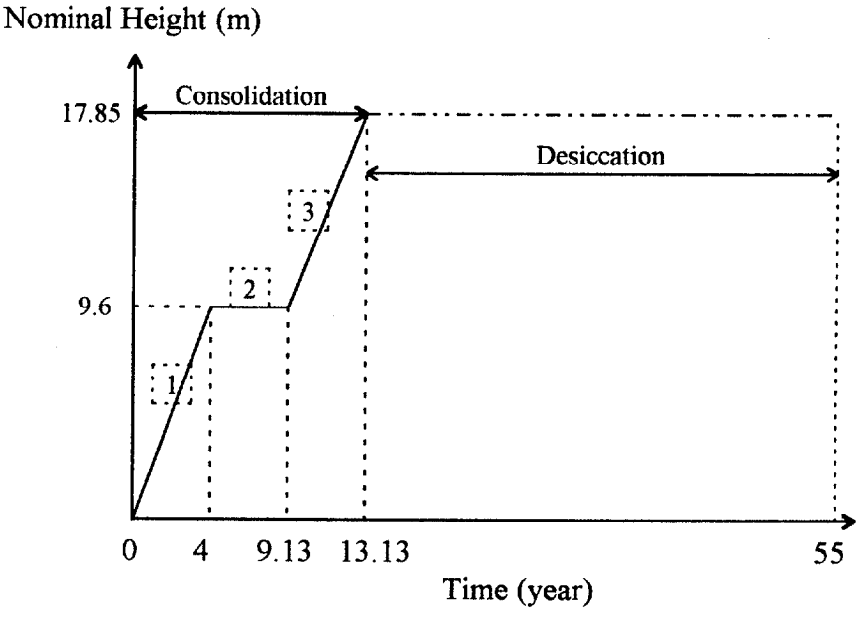


Figure EX5-1

D = 3.5

A2 =13.49
B2 = - 0.319

Gs = 2.71
Gw = 9.81 kN/$m^3$
$e_{(min)}$ = 0.5

Because two different boundary conditions required on top of soil in this analysis, the zero effective stress for stage filling and evaporation rate for desiccation, two consecutive analyses (consolidation and desiccation) should be performed separately,

Step 1: Consolidation analysis from 0.0 to 13.13 years

H0 = 0.0
T0 = 0.0
MAXDT = 0.5 year

The information requires at T=0.2, 0.5, 1, 1.5, 2.5, 4, 4.1, 4.5, 5.0, 5.5, 6, 7, 8, 9.13, 9.2, 10, 10.5, 11.5, 12.5, 13.13.

| | |
|---|---|
| Boundary Conditions: | Top - zero surcharge |
| | Bottom - impervious |
| Analysis Status: | Consolidation (No desiccation) |
| | Stage filling |
| | New analysis |

*Input and Output*

The complete input file, output files such as TS.OUT and INPUT, and part of the VD.OUT are provided in following pages. The INPUT file will be modified to the input file for desiccation analysis (Step 2).

Example 5 - **Input File** (Step 1 - Consolidation Analysis 0.0-13.13 years)

```
13.490 -.3190 .12110E-03 3.5000 .64000E-01      A,B,C,D,Z
 2                                              3-D DESSICATION STATUS
 2.7100                                         SPECIFIC GRAVITY OF SOLIDS
 9.8100                                         UNIT WEIGHT OF WATER
 .00000                                         INITIAL HEIGHT OF SOIL
 1                                              STAGE FILLING STATUS
   3                                            NUMBER OF FILLING STAGES
.00000    4.0000    2.4000          BEGINNING TIME,ENDING TIME,HEIGHTS OR RATES
4.0000    9.1300    .00000          BEGINNING TIME,ENDING TIME,HEIGHTS OR RATES
9.1300    13.130    2.0625          BEGINNING TIME,ENDING TIME,HEIGHTS OR RATES
 2                                              TOP BOUNDARY CONDITION
 .00000                                         TOP BOUNDARY CONDITION VALUES
 1                                              BOTTOM BOUNDARY CONDITION
.50000                                          MINIMUM VOID RATIO
 .00000                                         STARTING TIME
  20                                            NUMBER OF OUTPUT FILES
 .20000                                         SPECIFIED TIME FOR OUTPUT
 .50000                                         SPECIFIED TIME FOR OUTPUT
 1.0000                                         SPECIFIED TIME FOR OUTPUT
 1.5000                                         SPECIFIED TIME FOR OUTPUT
 2.5000                                         SPECIFIED TIME FOR OUTPUT
 4.0000                                         SPECIFIED TIME FOR OUTPUT
 4.1000                                         SPECIFIED TIME FOR OUTPUT
 4.5000                                         SPECIFIED TIME FOR OUTPUT
 5.0000                                         SPECIFIED TIME FOR OUTPUT
 5.5000                                         SPECIFIED TIME FOR OUTPUT
 6.0000                                         SPECIFIED TIME FOR OUTPUT
 7.0000                                         SPECIFIED TIME FOR OUTPUT
 8.0000                                         SPECIFIED TIME FOR OUTPUT
 9.1300                                         SPECIFIED TIME FOR OUTPUT
 9.2000                                         SPECIFIED TIME FOR OUTPUT
 10.000                                         SPECIFIED TIME FOR OUTPUT
 10.500                                         SPECIFIED TIME FOR OUTPUT
 11.500                                         SPECIFIED TIME FOR OUTPUT
 12.500                                         SPECIFIED TIME FOR OUTPUT
 13.130                                         SPECIFIED TIME FOR OUTPUT
 .50000                                         MAXIMUM TIME INTERVAL
 2                                              INITIAL STATUS
```

Example 5 - **TS.OUT** (Step 1 - Consolidation Analysis)

| -TIME- | SOIL -HEIGHT- | AVERAGE DRY -DENSITY- | CUMULATED OUTFLOW -TOP- | CUMULATED OUTFLOW -BOTTOM- | CRUST -THINKNESS- |
|---|---|---|---|---|---|
| .0000E+00 | .1375E-03 | .7954E+00 | .0000E+00 | .0000E+00 | .0000E+00 |
| .2000E+00 | .3985E+00 | .9565E+00 | .1561E+00 | .0000E+00 | .0000E+00 |
| .5000E+00 | .8357E+00 | .1087E+01 | .4468E+00 | .0000E+00 | .0000E+00 |
| .1000E+01 | .1663E+01 | .1144E+01 | .9544E+00 | .0000E+00 | .0000E+00 |
| .1500E+01 | .2270E+01 | .1220E+01 | .1505E+01 | .0000E+00 | .0000E+00 |
| .2500E+01 | .3541E+01 | .1294E+01 | .2611E+01 | .0000E+00 | .0000E+00 |
| .4000E+01 | .5554E+01 | .1341E+01 | .4302E+01 | .0000E+00 | .0000E+00 |
| .4100E+01 | .5461E+01 | .1363E+01 | .4409E+01 | .0000E+00 | .0000E+00 |
| .4500E+01 | .5178E+01 | .1438E+01 | .4758E+01 | .0000E+00 | .0000E+00 |
| .5000E+01 | .4921E+01 | .1513E+01 | .5067E+01 | .0000E+00 | .0000E+00 |
| .5500E+01 | .4722E+01 | .1577E+01 | .5300E+01 | .0000E+00 | .0000E+00 |
| .6000E+01 | .4560E+01 | .1633E+01 | .5499E+01 | .0000E+00 | .0000E+00 |
| .7000E+01 | .4316E+01 | .1725E+01 | .5787E+01 | .0000E+00 | .0000E+00 |
| .8000E+01 | .4140E+01 | .1799E+01 | .5994E+01 | .0000E+00 | .0000E+00 |
| .9130E+01 | .3994E+01 | .1864E+01 | .6158E+01 | .0000E+00 | .0000E+00 |
| .9200E+01 | .4149E+01 | .1834E+01 | .6196E+01 | .0000E+00 | .0000E+00 |
| .1000E+02 | .5010E+01 | .1760E+01 | .6994E+01 | .0000E+00 | .0000E+00 |
| .1050E+02 | .5673E+01 | .1713E+01 | .7525E+01 | .0000E+00 | .0000E+00 |
| .1150E+02 | .6675E+01 | .1689E+01 | .8604E+01 | .0000E+00 | .0000E+00 |
| .1250E+02 | .7953E+01 | .1645E+01 | .9697E+01 | .0000E+00 | .0000E+00 |
| .1313E+02 | .8414E+01 | .1658E+01 | .1040E+02 | .0000E+00 | .0000E+00 |

THE TOTAL HEIGHT OF SOIL SOLID IS 5.340784702856478E-001

Example 5 - **INPUT** (Step 1 - Consolidation Analysis)

```
13.490 -.3190 .12110E-03 3.5000 .64000E-01      A,B,C,D,Z
 2           3-D DESSICATION STATUS
 2.7100      SPECIFIC GRAVITY OF SOLIDS
 9.8100      UNIT WEIGHT OF WATER
 .00000      INITIAL HEIGHT OF SOIL
 1           STAGE FILLING STATUS
   3         NUMBER OF FILLING STAGES
.00000    4.0000    2.4000          BEGINNING TIME,ENDING TIME,HEIGHTS OR RATES
4.0000    9.1300    .00000          BEGINNING TIME,ENDING TIME,HEIGHTS OR RATES
9.1300    13.130    2.0625          BEGINNING TIME,ENDING TIME,HEIGHTS OR RATES
 2           TOP BOUNDARY CONDITION
 .00000      TOP BOUNDARY CONDITION VALUES
 1           BOTTOM BOUNDARY CONDITION
.50000       MINIMUM VOID RATIO
 .00000      STARTING TIME
  20         NUMBER OF OUTPUT FILES
 .20000      SPECIFIED TIME FOR OUTPUT
 .50000      SPECIFIED TIME FOR OUTPUT
 1.0000      SPECIFIED TIME FOR OUTPUT
 1.5000      SPECIFIED TIME FOR OUTPUT
 2.5000      SPECIFIED TIME FOR OUTPUT
 4.0000      SPECIFIED TIME FOR OUTPUT
 4.1000      SPECIFIED TIME FOR OUTPUT
 4.5000      SPECIFIED TIME FOR OUTPUT
 5.0000      SPECIFIED TIME FOR OUTPUT
 5.5000      SPECIFIED TIME FOR OUTPUT
 6.0000      SPECIFIED TIME FOR OUTPUT
 7.0000      SPECIFIED TIME FOR OUTPUT
 8.0000      SPECIFIED TIME FOR OUTPUT
 9.1300      SPECIFIED TIME FOR OUTPUT
 9.2000      SPECIFIED TIME FOR OUTPUT
 10.000      SPECIFIED TIME FOR OUTPUT
 10.500      SPECIFIED TIME FOR OUTPUT
 11.500      SPECIFIED TIME FOR OUTPUT
 12.500      SPECIFIED TIME FOR OUTPUT
 13.130      SPECIFIED TIME FOR OUTPUT
 .50000      MAXIMUM TIME INTERVAL
 2           INITIAL STATUS
  51         NUMBER OF NODE
       32.422054984641240        8.413762513818154
       30.412686849819320        8.237069465348100
       28.887613456126370        8.071943592369426
       27.506327687269440        7.906287927335709
       26.361306864013590        7.739629221617365
       25.426647920266860        7.572417932027064
       24.653172620972490        7.404917044796672
       23.984493754092270        7.237274827351167
       23.382143701458360        7.069549431197523
       22.822945427169800        6.901759469883452
       22.293692653224660        6.733914401153508
       21.786657726511170        6.566020719435556
       21.296999786993220        6.398083799546368
       20.821498214726420        6.230107917189084
       20.357920733952710        6.062096460676524
       19.904683321197780        5.894052100595108
       19.460659029245050        5.725976923669911
       19.025055558381230        5.557872588180830
```

Input Data

| | |
|---|---|
| 18.597334263480290 | 5.389740430456773 |
| 18.177148223201840 | 5.221581560421134 |
| 17.764298051768740 | 5.053396931091026 |
| 17.358693785850560 | 4.885187396490298 |
| 16.960326831577990 | 4.716953753311470 |
| 16.569243362455600 | 4.548696778813882 |
| 16.185525518962110 | 4.380417245070725 |
| 15.809272159325810 | 4.212115952223631 |
| 15.440585392920160 | 4.043793718008817 |
| 15.079558181428440 | 3.875451405857143 |
| 14.726263849967270 | 3.707089905815025 |
| 14.380750678860870 | 3.538710139363449 |
| 14.043034512170430 | 3.370313060250872 |
| 13.713097304281450 | 3.201899624619672 |
| 13.390886121527660 | 3.033470803854908 |
| 13.076311966643770 | 2.865027560880529 |
| 12.769254710418630 | 2.696570826435410 |
| 12.469566890680190 | 2.528101512662615 |
| 12.177072074078640 | 2.359620519124606 |
| 11.891574831450330 | 2.191128653218195 |
| 11.612868259410600 | 2.022626682166508 |
| 11.340737911927600 | 1.854115307056225 |
| 11.074969554375460 | 1.685595156684733 |
| 10.815353996044060 | 1.517066803232915 |
| 10.561691038284070 | 1.348530748507344 |
| 10.313796419920690 | 1.179987412936693 |
| 10.071504107166150 | 1.011437200558244 |
| 9.834662209566139 | 8.428804523600704E-001 |
| 9.603142099803558 | 6.743174351210859E-001 |
| 9.376839995058257 | 5.057483681999894E-001 |
| 9.155683011199777 | 3.371733393951784E-001 |
| 8.939674552729253 | 1.685918057562472E-001 |
| 8.729139331859662 | 0.000000000000000E+000 |
| 8.4138 | FINAL HEIGHT OF SOIL |
| 13.130 | STOPPING TIME |

Void Ratio Distribution at the end of current analysis and informative messages such as final height and stopping time

Example 5 - **VD.OUT** (Step 1 - Consolidation Analysis)

TIME = .0000

| | INITIAL STATE | | | | STEADY STATE | |
|---|---|---|---|---|---|---|
| | | VOID | SOLID | WATER | | VOID |
| -NODE- | -ELEVATION- | -RATIO- | -CONTENT- | -PRESSURE- | -ELEVATION- | -RATIO- |
| 51 | .1375E-03 | .3242E+02 | .7714E-01 | .0000E+00 | .5635E+01 | .3242E+02 |
| 50 | .1347E-03 | .3242E+02 | .7714E-01 | .2836E-04 | .5355E+01 | .2118E+02 |
| 49 | .1320E-03 | .3242E+02 | .7714E-01 | .5671E-04 | .5138E+01 | .1776E+02 |
| 48 | .1292E-03 | .3242E+02 | .7714E-01 | .8507E-04 | .4949E+01 | .1586E+02 |
| 47 | .1265E-03 | .3242E+02 | .7714E-01 | .1134E-03 | .4776E+01 | .1460E+02 |
| 46 | .1237E-03 | .3242E+02 | .7714E-01 | .1418E-03 | .4614E+01 | .1367E+02 |
| 45 | .1210E-03 | .3242E+02 | .7714E-01 | .1701E-03 | .4462E+01 | .1294E+02 |
| 44 | .1182E-03 | .3242E+02 | .7714E-01 | .1985E-03 | .4316E+01 | .1235E+02 |
| 43 | .1155E-03 | .3242E+02 | .7714E-01 | .2268E-03 | .4176E+01 | .1186E+02 |
| 42 | .1127E-03 | .3242E+02 | .7714E-01 | .2552E-03 | .4041E+01 | .1144E+02 |
| 41 | .1100E-03 | .3242E+02 | .7714E-01 | .2836E-03 | .3910E+01 | .1108E+02 |
| 40 | .1072E-03 | .3242E+02 | .7714E-01 | .3119E-03 | .3783E+01 | .1075E+02 |
| 39 | .1045E-03 | .3242E+02 | .7714E-01 | .3403E-03 | .3659E+01 | .1047E+02 |
| 38 | .1017E-03 | .3242E+02 | .7714E-01 | .3686E-03 | .3538E+01 | .1021E+02 |
| 37 | .9899E-04 | .3242E+02 | .7714E-01 | .3970E-03 | .3419E+01 | .9979E+01 |
| 36 | .9624E-04 | .3242E+02 | .7714E-01 | .4253E-03 | .3303E+01 | .9767E+01 |
| 35 | .9349E-04 | .3242E+02 | .7714E-01 | .4537E-03 | .3189E+01 | .9573E+01 |
| 34 | .9074E-04 | .3242E+02 | .7714E-01 | .4820E-03 | .3077E+01 | .9393E+01 |
| 33 | .8799E-04 | .3242E+02 | .7714E-01 | .5104E-03 | .2967E+01 | .9227E+01 |
| 32 | .8524E-04 | .3242E+02 | .7714E-01 | .5387E-03 | .2859E+01 | .9072E+01 |
| 31 | .8249E-04 | .3242E+02 | .7714E-01 | .5671E-03 | .2752E+01 | .8927E+01 |
| 30 | .7974E-04 | .3242E+02 | .7714E-01 | .5955E-03 | .2647E+01 | .8792E+01 |
| 29 | .7699E-04 | .3242E+02 | .7714E-01 | .6238E-03 | .2543E+01 | .8665E+01 |
| 28 | .7424E-04 | .3242E+02 | .7714E-01 | .6522E-03 | .2440E+01 | .8544E+01 |
| 27 | .7149E-04 | .3242E+02 | .7714E-01 | .6805E-03 | .2339E+01 | .8431E+01 |
| 26 | .6874E-04 | .3242E+02 | .7714E-01 | .7089E-03 | .2239E+01 | .8323E+01 |
| 25 | .6599E-04 | .3242E+02 | .7714E-01 | .7372E-03 | .2140E+01 | .8221E+01 |
| 24 | .6324E-04 | .3242E+02 | .7714E-01 | .7656E-03 | .2042E+01 | .8124E+01 |
| 23 | .6049E-04 | .3242E+02 | .7714E-01 | .7939E-03 | .1945E+01 | .8032E+01 |
| 22 | .5774E-04 | .3242E+02 | .7714E-01 | .8223E-03 | .1849E+01 | .7943E+01 |
| 21 | .5500E-04 | .3242E+02 | .7714E-01 | .8507E-03 | .1754E+01 | .7859E+01 |
| 20 | .5225E-04 | .3242E+02 | .7714E-01 | .8790E-03 | .1659E+01 | .7778E+01 |
| 19 | .4950E-04 | .3242E+02 | .7714E-01 | .9074E-03 | .1566E+01 | .7701E+01 |
| 18 | .4675E-04 | .3242E+02 | .7714E-01 | .9357E-03 | .1473E+01 | .7626E+01 |
| 17 | .4400E-04 | .3242E+02 | .7714E-01 | .9641E-03 | .1382E+01 | .7555E+01 |
| 16 | .4125E-04 | .3242E+02 | .7714E-01 | .9924E-03 | .1291E+01 | .7486E+01 |
| 15 | .3850E-04 | .3242E+02 | .7714E-01 | .1021E-02 | .1200E+01 | .7420E+01 |
| 14 | .3575E-04 | .3242E+02 | .7714E-01 | .1049E-02 | .1111E+01 | .7356E+01 |
| 13 | .3300E-04 | .3242E+02 | .7714E-01 | .1077E-02 | .1022E+01 | .7294E+01 |
| 12 | .3025E-04 | .3242E+02 | .7714E-01 | .1106E-02 | .9336E+00 | .7234E+01 |
| 11 | .2750E-04 | .3242E+02 | .7714E-01 | .1134E-02 | .8460E+00 | .7177E+01 |
| 10 | .2475E-04 | .3242E+02 | .7714E-01 | .1163E-02 | .7589E+00 | .7121E+01 |
| 9 | .2200E-04 | .3242E+02 | .7714E-01 | .1191E-02 | .6725E+00 | .7067E+01 |
| 8 | .1925E-04 | .3242E+02 | .7714E-01 | .1219E-02 | .5866E+00 | .7014E+01 |
| 7 | .1650E-04 | .3242E+02 | .7714E-01 | .1248E-02 | .5013E+00 | .6964E+01 |
| 6 | .1375E-04 | .3242E+02 | .7714E-01 | .1276E-02 | .4165E+00 | .6914E+01 |
| 5 | .1100E-04 | .3242E+02 | .7714E-01 | .1304E-02 | .3322E+00 | .6866E+01 |
| 4 | .8249E-05 | .3242E+02 | .7714E-01 | .1333E-02 | .2484E+00 | .6820E+01 |
| 3 | .5500E-05 | .3242E+02 | .7714E-01 | .1361E-02 | .1651E+00 | .6774E+01 |
| 2 | .2750E-05 | .3242E+02 | .7714E-01 | .1389E-02 | .8234E-01 | .6730E+01 |
| 1 | .0000E+00 | .3242E+02 | .7714E-01 | .1418E-02 | .0000E+00 | .6687E+01 |

TIME = .2000

| -NODE- | -ELEVATION- | VOID -RATIO- | SOLID -CONTENT- | WATER -PRESSURE- | ALPHA -VALUES- |
|---|---|---|---|---|---|
| 51 | .3985E+00 | .3242E+02 | .7714E-01 | .0000E+00 | .1000E+01 |
| 50 | .3904E+00 | .3234E+02 | .7731E-01 | .8272E-01 | .1000E+01 |
| 49 | .3824E+00 | .3226E+02 | .7748E-01 | .1645E+00 | .1000E+01 |
| 48 | .3745E+00 | .3218E+02 | .7767E-01 | .2462E+00 | .1000E+01 |
| 47 | .3665E+00 | .3209E+02 | .7787E-01 | .3278E+00 | .1000E+01 |
| 46 | .3585E+00 | .3199E+02 | .7809E-01 | .4093E+00 | .1000E+01 |
| 45 | .3506E+00 | .3188E+02 | .7834E-01 | .4907E+00 | .1000E+01 |
| 44 | .3426E+00 | .3176E+02 | .7862E-01 | .5719E+00 | .1000E+01 |
| 43 | .3347E+00 | .3162E+02 | .7894E-01 | .6530E+00 | .1000E+01 |
| 42 | .3267E+00 | .3146E+02 | .7930E-01 | .7340E+00 | .1000E+01 |
| 41 | .3188E+00 | .3129E+02 | .7971E-01 | .8148E+00 | .1000E+01 |
| 40 | .3108E+00 | .3110E+02 | .8015E-01 | .8955E+00 | .1000E+01 |
| 39 | .3029E+00 | .3089E+02 | .8065E-01 | .9761E+00 | .1000E+01 |
| 38 | .2949E+00 | .3067E+02 | .8118E-01 | .1056E+01 | .1000E+01 |
| 37 | .2870E+00 | .3044E+02 | .8176E-01 | .1137E+01 | .1000E+01 |
| 36 | .2791E+00 | .3019E+02 | .8238E-01 | .1217E+01 | .1000E+01 |
| 35 | .2711E+00 | .2993E+02 | .8304E-01 | .1297E+01 | .1000E+01 |
| 34 | .2632E+00 | .2966E+02 | .8373E-01 | .1377E+01 | .1000E+01 |
| 33 | .2552E+00 | .2938E+02 | .8445E-01 | .1457E+01 | .1000E+01 |
| 32 | .2473E+00 | .2910E+02 | .8520E-01 | .1537E+01 | .1000E+01 |
| 31 | .2393E+00 | .2881E+02 | .8598E-01 | .1616E+01 | .1000E+01 |
| 30 | .2313E+00 | .2852E+02 | .8679E-01 | .1696E+01 | .1000E+01 |
| 29 | .2234E+00 | .2822E+02 | .8761E-01 | .1775E+01 | .1000E+01 |
| 28 | .2154E+00 | .2793E+02 | .8845E-01 | .1855E+01 | .1000E+01 |
| 27 | .2075E+00 | .2763E+02 | .8931E-01 | .1934E+01 | .1000E+01 |
| 26 | .1995E+00 | .2734E+02 | .9019E-01 | .2013E+01 | .1000E+01 |
| 25 | .1915E+00 | .2705E+02 | .9107E-01 | .2092E+01 | .1000E+01 |
| 24 | .1836E+00 | .2676E+02 | .9197E-01 | .2171E+01 | .1000E+01 |
| 23 | .1756E+00 | .2647E+02 | .9288E-01 | .2250E+01 | .1000E+01 |
| 22 | .1676E+00 | .2618E+02 | .9379E-01 | .2329E+01 | .1000E+01 |
| 21 | .1596E+00 | .2590E+02 | .9471E-01 | .2408E+01 | .1000E+01 |
| 20 | .1517E+00 | .2563E+02 | .9564E-01 | .2487E+01 | .1000E+01 |
| 19 | .1437E+00 | .2535E+02 | .9657E-01 | .2566E+01 | .1000E+01 |
| 18 | .1357E+00 | .2509E+02 | .9750E-01 | .2644E+01 | .1000E+01 |
| 17 | .1277E+00 | .2482E+02 | .9843E-01 | .2723E+01 | .1000E+01 |
| 16 | .1198E+00 | .2457E+02 | .9936E-01 | .2802E+01 | .1000E+01 |
| 15 | .1118E+00 | .2431E+02 | .1003E+00 | .2880E+01 | .1000E+01 |
| 14 | .1038E+00 | .2407E+02 | .1012E+00 | .2959E+01 | .1000E+01 |
| 13 | .9582E-01 | .2382E+02 | .1021E+00 | .3037E+01 | .1000E+01 |
| 12 | .8783E-01 | .2359E+02 | .1031E+00 | .3115E+01 | .1000E+01 |
| 11 | .7985E-01 | .2335E+02 | .1040E+00 | .3194E+01 | .1000E+01 |
| 10 | .7187E-01 | .2313E+02 | .1049E+00 | .3272E+01 | .1000E+01 |
| 9 | .6389E-01 | .2291E+02 | .1058E+00 | .3350E+01 | .1000E+01 |
| 8 | .5590E-01 | .2269E+02 | .1067E+00 | .3428E+01 | .1000E+01 |
| 7 | .4792E-01 | .2248E+02 | .1076E+00 | .3507E+01 | .1000E+01 |
| 6 | .3993E-01 | .2228E+02 | .1085E+00 | .3585E+01 | .1000E+01 |
| 5 | .3195E-01 | .2208E+02 | .1093E+00 | .3663E+01 | .1000E+01 |
| 4 | .2396E-01 | .2188E+02 | .1102E+00 | .3741E+01 | .1000E+01 |
| 3 | .1598E-01 | .2170E+02 | .1110E+00 | .3820E+01 | .1000E+01 |
| 2 | .7988E-02 | .2152E+02 | .1119E+00 | .3898E+01 | .1000E+01 |
| 1 | .0000E+00 | .2123E+02 | .1132E+00 | .3972E+01 | .1000E+01 |

**Step 2:** Desiccation analysis from 13.13 to 50 years

HO = 8.4138 m
TO = 13.13 year
CV = 0.7 (Crust Void Ratio)
$\eta$ = 1.1 (Crack Side-Wall Loss Parameter)
Cracking Function Parameters (Fig. EX5-2): a = 0.0002
b = 0.001
c = 0.29
d = 0.3
MAXDT = 0.01 year (approximately 3.5 days, *see CONDES0 Input Instruction)*

The information requires at T = 13.4, 13.8, 14, 14.5, 15, 15.5, 16, 16.5, 17, 17.5, 18, 18.5, 19, 19.5, 20, 21, 23, 26, 30, 40.

Boundary Conditions: Top - evaporation rate (1.05 m/year)
Bottom - impervious
Analysis Status: Desiccation
No stage filling
Continuous analysis (void ratio distribution is needed at the end of input file)

The input file for Step 2 can be generated from INPUT obtained from Step 1. The INPUT from Step 1 contains the void ratio distribution at year 13.13, which is required for desiccation analysis.

*Input and Output*

The complete input file, output files such as TS.OUT, TC.OUT and INPUT, and part of the VD.OUT are provided in following pages. The time-settlement curve (Fig. EX5-3), solid content curve for desiccation, (Fig. EX5-4), time-crack depth curve (Fig. EX5-5), and time-crack volume curve (Fig. EX5-6) are also plotted.

Example 5 - **Input File** (Step 2 - Desiccation Analysis 13.13 - 50 years)

```
13.490 -.3190 .12110E-03 3.5000 .64000E-01      A1,B1,C,D,Z1
 1                                              3-D DESSICATION STATUS
 13.49 -0.319                                   A2,B2: 3-D SHRINKAGE PARAMETERS
 0.0002 0.001 0.29 0.3                          CRACKING FUNCTION PARAMETERS, a,b,c,d
 1.1                                            CRACK-WALL LOSS PARAMETER
 0.7                                            CRUST VOID RATIO
 2.7100                                         SPECIFIC GRAVITY OF SOLIDS
 9.8100                                         UNIT WEIGHT OF WATER
 8.4138                                         INITIAL HEIGHT OF SOIL
 2                                              STAGE FILLING STATUS
 1                                              TOP BOUNDARY CONDITION
 1.0500                                         TOP BOUNDARY CONDITION VALUES
 1                                              BOTTOM BOUNDARY CONDITION
.50000                                          MINIMUM VOID RATIO
 13.130                                         STARTING TIME
  20                                            NUMBER OF OUTPUT FILES
 13.400                                         SPECIFIED TIME FOR OUTPUT
 13.800                                         SPECIFIED TIME FOR OUTPUT
 14.000                                         SPECIFIED TIME FOR OUTPUT
 14.500                                         SPECIFIED TIME FOR OUTPUT
 15.000                                         SPECIFIED TIME FOR OUTPUT
 15.500                                         SPECIFIED TIME FOR OUTPUT
 16.000                                         SPECIFIED TIME FOR OUTPUT
 16.500                                         SPECIFIED TIME FOR OUTPUT
 17.000                                         SPECIFIED TIME FOR OUTPUT
 17.500                                         SPECIFIED TIME FOR OUTPUT
 18.000                                         SPECIFIED TIME FOR OUTPUT
 18.500                                         SPECIFIED TIME FOR OUTPUT
 19.000                                         SPECIFIED TIME FOR OUTPUT
 19.500                                         SPECIFIED TIME FOR OUTPUT
 20.000                                         SPECIFIED TIME FOR OUTPUT
 21.000                                         SPECIFIED TIME FOR OUTPUT
 23.000                                         SPECIFIED TIME FOR OUTPUT
 26.000                                         SPECIFIED TIME FOR OUTPUT
 30.000                                         SPECIFIED TIME FOR OUTPUT
 40.000                                         SPECIFIED TIME FOR OUTPUT
 .01000                                         MAXIMUM TIME INTERVAL
 1                                              INITIAL STATUS
  51                                            NUMBER OF NODE
       32.422054984641240        8.413762513818154
       30.412686849819320        8.237069465348100
       28.887613456126370        8.071943592369426
       27.506327687269440        7.906287927335709
       26.361306864013590        7.739629221617365
       25.426647920266860        7.572417932027064
       24.653172620972490        7.404917044796672
       23.984493754092270        7.237274827351167
       23.382143701458360        7.069549431197523
       22.822945427169800        6.901759469883452
       22.293692653224660        6.733914401153508
       21.786657726511170        6.566020719435556
       21.296999786993220        6.398083799546368
       20.821498214726420        6.230107917189084
       20.357920733952710        6.062096460676524
       19.904683321197780        5.894052100595108
       19.460659029245050        5.725976923669911
       19.025055558381230        5.557872588180830
```

| | |
|---|---|
| 18.597334263480290 | 5.389740430456773 |
| 18.177148223201840 | 5.221581560421134 |
| 17.764298051768740 | 5.053396931091026 |
| 17.358693785850560 | 4.885187396490298 |
| 16.960326831577990 | 4.716953753311470 |
| 16.569243362455600 | 4.548696778813882 |
| 16.185525518962110 | 4.380417245070725 |
| 15.809272159325810 | 4.212115952223631 |
| 15.440585392920160 | 4.043793718008817 |
| 15.079558181428440 | 3.875451405857143 |
| 14.726263849967270 | 3.707089905815025 |
| 14.380750678860870 | 3.538710139363449 |
| 14.043034512170430 | 3.370313060250872 |
| 13.713097304281450 | 3.201899624619672 |
| 13.390886121527660 | 3.033470803854908 |
| 13.076311966643770 | 2.865027560880529 |
| 12.769254710418630 | 2.696570826435410 |
| 12.469566890680190 | 2.528101512662615 |
| 12.177072074078640 | 2.359620519124606 |
| 11.891574831450330 | 2.191128653218195 |
| 11.612868259410600 | 2.022626682166508 |
| 11.340737911927600 | 1.854115307056225 |
| 11.074969554375460 | 1.685595156684733 |
| 10.815353996044060 | 1.517066803232915 |
| 10.561691038284070 | 1.348530748507344 |
| 10.313796419920690 | 1.179987412936693 |
| 10.071504107166150 | 1.011437200558244 |
| 9.834662209566139 | 8.428804523600704E-001 |
| 9.603142099803558 | 6.743174351210859E-001 |
| 9.376839995058257 | 5.057483681999894E-001 |
| 9.155683011199777 | 3.371733393951784E-001 |
| 8.939674552729253 | 1.685918057562472E-001 |
| 8.729139331859662 | 0.000000000000000E+000 |

VOID RATIO DISTRIBUTION
AT THE END OF
CONSOLIDATION ANALYSIS
(13.13 YEAR)

Example 5 - **TS.OUT** (Step 2 - Desiccation Analysis)

| -TIME- | SOIL -HEIGHT- | AVERAGE DRY -DENSITY- | CUMULATED OUTFLOW -TOP- | CUMULATED OUTFLOW -BOTTOM- | CRUST -THINKNESS- |
|---|---|---|---|---|---|
| .1313E+02 | .8414E+01 | .1658E+01 | .0000E+00 | .0000E+00 | .0000E+00 |
| .1340E+02 | .8127E+01 | .1716E+01 | .0000E+00 | .0000E+00 | .0000E+00 |
| .1380E+02 | .7715E+01 | .1810E+01 | .0000E+00 | .0000E+00 | .0000E+00 |
| .1400E+02 | .7515E+01 | .1862E+01 | .0000E+00 | .0000E+00 | .0000E+00 |
| .1450E+02 | .7046E+01 | .2022E+01 | .0000E+00 | .0000E+00 | .0000E+00 |
| .1500E+02 | .6615E+01 | .2244E+01 | .0000E+00 | .0000E+00 | .0000E+00 |
| .1550E+02 | .6214E+01 | .2569E+01 | .0000E+00 | .0000E+00 | .0000E+00 |
| .1573E+02 | .6037E+01 | .2768E+01 | .0000E+00 | .0000E+00 | .0000E+00 |

Example 5 - **TC.OUT** (Step 2 - Desiccation Analysis)

| -TIME- | CRACK -DEPTH- | SOIL -HEIGHT- | TOTAL -VOLUME- | CRACK -VOLUME- | FLUID -VOLUME- | SIDE-WALL -LOSS- | SIMULATED -RATE- |
|---|---|---|---|---|---|---|---|
| 13.5742 | .0077 | 7.9431 | 7.9428 | .0002 | .4710 | .0065 | 1.0290627 |
| 13.6442 | .0148 | 7.8733 | 7.8725 | .0009 | .5413 | .0097 | 1.0084178 |
| 13.6742 | .0217 | 7.8429 | 7.8415 | .0014 | .5723 | .0132 | 1.0147914 |
| 13.7142 | .0282 | 7.8024 | 7.8000 | .0023 | .6138 | .0193 | 1.0207648 |
| 13.7442 | .0345 | 7.7719 | 7.7687 | .0032 | .6451 | .0251 | 1.0245399 |
| 13.7742 | .0407 | 7.7415 | 7.7373 | .0042 | .6765 | .0317 | 1.0276110 |
| 13.7942 | .0469 | 7.7212 | 7.7162 | .0050 | .6976 | .0368 | 1.0300288 |
| 13.8000 | .0468 | 7.7153 | 7.7101 | .0052 | .7037 | .0383 | 1.0502870 |
| 13.8200 | .0529 | 7.6951 | 7.6890 | .0061 | .7248 | .0438 | 1.0326235 |
| 13.8500 | .0586 | 7.6649 | 7.6574 | .0074 | .7564 | .0525 | 1.0346269 |
| 13.8700 | .0645 | 7.6448 | 7.6363 | .0084 | .7775 | .0588 | 1.0359614 |
| 13.8900 | .0703 | 7.6247 | 7.6152 | .0095 | .7986 | .0654 | 1.0372918 |
| 13.9100 | .0760 | 7.6046 | 7.5940 | .0106 | .8198 | .0724 | 1.0385641 |
| 13.9300 | .0817 | 7.5846 | 7.5728 | .0118 | .8410 | .0796 | 1.0397436 |
| 13.9500 | .0873 | 7.5647 | 7.5516 | .0131 | .8622 | .0872 | 1.0408118 |
| 13.9800 | .0925 | 7.5350 | 7.5200 | .0150 | .8938 | .0988 | 1.0416260 |
| 14.0000 | .0980 | 7.5154 | 7.4990 | .0164 | .9148 | .1068 | 1.0420349 |
| 14.0000 | .0980 | 7.5154 | 7.4990 | .0164 | .9148 | .1068 | 1.0514755 |
| 14.0200 | .1034 | 7.4958 | 7.4780 | .0178 | .9358 | .1151 | 1.0423816 |
| 14.0400 | .1088 | 7.4763 | 7.4570 | .0192 | .9568 | .1236 | 1.0426608 |
| 14.0600 | .1141 | 7.4569 | 7.4361 | .0208 | .9777 | .1324 | 1.0428683 |
| 14.0800 | .1194 | 7.4375 | 7.4152 | .0223 | .9986 | .1413 | 1.0430028 |
| 14.0900 | .1250 | 7.4278 | 7.4046 | .0232 | 1.0092 | .1460 | 1.0432822 |
| 14.1100 | .1302 | 7.4084 | 7.3835 | .0249 | 1.0303 | .1554 | 1.0435820 |
| 14.1300 | .1354 | 7.3892 | 7.3626 | .0266 | 1.0512 | .1650 | 1.0437748 |
| 14.1500 | .1406 | 7.3700 | 7.3416 | .0284 | 1.0722 | .1748 | 1.0438685 |
| 14.1700 | .1457 | 7.3509 | 7.3208 | .0302 | 1.0930 | .1847 | 1.0438718 |
| 14.1900 | .1508 | 7.3320 | 7.2999 | .0320 | 1.1139 | .1948 | 1.0437925 |
| 14.2000 | .1563 | 7.3224 | 7.2894 | .0330 | 1.1244 | .2000 | 1.0439048 |
| 14.2200 | .1614 | 7.3035 | 7.2685 | .0350 | 1.1453 | .2105 | 1.0439245 |
| 14.2400 | .1664 | 7.2846 | 7.2477 | .0369 | 1.1661 | .2211 | 1.0438525 |
| 14.2600 | .1714 | 7.2659 | 7.2269 | .0389 | 1.1869 | .2319 | 1.0436968 |
| 14.2800 | .1764 | 7.2472 | 7.2062 | .0410 | 1.2076 | .2427 | 1.0434657 |
| 14.2900 | .1819 | 7.2378 | 7.1958 | .0421 | 1.2180 | .2483 | 1.0434741 |
| 14.3100 | .1868 | 7.2192 | 7.1750 | .0442 | 1.2388 | .2596 | 1.0433190 |
| 14.3300 | .1917 | 7.2007 | 7.1543 | .0464 | 1.2595 | .2709 | 1.0430852 |
| 14.3500 | .1966 | 7.1823 | 7.1337 | .0485 | 1.2801 | .2823 | 1.0427799 |
| 14.3600 | .2021 | 7.1730 | 7.1233 | .0497 | 1.2905 | .2882 | 1.0427345 |
| 14.3800 | .2069 | 7.1546 | 7.1027 | .0520 | 1.3111 | .2999 | 1.0424906 |
| 14.4000 | .2118 | 7.1364 | 7.0821 | .0543 | 1.3317 | .3118 | 1.0421752 |
| 14.4200 | .2166 | 7.1182 | 7.0616 | .0566 | 1.3522 | .3237 | 1.0417950 |
| 14.4300 | .2220 | 7.1090 | 7.0512 | .0578 | 1.3626 | .3298 | 1.0417002 |
| 14.4500 | .2268 | 7.0909 | 7.0307 | .0602 | 1.3831 | .3420 | 1.0413739 |
| 14.4700 | .2316 | 7.0729 | 7.0102 | .0626 | 1.4036 | .3543 | 1.0409839 |
| 14.4900 | .2364 | 7.0549 | 6.9898 | .0651 | 1.4240 | .3667 | 1.0405360 |
| 14.5000 | .2418 | 7.0459 | 6.9795 | .0664 | 1.4343 | .3730 | 1.0403979 |
| 14.5000 | .2418 | 7.0459 | 6.9795 | .0664 | 1.4343 | .3730 | 1.0469118 |
| 14.5200 | .2465 | 7.0280 | 6.9591 | .0689 | 1.4547 | .3856 | 1.0399991 |
| 14.5400 | .2513 | 7.0102 | 6.9387 | .0714 | 1.4751 | .3983 | 1.0395432 |
| 14.5500 | .2566 | 7.0013 | 6.9285 | .0728 | 1.4853 | .4048 | 1.0393942 |
| 14.5700 | .2613 | 6.9835 | 6.9081 | .0754 | 1.5057 | .4177 | 1.0389803 |
| 14.5900 | .2660 | 6.9658 | 6.8878 | .0780 | 1.5260 | .4307 | 1.0385115 |
| 14.6000 | .2714 | 6.9570 | 6.8776 | .0794 | 1.5362 | .4374 | 1.0383504 |
| 14.6200 | .2760 | 6.9394 | 6.8573 | .0821 | 1.5565 | .4506 | 1.0379190 |
| 14.6400 | .2807 | 6.9218 | 6.8371 | .0848 | 1.5767 | .4638 | 1.0374351 |

| | | | | | | | |
|---|---|---|---|---|---|---|---|
| 14.6500 | .2860 | 6.9131 | 6.8269 | .0862 | 1.5869 | .4706 | 1.0372617 |
| 14.6700 | .2906 | 6.8956 | 6.8066 | .0890 | 1.6072 | .4840 | 1.0368118 |
| 14.6900 | .2953 | 6.8782 | 6.7865 | .0918 | 1.6273 | .4976 | 1.0363118 |
| 14.7000 | .3006 | 6.8695 | 6.7763 | .0932 | 1.6375 | .5044 | 1.0361263 |
| 14.7200 | .3052 | 6.8522 | 6.7561 | .0961 | 1.6577 | .5181 | 1.0356577 |
| 14.7400 | .3097 | 6.8349 | 6.7360 | .0989 | 1.6778 | .5319 | 1.0351417 |
| 14.7500 | .3150 | 6.8263 | 6.7259 | .1004 | 1.6879 | .5389 | 1.0349444 |
| 14.7700 | .3196 | 6.8091 | 6.7058 | .1033 | 1.7080 | .5528 | 1.0344580 |
| 14.7900 | .3242 | 6.7920 | 6.6857 | .1063 | 1.7281 | .5668 | 1.0339266 |
| 14.8000 | .3294 | 6.7835 | 6.6757 | .1078 | 1.7381 | .5739 | 1.0337185 |
| 14.8200 | .3340 | 6.7664 | 6.6556 | .1108 | 1.7582 | .5880 | 1.0332153 |
| 14.8300 | .3392 | 6.7579 | 6.6455 | .1123 | 1.7683 | .5952 | 1.0330182 |
| 14.8500 | .3437 | 6.7409 | 6.6255 | .1154 | 1.7883 | .6095 | 1.0325377 |
| 14.8700 | .3483 | 6.7240 | 6.6055 | .1185 | 1.8083 | .6238 | 1.0320136 |
| 14.8800 | .3535 | 6.7155 | 6.5955 | .1200 | 1.8183 | .6310 | 1.0318039 |
| 14.9000 | .3580 | 6.6987 | 6.5755 | .1231 | 1.8383 | .6455 | 1.0313032 |
| 14.9200 | .3625 | 6.6819 | 6.5556 | .1263 | 1.8582 | .6600 | 1.0307618 |
| 14.9300 | .3677 | 6.6735 | 6.5456 | .1279 | 1.8682 | .6674 | 1.0305412 |
| 14.9500 | .3722 | 6.6568 | 6.5257 | .1311 | 1.8881 | .6820 | 1.0300229 |
| 14.9600 | .3774 | 6.6484 | 6.5157 | .1327 | 1.8981 | .6894 | 1.0298113 |
| 14.9800 | .3819 | 6.6318 | 6.4958 | .1359 | 1.9180 | .7042 | 1.0293119 |
| 15.0000 | .3863 | 6.6152 | 6.4760 | .1392 | 1.9378 | .7190 | 1.0287737 |
| 15.0000 | .3863 | 6.6152 | 6.4760 | .1392 | 1.9378 | .7190 | 1.0362450 |
| 15.0100 | .3915 | 6.6069 | 6.4661 | .1408 | 1.9477 | .7265 | 1.0285507 |
| 15.0300 | .3959 | 6.5903 | 6.4462 | .1441 | 1.9676 | .7414 | 1.0280326 |
| 15.0400 | .4012 | 6.5821 | 6.4363 | .1458 | 1.9775 | .7489 | 1.0278175 |
| 15.0600 | .4056 | 6.5656 | 6.4165 | .1491 | 1.9973 | .7640 | 1.0273159 |
| 15.0800 | .4100 | 6.5492 | 6.3967 | .1525 | 2.0171 | .7790 | 1.0267776 |
| 15.0900 | .4152 | 6.5410 | 6.3868 | .1542 | 2.0270 | .7866 | 1.0265513 |
| 15.1100 | .4195 | 6.5247 | 6.3671 | .1576 | 2.0467 | .8018 | 1.0260312 |
| 15.1200 | .4248 | 6.5165 | 6.3572 | .1593 | 2.0566 | .8094 | 1.0258121 |
| 15.1400 | .4291 | 6.5002 | 6.3375 | .1627 | 2.0763 | .8247 | 1.0253071 |
| 15.1500 | .4343 | 6.4920 | 6.3275 | .1645 | 2.0863 | .8324 | 1.0250940 |
| 15.1700 | .4387 | 6.4758 | 6.3078 | .1680 | 2.1060 | .8478 | 1.0246019 |
| 15.1900 | .4430 | 6.4596 | 6.2882 | .1714 | 2.1256 | .8632 | 1.0240752 |
| 15.2000 | .4482 | 6.4515 | 6.2783 | .1732 | 2.1355 | .8710 | 1.0238507 |
| 15.2200 | .4525 | 6.4354 | 6.2587 | .1767 | 2.1551 | .8864 | 1.0233393 |
| 15.2300 | .4577 | 6.4274 | 6.2488 | .1785 | 2.1650 | .8943 | 1.0231208 |
| 15.2500 | .4621 | 6.4113 | 6.2292 | .1821 | 2.1846 | .9098 | 1.0226220 |
| 15.2600 | .4673 | 6.4033 | 6.2193 | .1839 | 2.1945 | .9177 | 1.0224086 |
| 15.2800 | .4716 | 6.3872 | 6.1997 | .1875 | 2.2141 | .9333 | 1.0219209 |
| 15.3000 | .4759 | 6.3713 | 6.1802 | .1911 | 2.2336 | .9490 | 1.0214009 |
| 15.3100 | .4810 | 6.3633 | 6.1704 | .1930 | 2.2434 | .9569 | 1.0211766 |
| 15.3300 | .4853 | 6.3475 | 6.1508 | .1966 | 2.2630 | .9726 | 1.0206701 |
| 15.3400 | .4905 | 6.3395 | 6.1410 | .1985 | 2.2728 | .9806 | 1.0204510 |
| 15.3600 | .4948 | 6.3237 | 6.1215 | .2022 | 2.2923 | .9964 | 1.0199557 |
| 15.3700 | .5000 | 6.3157 | 6.1117 | .2041 | 2.3021 | 1.0044 | 1.0197412 |
| 15.3900 | .5043 | 6.3000 | 6.0922 | .2078 | 2.3216 | 1.0203 | 1.0192557 |
| 15.4000 | .5094 | 6.2921 | 6.0824 | .2097 | 2.3314 | 1.0283 | 1.0190452 |
| 15.4200 | .5137 | 6.2763 | 6.0629 | .2134 | 2.3509 | 1.0443 | 1.0185687 |
| 15.4300 | .5189 | 6.2684 | 6.0531 | .2154 | 2.3607 | 1.0523 | 1.0183618 |
| 15.4500 | .5231 | 6.2528 | 6.0336 | .2192 | 2.3802 | 1.0684 | 1.0178933 |
| 15.4600 | .5283 | 6.2449 | 6.0238 | .2211 | 2.3900 | 1.0765 | 1.0176897 |
| 15.4800 | .5325 | 6.2293 | 6.0043 | .2249 | 2.4095 | 1.0926 | 1.0172286 |
| 15.5000 | .5368 | 6.2137 | 5.9849 | .2288 | 2.4289 | 1.1087 | 1.0167381 |
| 15.5000 | .5368 | 6.2137 | 5.9849 | .2288 | 2.4289 | 1.1087 | 1.0248382 |
| 15.5100 | .5419 | 6.2059 | 5.9752 | .2307 | 2.4386 | 1.1168 | 1.0165235 |
| 15.5300 | .5462 | 6.1904 | 5.9558 | .2346 | 2.4580 | 1.1329 | 1.0160432 |
| 15.5400 | .5514 | 6.1826 | 5.9461 | .2366 | 2.4677 | 1.1411 | 1.0158325 |
| 15.5600 | .5556 | 6.1672 | 5.9267 | .2405 | 2.4871 | 1.1573 | 1.0153605 |

| | | | | | | | |
|---|---|---|---|---|---|---|---|
| 15.5700 | .5608 | 6.1594 | 5.9169 | .2425 | 2.4969 | 1.1654 | 1.0151532 |
| 15.5900 | .5650 | 6.1440 | 5.8976 | .2464 | 2.5162 | 1.1817 | 1.0146887 |
| 15.6000 | .5701 | 6.1363 | 5.8878 | .2484 | 2.5260 | 1.1899 | 1.0144844 |
| 15.6200 | .5743 | 6.1209 | 5.8685 | .2524 | 2.5453 | 1.2062 | 1.0140267 |
| 15.6300 | .5795 | 6.1132 | 5.8588 | .2544 | 2.5550 | 1.2145 | 1.0138253 |
| 15.6500 | .5837 | 6.0979 | 5.8394 | .2584 | 2.5744 | 1.2308 | 1.0133739 |
| 15.6600 | .5889 | 6.0902 | 5.8297 | .2605 | 2.5841 | 1.2391 | 1.0131751 |
| 15.6800 | .5931 | 6.0749 | 5.8104 | .2645 | 2.6034 | 1.2555 | 1.0127296 |
| 15.6900 | .5983 | 6.0673 | 5.8007 | .2666 | 2.6131 | 1.2638 | 1.0125331 |
| 15.7100 | .6025 | 6.0520 | 5.7814 | .2707 | 2.6324 | 1.2803 | 1.0120930 |
| 15.7200 | .6076 | 6.0444 | 5.7717 | .2727 | 2.6421 | 1.2886 | 1.0118988 |

Example 5 - **VD.OUT** (Step 2 - Desiccation Analysis)

TIME = 13.13

| | INITIAL STATE | | | | STEADY STATE | |
|---|---|---|---|---|---|---|
| -NODE- | -ELEVATION- | VOID -RATIO- | SOLID -CONTENT- | WATER -PRESSURE- | -ELEVATION- | VOID -RATIO- |
| 51 | .8414E+01 | .3242E+02 | .7714E-01 | .0000E+00 | .1000E-19 | .3242E+02 |
| 50 | .8245E+01 | .3051E+02 | .8158E-01 | .0000E+00 | .1000E-19 | .3242E+02 |
| 49 | .8077E+01 | .2894E+02 | .8563E-01 | .0000E+00 | .1000E-19 | .3242E+02 |
| 48 | .7909E+01 | .2753E+02 | .8962E-01 | .0000E+00 | .1000E-19 | .3242E+02 |
| 47 | .7741E+01 | .2637E+02 | .9320E-01 | .0000E+00 | .1000E-19 | .3242E+02 |
| 46 | .7572E+01 | .2543E+02 | .9632E-01 | .0000E+00 | .1000E-19 | .3242E+02 |
| 45 | .7404E+01 | .2465E+02 | .9905E-01 | .0000E+00 | .1000E-19 | .3242E+02 |
| 44 | .7236E+01 | .2398E+02 | .1015E+00 | .0000E+00 | .1000E-19 | .3242E+02 |
| 43 | .7068E+01 | .2338E+02 | .1039E+00 | .0000E+00 | .1000E-19 | .3242E+02 |
| 42 | .6899E+01 | .2282E+02 | .1062E+00 | .0000E+00 | .1000E-19 | .3242E+02 |
| 41 | .6731E+01 | .2228E+02 | .1084E+00 | .0000E+00 | .1000E-19 | .3242E+02 |
| 40 | .6563E+01 | .2178E+02 | .1107E+00 | .0000E+00 | .1000E-19 | .3242E+02 |
| 39 | .6394E+01 | .2129E+02 | .1129E+00 | .0000E+00 | .1000E-19 | .3242E+02 |
| 38 | .6226E+01 | .2081E+02 | .1152E+00 | .0000E+00 | .1000E-19 | .3242E+02 |
| 37 | .6058E+01 | .2035E+02 | .1175E+00 | .0000E+00 | .1000E-19 | .3242E+02 |
| 36 | .5890E+01 | .1989E+02 | .1199E+00 | .0000E+00 | .1000E-19 | .3242E+02 |
| 35 | .5721E+01 | .1945E+02 | .1223E+00 | .0000E+00 | .1000E-19 | .3242E+02 |
| 34 | .5553E+01 | .1901E+02 | .1248E+00 | .0000E+00 | .1000E-19 | .3242E+02 |
| 33 | .5385E+01 | .1859E+02 | .1273E+00 | .0000E+00 | .1000E-19 | .3242E+02 |
| 32 | .5217E+01 | .1816E+02 | .1298E+00 | .0000E+00 | .1000E-19 | .3242E+02 |
| 31 | .5048E+01 | .1775E+02 | .1324E+00 | .0000E+00 | .1000E-19 | .3242E+02 |
| 30 | .4880E+01 | .1735E+02 | .1351E+00 | .0000E+00 | .1000E-19 | .3242E+02 |
| 29 | .4712E+01 | .1695E+02 | .1379E+00 | .0000E+00 | .1000E-19 | .3242E+02 |
| 28 | .4543E+01 | .1656E+02 | .1407E+00 | .0000E+00 | .1000E-19 | .3242E+02 |
| 27 | .4375E+01 | .1617E+02 | .1435E+00 | .0000E+00 | .1000E-19 | .3242E+02 |
| 26 | .4207E+01 | .1580E+02 | .1464E+00 | .0000E+00 | .1000E-19 | .3242E+02 |
| 25 | .4039E+01 | .1543E+02 | .1494E+00 | .0000E+00 | .1000E-19 | .3242E+02 |
| 24 | .3870E+01 | .1507E+02 | .1524E+00 | .0000E+00 | .1000E-19 | .3242E+02 |
| 23 | .3702E+01 | .1472E+02 | .1555E+00 | .0000E+00 | .1000E-19 | .3242E+02 |
| 22 | .3534E+01 | .1437E+02 | .1587E+00 | .0000E+00 | .1000E-19 | .3242E+02 |
| 21 | .3366E+01 | .1403E+02 | .1619E+00 | .0000E+00 | .1000E-19 | .3242E+02 |
| 20 | .3197E+01 | .1370E+02 | .1651E+00 | .0000E+00 | .1000E-19 | .3242E+02 |
| 19 | .3029E+01 | .1338E+02 | .1684E+00 | .0000E+00 | .1000E-19 | .3242E+02 |
| 18 | .2861E+01 | .1307E+02 | .1718E+00 | .0000E+00 | .1000E-19 | .3242E+02 |
| 17 | .2692E+01 | .1276E+02 | .1752E+00 | .0000E+00 | .1000E-19 | .3242E+02 |
| 16 | .2524E+01 | .1246E+02 | .1786E+00 | .0000E+00 | .1000E-19 | .3242E+02 |
| 15 | .2356E+01 | .1217E+02 | .1821E+00 | .0000E+00 | .1000E-19 | .3242E+02 |
| 14 | .2188E+01 | .1189E+02 | .1857E+00 | .0000E+00 | .1000E-19 | .3242E+02 |
| 13 | .2019E+01 | .1161E+02 | .1893E+00 | .0000E+00 | .1000E-19 | .3242E+02 |
| 12 | .1851E+01 | .1134E+02 | .1929E+00 | .0000E+00 | .1000E-19 | .3242E+02 |
| 11 | .1683E+01 | .1107E+02 | .1967E+00 | .0000E+00 | .1000E-19 | .3242E+02 |
| 10 | .1514E+01 | .1081E+02 | .2004E+00 | .0000E+00 | .1000E-19 | .3242E+02 |
| 9 | .1346E+01 | .1056E+02 | .2042E+00 | .0000E+00 | .1000E-19 | .3242E+02 |
| 8 | .1178E+01 | .1031E+02 | .2081E+00 | .0000E+00 | .1000E-19 | .3242E+02 |
| 7 | .1010E+01 | .1007E+02 | .2121E+00 | .0000E+00 | .1000E-19 | .3242E+02 |
| 6 | .8414E+00 | .9833E+01 | .2161E+00 | .0000E+00 | .1000E-19 | .3242E+02 |
| 5 | .6731E+00 | .9602E+01 | .2201E+00 | .0000E+00 | .1000E-19 | .3242E+02 |
| 4 | .5048E+00 | .9376E+01 | .2242E+00 | .0000E+00 | .1000E-19 | .3242E+02 |
| 3 | .3366E+00 | .9155E+01 | .2284E+00 | .0000E+00 | .1000E-19 | .3242E+02 |
| 2 | .1683E+00 | .8939E+01 | .2326E+00 | .0000E+00 | .1000E-19 | .3242E+02 |
| 1 | .0000E+00 | .8729E+01 | .2369E+00 | .0000E+00 | .1000E-19 | .3242E+02 |

TIME = 13.40

| -NODE- | -ELEVATION- | VOID -RATIO- | SOLID -CONTENT- | WATER -PRESSURE- | ALPHA -VALUES- |
|---|---|---|---|---|---|
| 51 | .8127E+01 | .1856E+02 | .1274E+00 | .0000E+00 | .1000E+01 |
| 50 | .8016E+01 | .2183E+02 | .1104E+00 | .0000E+00 | .1000E+01 |
| 49 | .7885E+01 | .2381E+02 | .1022E+00 | .0000E+00 | .1000E+01 |
| 48 | .7740E+01 | .2444E+02 | .9983E-01 | .0000E+00 | .1000E+01 |
| 47 | .7587E+01 | .2429E+02 | .1004E+00 | .0000E+00 | .1000E+01 |
| 46 | .7430E+01 | .2386E+02 | .1020E+00 | .0000E+00 | .1000E+01 |
| 45 | .7271E+01 | .2335E+02 | .1040E+00 | .0000E+00 | .1000E+01 |
| 44 | .7111E+01 | .2284E+02 | .1061E+00 | .0000E+00 | .1000E+01 |
| 43 | .6950E+01 | .2234E+02 | .1082E+00 | .0000E+00 | .1000E+01 |
| 42 | .6789E+01 | .2187E+02 | .1103E+00 | .0000E+00 | .1000E+01 |
| 41 | .6627E+01 | .2141E+02 | .1124E+00 | .0000E+00 | .1000E+01 |
| 40 | .6465E+01 | .2096E+02 | .1145E+00 | .0000E+00 | .1000E+01 |
| 39 | .6302E+01 | .2053E+02 | .1166E+00 | .0000E+00 | .1000E+01 |
| 38 | .6140E+01 | .2011E+02 | .1188E+00 | .0000E+00 | .1000E+01 |
| 37 | .5977E+01 | .1969E+02 | .1210E+00 | .0000E+00 | .1000E+01 |
| 36 | .5814E+01 | .1928E+02 | .1232E+00 | .0000E+00 | .1000E+01 |
| 35 | .5650E+01 | .1888E+02 | .1255E+00 | .0000E+00 | .1000E+01 |
| 34 | .5486E+01 | .1848E+02 | .1279E+00 | .0000E+00 | .1000E+01 |
| 33 | .5323E+01 | .1809E+02 | .1303E+00 | .0000E+00 | .1000E+01 |
| 32 | .5158E+01 | .1770E+02 | .1328E+00 | .0000E+00 | .1000E+01 |
| 31 | .4994E+01 | .1732E+02 | .1353E+00 | .0000E+00 | .1000E+01 |
| 30 | .4830E+01 | .1695E+02 | .1379E+00 | .0000E+00 | .1000E+01 |
| 29 | .4665E+01 | .1658E+02 | .1405E+00 | .0000E+00 | .1000E+01 |
| 28 | .4500E+01 | .1621E+02 | .1432E+00 | .0000E+00 | .1000E+01 |
| 27 | .4335E+01 | .1586E+02 | .1460E+00 | .0000E+00 | .1000E+01 |
| 26 | .4170E+01 | .1551E+02 | .1488E+00 | .0000E+00 | .1000E+01 |
| 25 | .4004E+01 | .1516E+02 | .1517E+00 | .0000E+00 | .1000E+01 |
| 24 | .3839E+01 | .1482E+02 | .1546E+00 | .0000E+00 | .1000E+01 |
| 23 | .3673E+01 | .1449E+02 | .1576E+00 | .0000E+00 | .1000E+01 |
| 22 | .3507E+01 | .1416E+02 | .1606E+00 | .0000E+00 | .1000E+01 |
| 21 | .3341E+01 | .1384E+02 | .1637E+00 | .0000E+00 | .1000E+01 |
| 20 | .3175E+01 | .1353E+02 | .1669E+00 | .0000E+00 | .1000E+01 |
| 19 | .3008E+01 | .1322E+02 | .1701E+00 | .0000E+00 | .1000E+01 |
| 18 | .2842E+01 | .1292E+02 | .1734E+00 | .0000E+00 | .1000E+01 |
| 17 | .2675E+01 | .1262E+02 | .1767E+00 | .0000E+00 | .1000E+01 |
| 16 | .2509E+01 | .1234E+02 | .1801E+00 | .0000E+00 | .1000E+01 |
| 15 | .2342E+01 | .1206E+02 | .1835E+00 | .0000E+00 | .1000E+01 |
| 14 | .2175E+01 | .1178E+02 | .1870E+00 | .0000E+00 | .1000E+01 |
| 13 | .2008E+01 | .1151E+02 | .1906E+00 | .0000E+00 | .1000E+01 |
| 12 | .1841E+01 | .1125E+02 | .1942E+00 | .0000E+00 | .1000E+01 |
| 11 | .1674E+01 | .1099E+02 | .1978E+00 | .0000E+00 | .1000E+01 |
| 10 | .1507E+01 | .1074E+02 | .2016E+00 | .0000E+00 | .1000E+01 |
| 9 | .1340E+01 | .1049E+02 | .2053E+00 | .0000E+00 | .1000E+01 |
| 8 | .1173E+01 | .1025E+02 | .2092E+00 | .0000E+00 | .1000E+01 |
| 7 | .1005E+01 | .1001E+02 | .2130E+00 | .0000E+00 | .1000E+01 |
| 6 | .8379E+00 | .9779E+01 | .2170E+00 | .0000E+00 | .1000E+01 |
| 5 | .6704E+00 | .9552E+01 | .2210E+00 | .0000E+00 | .1000E+01 |
| 4 | .5029E+00 | .9331E+01 | .2251E+00 | .0000E+00 | .1000E+01 |
| 3 | .3353E+00 | .9114E+01 | .2292E+00 | .0000E+00 | .1000E+01 |
| 2 | .1677E+00 | .8903E+01 | .2334E+00 | .0000E+00 | .1000E+01 |
| 1 | .0000E+00 | .8697E+01 | .2376E+00 | .0000E+00 | .1000E+01 |

**Material Characteristics of Example Problem**
**Figure EX5-2 Cracking Function Curve**
**(Cracking Void Ratio - Total Stress Curve)**

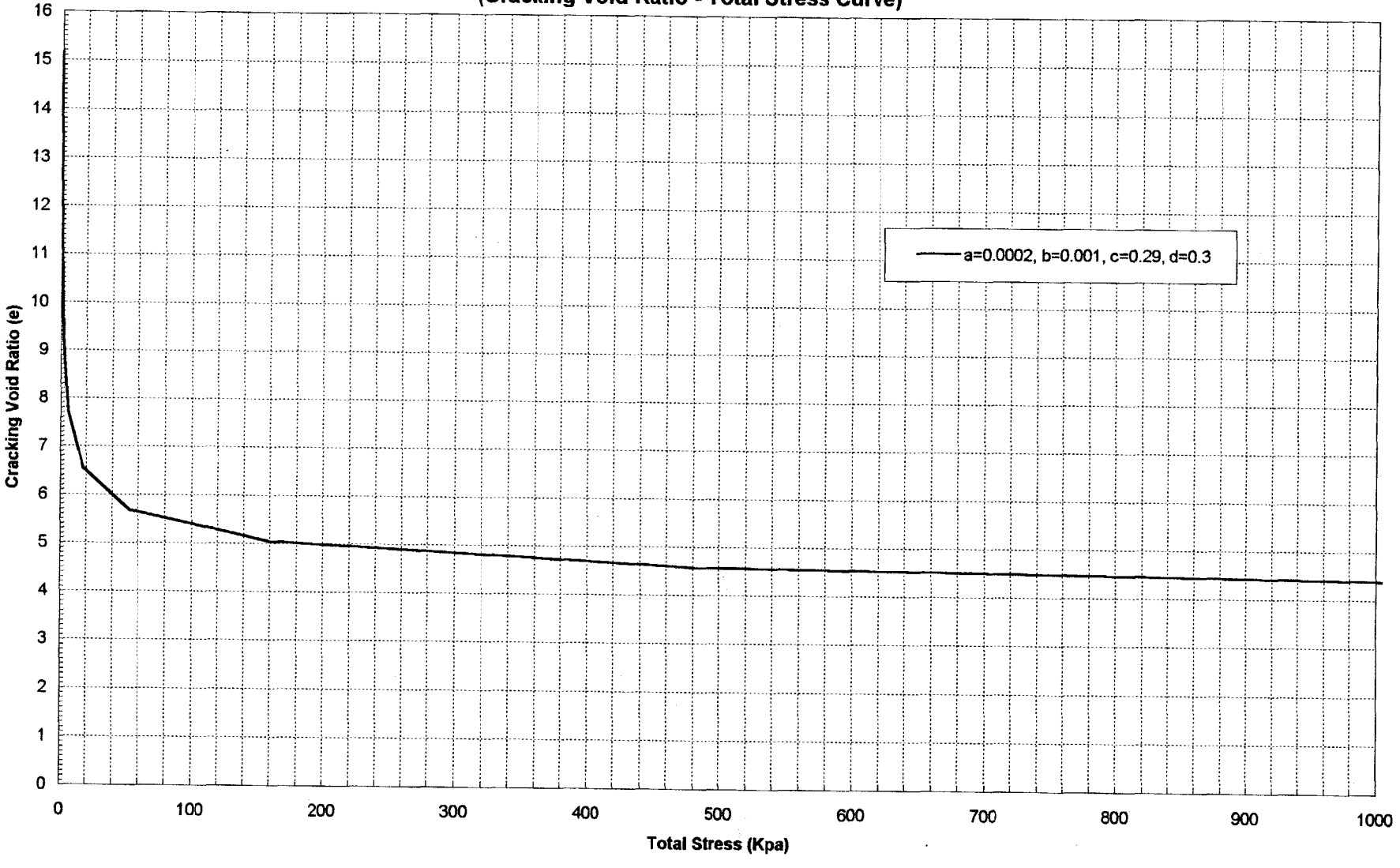

**Figure EX5-3 Time - Settlement Curve**

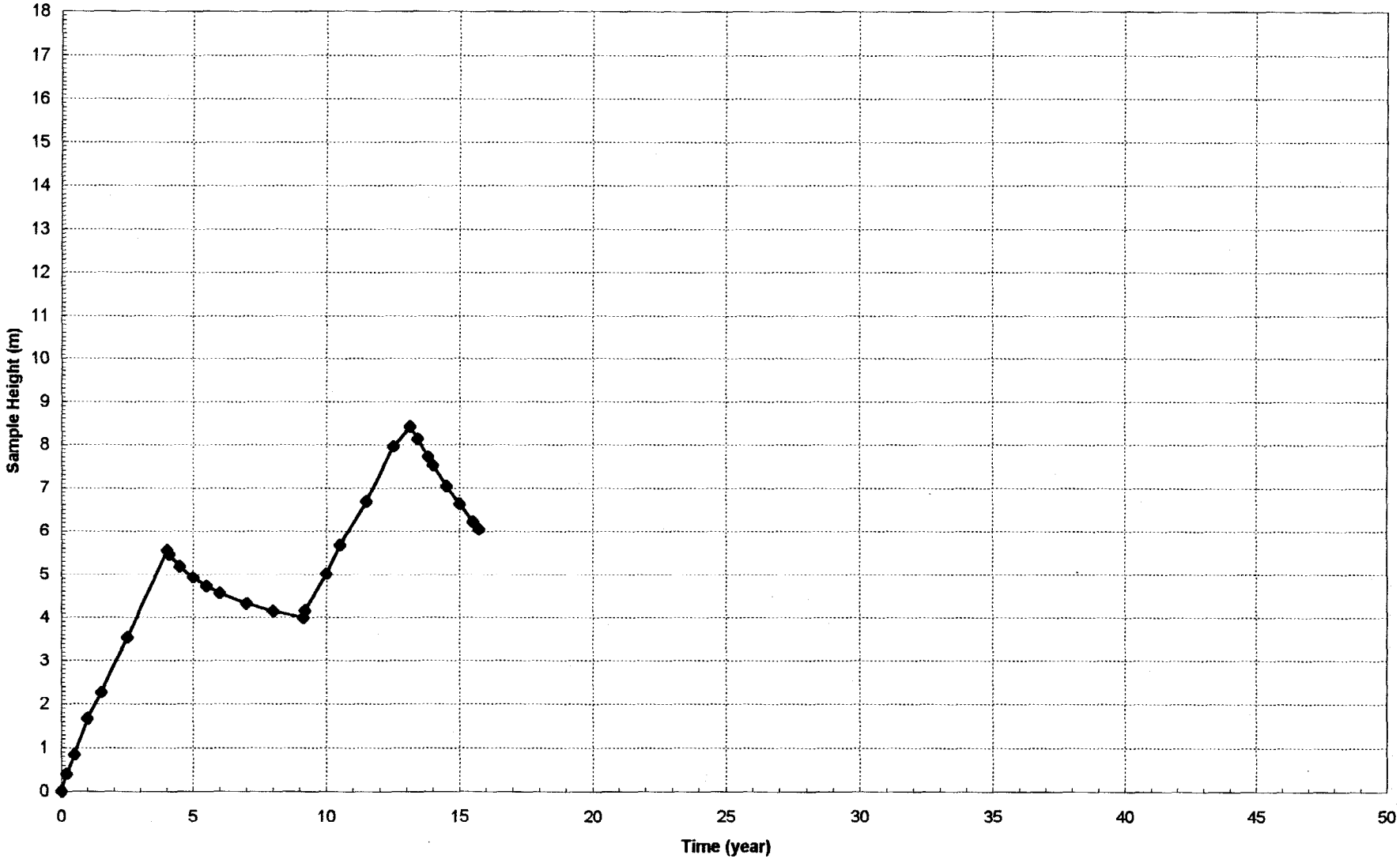

**Figure EX5-4 Solid Content Curve (Desiccation)**

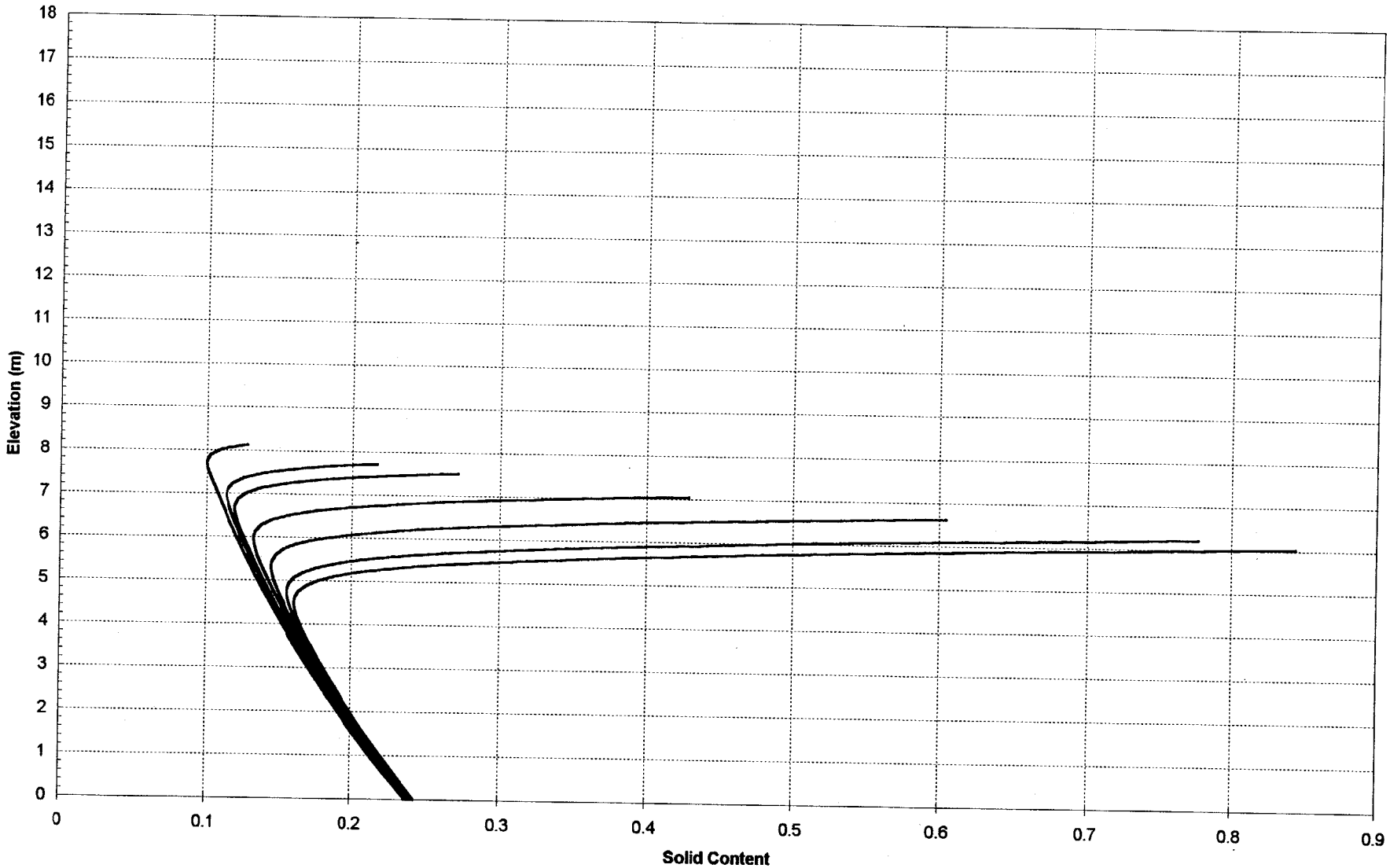

**Figure EX5-5 Time - Crack Depth Curve**

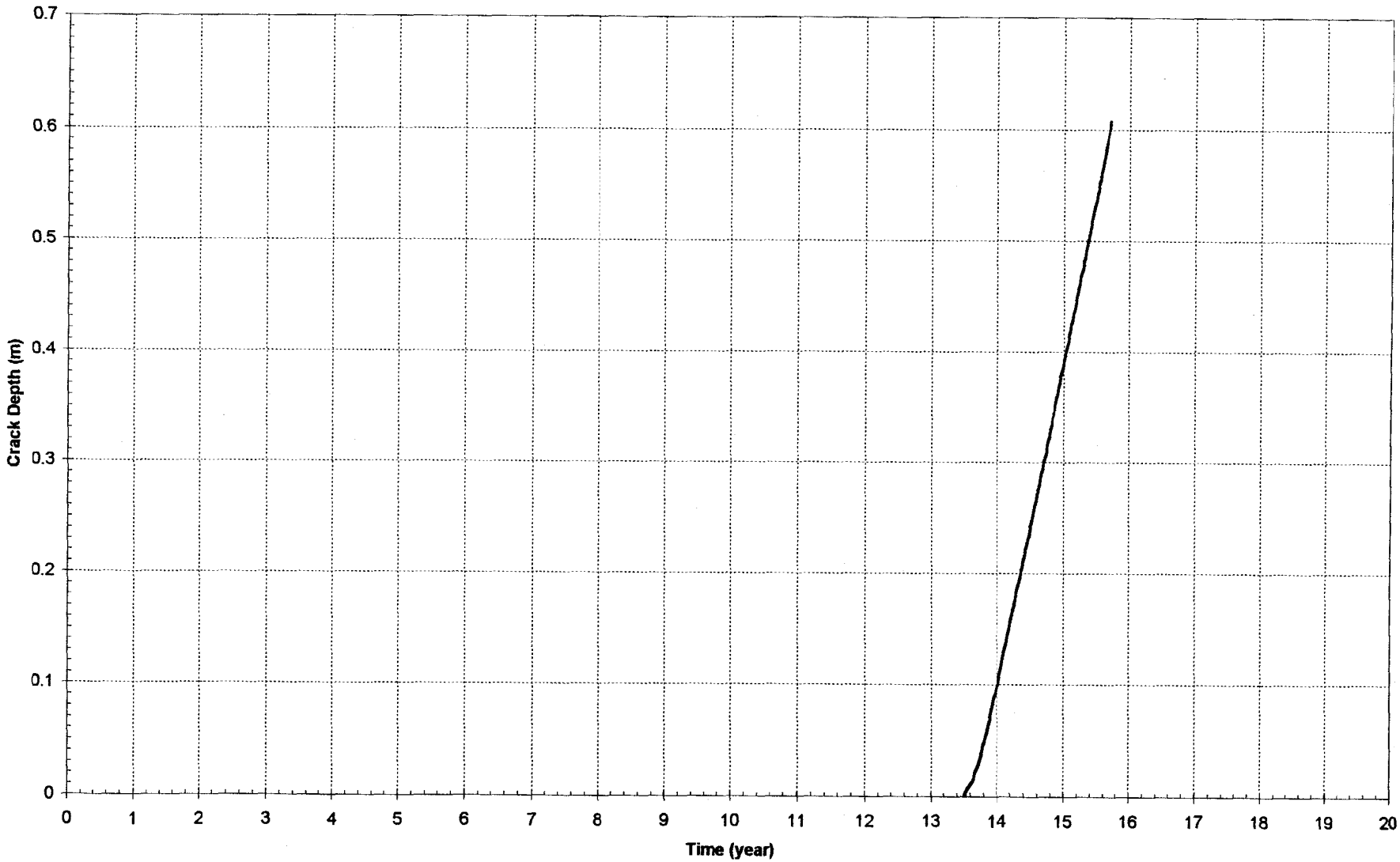

**Figure EX5-6 Time - Crack Volume Curve**

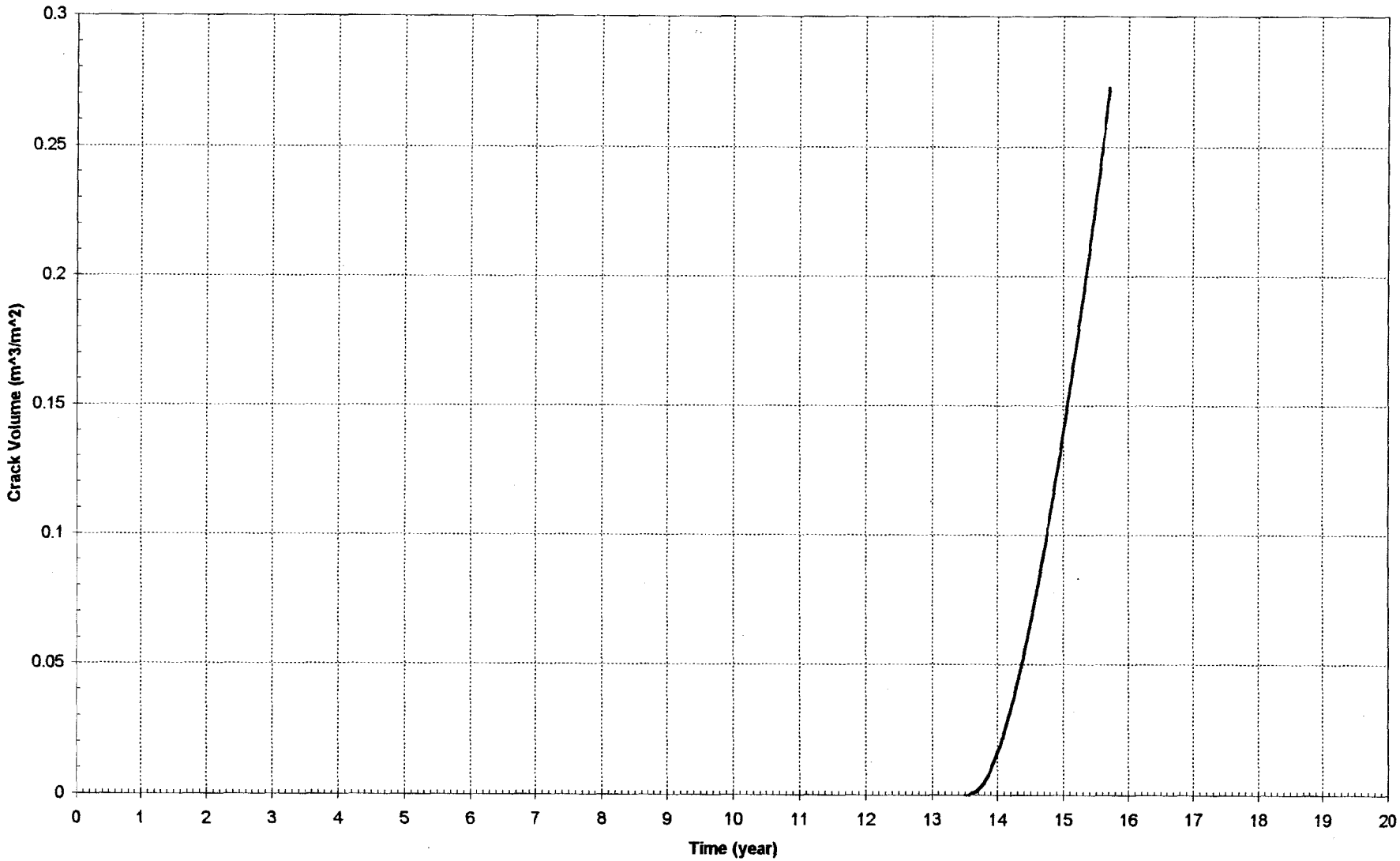

# Publications

# CONSOLIDATION CHARACTERISTICS OF PHOSPHATIC CLAYS

By A. Naser Abu-Hejleh,[1] Associate Member, ASCE,
Dobroslav Znidarčić,[2] Associate Member, ASCE, and Bobby L. Barnes[3]

**ABSTRACT:** Reliable and convenient testing technique and analysis are used to evaluate the void ratio-effective stress and void ratio-permeability relations for several types of very soft phosphatic waste clays. The technique is based on the seepage-induced consolidation test in which a soft soil sample is subjected to a constant downward flow rate and its final consolidated height and bottom effective stress are measured as the sample reaches steady state conditions. These two data points and the measured zero effective stress void ratio represent three reliable experimental data in the low range of effective stress, where the consolidation constitutive relations are highly nonlinear. In the higher effective stress range, the loading and permeability tests are used to determine the coefficient of permeability and effective stress corresponding to a given void ratio. An efficient algorithm to describe the steady-state flow in soft soils and a parameter-estimation scheme are employed for the determination of the soil consolidation parameters needed in the finite strain consolidation theory. The laboratory data of the restricted flow test and the transient seepage-induced consolidation test and the field measurements in three phosphatic clay settling ponds confirm the results obtained from the seepage-induced consolidation testing and analysis.

## INTRODUCTION

It is estimated that 30% of the world's phosphate is produced in the state of Florida, leading to the creation of large quantities of very soft, fine, and highly plastic phosphatic waste clays (McVay et al. 1986). According to Carrier et al. (1983). more than 50,000.000 t (dry weight) of such waste materials are generated annually in Florida's phosphate industry. The resulting slurry waste clay is typically pumped into large retention ponds at an initial void ratio of between 40 and 130. Within a few days to a few weeks after deposition, the sedimentation of the suspended soil particles brings the slurry clay to the zero effective stress void ratio, $e_0$, at which a soil is formed and the effective stress principle begins to apply. At that point, the very long consolidation process starts and might continue for decades. The soil formation void ratio, $e_0$, is not a material constant but depends on the initial slurry void ratio (Liu 1990). Carrier et al. (1983) listed typical values of $e_0$ for various fine-grained waste materials, with a value of around 30 for the phosphatic waste clays. The magnitude of densification that a deposit of soft soil undergoes during the consolidation phase is directly dependent on the soil void ratio-effective stress relation and the time-dependent progress of densification is directly dependent on the soil permeability-void ratio relation. Many computer models, based on finite strain consolidation analysis, have proven to be valuable tools in planning disposal site capacity, predicting the time at which site reclamation is technically feasible, and predicting the development of soil shear strength. However, the success of such analyses depends on the accuracy of the input data, especially the consolidation constitutive relations.

The changes of void ratio and permeability with the effective stress are very significant for soft phosphatic waste clays and other fine-grained materials, especially in the early stages of consolidation when the effective stresses are low. The direct determination of the consolidation characteristics for such soils is difficult if not impossible to achieve (Znidarčić 1982). For example, the application of a constant hydraulic gradient across a sample to measure its permeability results in a varying effective stress along the sample depth. For a very soft soil sample in the low effective Stress range, this variation in effective stress produces a nonuniform void ratio distribution, and, therefore, the permeability within the sample changes significantly and can't be assumed constant. McVay et al. (1986) also concluded that the laboratory measurements for determining the permeability relationships of phosphatic clays were deficient, but that acceptable results for their compressibility relationships could be obtained from the tests. Indeed, reliable effective stress-void ratio relations for soft soils could be determined from the field measurements or laboratory tests, but only if the soil layer (or soil sample) is fully consolidated (e.g., Cargill 1986). Obtaining such data, however, requires excessive testing time for fine-grained soils. For example, Carrier et al. (1983) reported that the time needed to conduct a direct stress-controlled slurry consolidometer test on a Florida phosphatic clay sample is 6-7 months. To provide more practical and reliable methodology for the determination of the consolidation characteristics of soft soils, Znidarčić (1982) introduced the concept of the inverse solution (or indirect) approach, in which the variation of void ratio across the sample is recognized. in the analysis.

Imai (1979) proposed a seepage induced consolidation test, in which, besides the self-weight of the specimen, a downward seepage force is imposed by creating a constant head difference across the specimen. The pore-water pressure within the sample is measured during the experiment and the void ratio distribution is obtained at the end of the test by slicing the specimen. From the obtained test data, the soil permeability-void ratio and effective stress-void ratio relations can be determined. Huerta et al. (1988) presented a new analysis for the seepage induced consolidation test, in which the inverse solution algorithm is adopted. While the two methods have enhanced our ability to determine the consolidation characteristics of soft soils, especially the permeability relation, they have not been widely used in practical applications. Both have some shortcomings that make their application difficult, or at least cumbersome. Imai's approach requires specialized equipment, for which the quality of the measured data is operator-dependent. In addition, the process of the determination of void ratio distribution is unreliable and may produce erroneous results. The analysis of the constant rate deformation technique sug-

[1]Colorado Dept. of Transp.. Sterling. CO 80751; formerly. Res. Assoc., Dept. of Civ., Envir., and Arch. Engrg.. Univ. of Colorado, Boulder, CO 80309.

[2]Assoc. Prof., Dept. of Civ.. Envir., and Arch. Engrg., Univ. of Colorado, Boulder, CO.

[3]Froehling and Robertson, Inc., Asheville, NC 28802; formerly, BCI, Lakeland, FL.

Note.. Discussion open until September 1,1996. To extend the closing date one month, a written request must be filed with the ASCE Manager of Journals. The manuscript for this paper was submitt for review and possible publication on January 23. 1995. This paper is part of the *Journal of Geotechnical Engineering,* Vol. 122. No. 4. April, 1996. ©ASCE, ISSN 0733-9410/96/0004-0295-0301/$4.00 + $.50 per page. Paper No. 9949.

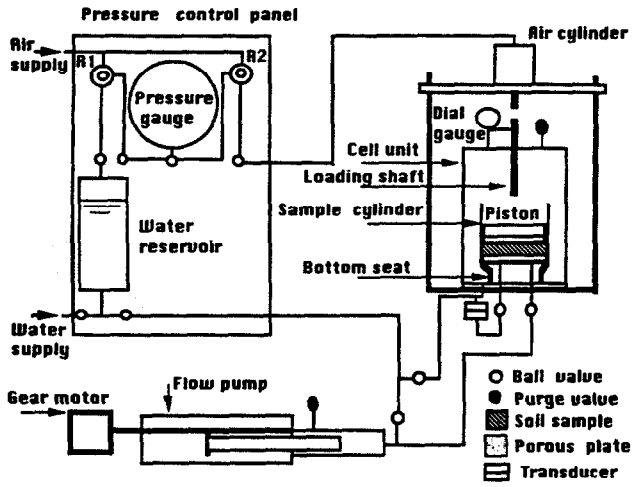


**FIG. 1. Seepage-Induced Consolidation Testing Equipment**

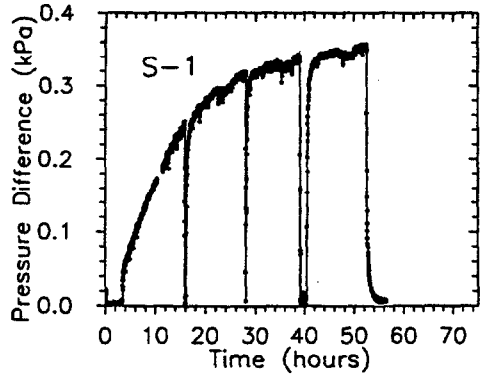


**FIG. 2. Experimental Results of Seepage-Induced Consolidation Test on Sample S-1**

gested by Znidarčić et al. (1986) is based on the linearized consolidation theory, which may not be appropriate for very soft, cohesive soils. In addition, the sensitivity of the developed equipment limits its application to stress levels above 1 kPa. The method proposed by Huerta et al. (1988) is the most comprehensive one, but still requires a direct measurement of the void ratio at the bottom of the sample and a precise determination of the steady-state flow rate. Both of these requirements make it a difficult and operator-dependent procedure. In addition, the associated analysis of the test results is inconvenient,

A reliable testing technique to evaluate the highly nonlinear consolidation constitutive relations of soft, cohesive soils was developed by Znidarčić and Liu (1989). The technique is based on the seepage induced consolidation test suggested originally by Imai (1979). This experiment has been enhanced and a new analysis has been developed (Abu-Hejleh and Znidarčić 1992; Znidarčić et al. 1992; Abu-Hejleh et al. 1992; and Abu-Hejleh and Znidarčić 1994). The new procedure eliminates most of the limitations of the existing methods. This paper presents the new version of the seepage induced consolidation testing and analysis and demonstrates its advantages over existing methods. Consolidation characteristics for several samples of very soft phosphatic clays obtained by the new procedure are also included. These characteristics are verified by utilizing independent experimental and field measurements.

## EXPERIMENTS

The experimental part of the procedure consists of three distinct phases that all provide data for the test analysis. These include the determination of the zero effective stress void ratio, $e_0$, the steady-state stage of the seepage induced consolidation test, and the step loading test with the direct permeability measurements at high effective stresses.

A sufficient amount of the soft clay is thoroughly mixed at the consistency corresponding to the deposited characteristics at the beginning of the disposal. For the $e_0$ determination, two laboratory jars are filled with a 25 mm (1 in.) thick layer of the slurry clay and covered to prevent evaporation. The slurry clay is left for several days to settle. At the end of its consolidation, any supernatant is carefully removed and few samples are taken from the surface of the settled clay, where the effective stress is very close to zero, to determine $e_0$. The overall contribution of the sedimentation process in densifying the slurry clay can be estimated by the difference between the initial mixing void ratio and $e_0$.

The testing system for the seepage induced consolidation, step loading, and permeability tests consists of five major parts: a triaxial cell unit with a differential pressure transducer, a pressure control panel, a loading system, a flow pump, and a data acquisition system. A schematic diagram of the experimental apparatus is shown in Fig. 1. The testing system is self-contained and requires only electrical power and an air-pressure supply. The cell unit contains a transparent sample ring for housing the soft soil sample, a plastic piston, and a bottom seat that are equipped with a coarse porous plate, a loading shaft, and a dial gauge to measure the sample height. The pressure control panel has a dual purpose: to apply the necessary back pressure and to control the air pressure in the air cylinder for loading the sample in the step loading test. Two ports beneath the bottom seat connect the pore water at the bottom of the soil sample to the flow pump and to the transducer. The use of the flow pump facilitates a precise control of the flow rate through the sample. The pressure difference across the sample is measured with the precision differential pressure transducer connected to a personal computer-based data acquisition system to collect the data of pressure changes with time.

The slurry clay is poured into the transparent container and the loading piston is allowed to rest freely on top of the sample. The triaxial cell is filled with water and the entire testing system is saturated under a back pressure of 200 kPa. The slurry soil sample is left to consolidate overnight under both its own weight and the top effective stress produced by the plastic piston. Due to the piston's buoyancy, an effective stress of only 0.1 kPa is applied to the top sample boundary. This small surface load is used to prevent the creation of flow channels during the seepage induced consolidation test that would otherwise form in the sample (You 1993).

In the seepage induced consolidation test, a constant flow rate is imposed across the sample by withdrawing water from the bottom of the sample using the flow pump. Due to the downward flow of water, the sample consolidates and the resulting pressure difference across the sample increases with time. The pressure difference is continuously measured with the pressure transducer and recorded by the data acquisition system (Fig. 2). The same flow rate is maintained until the steady state condition is reached where no further consolidation takes place and the pressure difference across the sample, $\Delta P_s$, becomes constant. The water flux across the sample, $v$, is constant at the steady state, and it is calculated as the imposed flow rate divided by the sample area, $A_x$. At that stage, the sample height, $H_f$, is measured and $\Delta P_s$ is used to evaluate the sample's bottom effective stress, $\sigma_b'$, as

$$\sigma_b' = \sigma_0' + \gamma_w H_f (G_s - 1) + \Delta P_s \quad (1)$$

where $\sigma_0'$ = effective stress produced by the loading piston; $\gamma_w$ = water unit weight; $G_s$ = specific gravity of solids; and $H_s$ =

height of solids contained in the sample calculated as $W_d/(G_s\gamma_w A_s)$, in which $W_d$ is the dry weight of the sample.

Once the steady-state conditions under a given flow rate are reached, the seepage-induced consolidation test with a higher flow rate can be performed. This will produce further compression of the sample and a higher pressure difference. The seepage-induced consolidation test should be performed under relatively high flow rate that will produce significant variations of void ratio and effective stress across the specimen. This provides more reliable values of $v$, $\sigma'_b$, and $H_f$ for the analysis of test results. Based on experience, the flow rate should be increased from low flow rate until the resulting pressure difference is between 2 kPa and 5 kPa, and not less than 0.3 kPa or more than 10 kPa. Note that only one set of $v$, $\sigma'_b$, and $H_f$ is needed for the analysis of test results.

To obtain compressibility and permeability data in the higher effective stress range, step loading and permeability tests are performed. At the conclusion of the seepage-induced consolidation test, the sample is consolidated under a large vertical effective stress, $\sigma'_c$. At the end of its consolidation, the sample height is measured and the corresponding uniform void ratio of the compressed sample, $e_c$, is calculated. A small downward water flux is imposed across the sample with the flow pump. The resulting pressure change across the sample is obtained and used to calculate the permeability of the sample, $k_c$ (Aiban and Znidarčić 1989). The two tests can be repeated several times under increasing loads in order to obtain redundant data, but only one set of $\sigma'_c$, $e_c$, and $k_c$ are needed for the analysis. The sample is removed from the testing apparatus and the weight of solids, $W_d$, is determined.

## TEST ANALYSIS

An extended power function (Liu and Znidarčić 1991) is used to relate the vertical effective stress, $\sigma'_v$, to the void ratio, $e$

$$e = A(\sigma'_v + Z)^B \tag{2}$$

This form, representing an expanded form of a widely used power function, removes all major deficiencies of the conventional logarithmic models. Namely, the void ratio is well defined at zero effective stress and, irrespective of the stress magnitude, the void ratio never becomes negative. The conventional form of the power function is used to relate the coefficient of permeability, $k$, to the void ratio

$$k = Ce^D \tag{3}$$

This form describes the permeability relations for soft soils quite well, as demonstrated by Somogyi (1979) and Al Tabaa and Wood (1987). The empirical parameters $A$, $B$, $C$, $D$, and Z are the consolidation constitutive parameters to be determined for a given soil. An efficient solution describing the steady state conditions in the seepage induced consolidation test and a parameter-estimation algorithm are developed and coded in the computer program SICTA (Seepage Induced Consolidation Test Analysis). The parameters $A$, $B$, $C$, $D$, and Z are determined in program SICTA from the test results. A brief description of the overall analysis procedure follows.

The consolidation of soft phosphatic clays and other cohesive materials is properly described by the finite strain consolidation theory (Gibson et al. 1967; McVay et al. 1986). The governing equation for the process can be written in the material coordinate system as:

$$(G_s - 1)\left[\frac{d}{de}\left(\frac{k}{1+e}\right)\right]\frac{\partial e}{\partial z} - \frac{\partial}{\partial z}\left[\frac{k}{\gamma_w(1+e)}\frac{d\sigma'_v}{de}\frac{\partial e}{\partial z}\right] = \frac{\partial e}{\partial t} \tag{4}$$

where the material coordinate $z$ is taken positive in the direction of gravity, and $t$ = time. For the steady-state condition the right-hand side of the equation is equal to zero, since there is no further change of the void ratio with time. The equation is thus written in the form

$$(G_s - 1)\left[\frac{d}{de}\left(\frac{k}{1+e}\right)\right]\frac{de}{dz} - \frac{d}{dz}\left[\frac{k}{\gamma_w(1+e)}\frac{d\sigma'_v}{de}\frac{de}{dz}\right] = 0 \tag{5}$$

This new equation describes, together with the appropriate boundary conditions, the steady-state flow of water through a soft soil layer. Its solution gives the void ratio distribution at steady state, from which the effective stresses and layer height can be determined. It is clear from (5) that both the compressibility and permeability constitutive relations influence the steady-state void ratio distribution. Thus, the steady state in the seepage induced consolidation experiment is also an appropriate and sufficient test from which the consolidation constitutive properties can be determined. The use of the steady state, rather than the transient part of the test, has several benefits. It is easier to make reliable measurements in the steady state than during the transient part of the test. The delay in the instrumentation response, caused by the system compliance, has less effect on the quantities measured in the steady state than during the transient phase of the test. The analysis of the steady-state flow is also much simpler and involves less computational effort. The use of the steady state as the basis for the determination of the consolidation characteristics of soft soils distinguishes this method from others that are based on the analysis of transient tests (Been and Sills 1981).

At the steady-state condition in the seepage-induced consolidation test, the velocity of the sample solid phase is zero (no vertical deformation) and the apparent velocity of the water phase is constant along the sample depth and does not change with time. Hence, the steady-state apparent relative velocity between the water phase and the solid phase is the applied water flux, $v$. By combining the equilibrium equation, the principle of effective stress, and Darcy's Law in terms of the relative apparent velocity between the water and solid phases, an expression for v can be obtained as

$$v = \frac{k}{\gamma_w(1+e)}\frac{d\sigma'_v(z)}{dz} - \frac{k}{1+e}(G_s - 1) \tag{6}$$

Note that (6) is equivalent to (5). but the use of (6) to simulate the test is more convenient since the steady-state water flux, $v$, is known. The material coordinate, $z$, identifies the height of solids from the top of the sample, where $z = 0$, to the point of interest; note that $z = H_s$ at the bottom of the sample. The rearrangement of (6) followed by the integration from $z = 0$ to any $z$ leads to

$$\sigma'_v(z) = \sigma'_0 + \gamma_w(G_s - 1)z + \int_0^z \frac{v\gamma_w}{k}(1+e)\,dz \tag{7}$$

The integral equation, (7), relates the vertical effective stress at any material depth z in the soil sample (or a soil layer) at steady state to the sample void ratio distribution above z. The effective stress and permeability in the integral equation are expressed in terms of the void ratio using (2) and (3). A simple iterative numerical solution for the integral equation was developed and used to describe the steady state conditions in the seepage induced consolidation test. With the known values of $H_s$, $\sigma'_0$, $v$, $e_0$, $G_s$, and $\gamma_w$, the numerical solution predicts the steady-state sample bottom effective stress, $\sigma'_{bn}$, and height, $H_{fn}$, for any set of parameters $A$, $B$, $Z$, C, and $D$. The numerical solution is very accurate and always stable irrespective of the degree of nonlinearity of the consolidation constitutive relations.

With the measured zero effective stress void ratio and the compressibility and permeability data in the higher effective

stress range, the number of parameters needed to be estimated is reduced from five to two. Parameters $B$ and $D$ are chosen to be the free parameters and the other parameters are determined as

$$Z = \frac{\sigma_c'}{(e_c/e_0)^{1/B} - 1}, \quad A = \frac{e_0}{Z^B}, \quad C = \frac{k_c}{(e_c)^D} \tag{8}$$

By utilizing the steady-state results of the seepage induced consolidation test and their numerical predictions for any set of consolidation constitutive parameters, parameters $B$ and $D$ are determined by minimizing the objective function, $Q$, defined as

$$Q = \left|1 - \frac{\sigma_{bm}'}{\sigma_b'}\right| + \left|1 - \frac{H_{fm}}{H_f}\right| \tag{9}$$

An iterative parameter estimation algorithm, based on the Newton method coupled with the line search procedure (Dennis and Schnabel 1983). is used to minimize $Q$ by calculating improved values for $A$, $B$, $C$, $D$, and Z in each successive iteration until an arbitrary small value of $Q$ is reached. Both the efficiency of the numerical simulation of the test and the requirement that only two free parameters need to be determined prevent the parameter estimation analysis from converging to inaccurate optimized constitutive parameters. The complete analysis of any set of experimental data with the SICTA program usually requires between 3 and 20 iterations and can be completed within a few seconds on any personal computer.

The seepage-induced consolidation test with the controlled flow rate has many advantages when compared to the controlled head difference techniques (Imai 1979; Huerta et al. 1988). First, the flow pump facilitates a precise determination of the steady-state flow rates with a resolution in the range of $10^{-6}$ mL/s, that is four orders of magnitude better than with the conventional methods of volume change measurement (Alva-Hurtado and Selig 1981). Second, the precise control of low flow rates with the flow pump enables testing under small gradients that are easily measured with the sensitive pressure transducer. This leads to more reliable results in the low effective stress range for soft cohesive soils. Third, since the response of the transducer is essentially instantaneous, the steady-state condition will be detected as soon as it is reached in the experiment. This is a major advantage over the constant head test in which a sufficient water quantity has to be accumulated for a reliable calculation of the steady-state average flow rate. Thus, the constant head test has to be extended for some time into the steady-state regime, leading to prolonged tests.

**TABLE 1. Properties of Phosphatic Clays**

| Sample (1) | Specific gravity (2) | Plastic limit (%) (3) | Liquid limit (%) (4) |
|---|---|---|---|
| A-1 | 2.6 | 74 | 318 |
| A-9 | 2.82 | 49 | 233 |
| C-1 | 2.92 | 33 | 114 |
| S-1 | 2.71 | 50 | 198 |

## TEST AND ANALYSIS RESULTS FOR PHOSPHATIC CLAYS

The consolidation characteristics for samples of very soft and cohesive waste phosphatic clay were determined with the presented seepage-induced consolidation testing and analysis. The samples were obtained from several phosphate mines in Florida. The specific gravity, plastic limit, and liquid limit for the samples are included in Table 1. The results of all three phases of the testing programs are summarized in Table 2, and an example of the recorded pore water pressure during the seepage induced consolidation test is given in Fig. 2. The several pressure drops noticed in Fig. 2 were caused by the resetting of the flow pump at the end of its travel distance. The data indicate that the short flow interruptions do not affect the pore pressure response significantly. The test data from Table 2 are used as the input variables for the SICTA program and the analysis results, constitutive parameters, are listed in Table 3. Graphical presentations of the obtained compressibility and permeability relations are shown in Figs. 3 and 4. respectively. The low permeability of the phosphatic clays and their high compressibility are demonstrated in these figures.

## VERIFICATION RESULTS

Three types of independent measurements are used to verify the seepage-induced consolidation teat and analysis results for the phosphatic clays. The obtained consolidation constitutive relations are first compared with the results of the restricted flow consolidation test which produces the same relations with a completely different testing procedure and analysis. Second, the obtained consolidation characteristics are used in the consolidation analysis to simulate the transient phase of the seep age-induced consolidation test and to predict the field conditions in several phosphatic clay settling ponds for which some direct measurements are available. The transient finite strain consolidation analysis is conducted with the CADA program (Abu-Hejleh 1993). in which an efficient, nonlinear, finite-element solution algorithm for (4) is implemented.

The testing technique and analysis procedure for the restricted flow consolidation test are documented in the report by Sills et al. (1984). In the analysis, the experimentally obtained compressibility and permeability data are fitted to the exponential curves, which correspond to linear functions in double log scale. The data from this test on sample A-9 and the fitted linear curves on double log scale plots are shown in Figs. 5 and 6, together with the obtained compressibility and permeability curves from the seepage-induced consolidation test and analysis. A good agreement between the two sets of results is noted with the only notable deviation in the low effective stress range. The data reported for the restricted flow consolidation test show substantial scatter in that range, indicating that the procedure may not be reliable for the low effective stress level. The seepage-induced consolidation test produces less ambiguous results at low effective stresses. In addition, a simpler power function is fitted to the compressibility data from the restricted flow test, while an expanded power function is used in the analysis of the seepage-induced consolidation test. Since the simple power function does not recognize the maximum void ratio for a given sample, the

**TABLE 2. Experimental Results of Tests Performed on Phosphatic Clays**

| Sample (1) | $e_0$ (2) | $H_0$ (m) (3) | $\sigma_b'$ (kPa) (4) | $v$ (m/s) (5) | $\sigma_b'$ (kPa) (6) | $H_f$ (m) (7) | $\sigma_c$ (kPa) (8) | $e_c$ (9) | $k_c$ (m/s) (10) |
|---|---|---|---|---|---|---|---|---|---|
| A-1 | 25.93 | 0.046 | 0.10 | $0.147 \times 10^{-6}$ | 2.29 | 0.0230 | 50.00 | 4.68 | $0.798 \times 10^{-9}$ |
| A-9 | 18.39 | 0.034 | 0.10 | $0.294 \times 10^{-6}$ | 2.82 | 0.0275 | 50.00 | 4.17 | $0.648 \times 10^{-9}$ |
| C-1 | 13.07 | 0.051 | 0.39 | $0.164 \times 10^{-6}$ | 2.94 | 0.0307 | 29.20 | 4.07 | $0.169 \times 10^{-8}$ |
| S-1 | 32.50 | 0.049 | 0.10 | $0.147 \times 10^{-6}$ | 0.474 | 0.0302 | 99.47 | 3.11 | $0.203 \times 10^{-9}$ |

**TABLE 3. Obtained Consolidation Constitutive Parameters for Phosphatic Clays**

| Sample (1) | A (2) | B (3) | Z (kPa) (4) | C (m/s) (5) | D (6) |
|---|---|---|---|---|---|
| A-1 | 11.50 | −0.230 | 0.029 | $0.625 \times 10^{-11}$ | 3.14 |
| A-9 | 12.74 | −0.285 | 0.277 | $0.361 \times 10^{-11}$ | 3.64 |
| C-1 | 7.75 | −0.191 | 0.065 | $0.429 \times 10^{-11}$ | 4.26 |
| S-1 | 13.49 | −0.319 | 0.064 | $0.384 \times 10^{-11}$ | 3.50 |

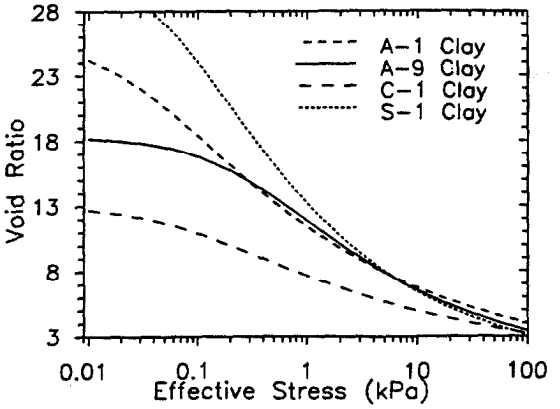


**FIG. 3. Consolidation Compressibility Relations for Phosphatic Clays**

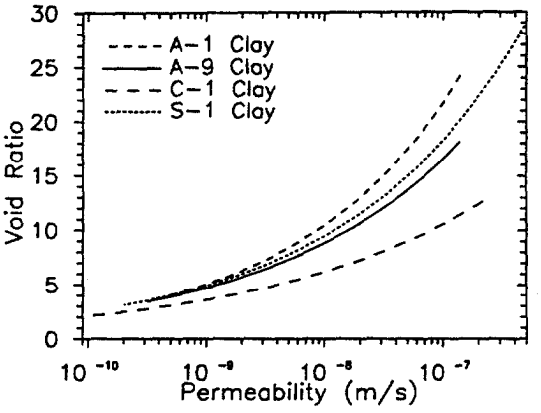


**FIG. 4. Consolidation Permeability Relations for Phosphatic Clays**

obtained data in the higher effective stress range are extrapolated to the low effective stress range, leading to a further disagreement between the two techniques.

In the seepage-induced consolidation test, the soil sample passes through a transient phase of consolidation before reaching the steady-state conditions. Thus, the obtained data in this phase gives the opportunity for an independent verification of the obtained consolidation characteristics in the low range of effective stresses. Note that the consolidation characteristics were obtained using only the steady state results of the seepage induced consolidation test. With the known testing conditions and measured consolidation material characteristics of the phosphatic clays, the CADA program is used to simulate the seepage induced consolidation tests. The measured test data on samples A-l and S-l and their numerical predictions are shown in Figs. 7 and 8. These figures show a good agreement between the test data and their numerical predictions, confirming the accuracy of the obtained consolidation characteristics of phosphatic clays in the low effective stress range.

Using the piston tube sampler, profiles of void ratio with depth were obtained from the phosphatic clay settling ponds where samples A-l, C-l, and S-l, were taken, and these are shown graphically in Figs. 9- 11. In order to predict these field data numerically using the experimentally obtained consolidation characteristics and the CADA program, information that describes the boundary conditions and the slurry deposition history of the phosphatic clays is needed. It was given that the bottom surface of the settling ponds can be assumed impervious and that the phosphatic clay deposits had been covered with water. Thus, the measured zero effective stress void ratio in our laboratory is assumed for the surface of the deposits, where the effective stress is zero, and it is included in the

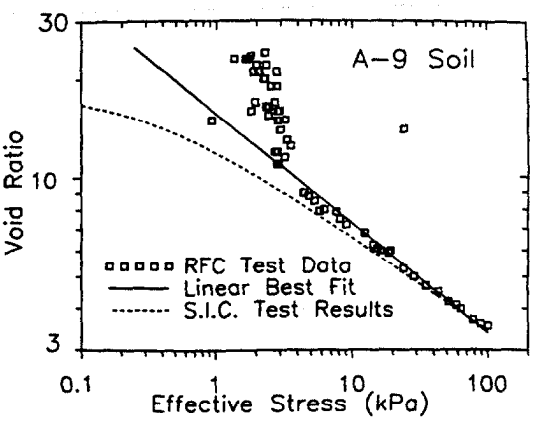


**FIG. 5. Consolidation Compressibility Relation for A-9 Phosphatic Soil**

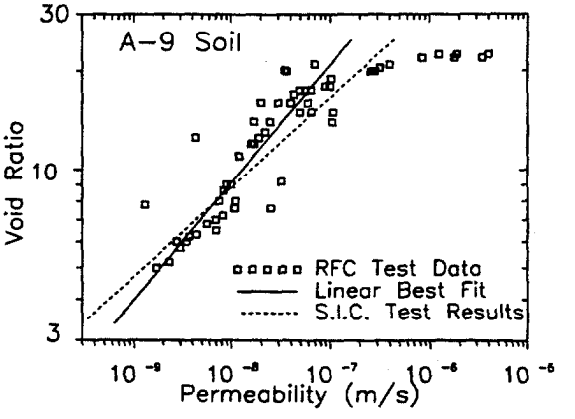


**FIG. 6. Consolidation Permeability Relation for A-9 Phosphatic Soil**

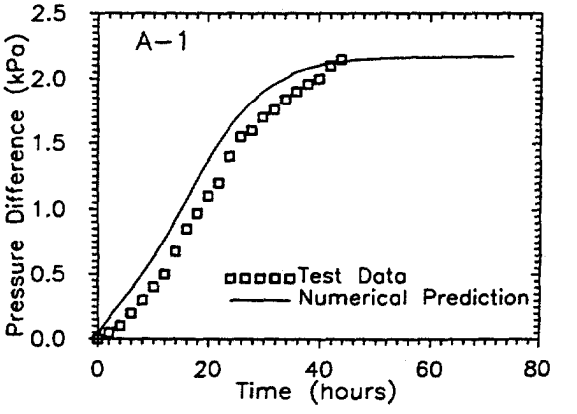


**FIG. 7. Measured and Predicted Data In Seepage Induced Consolidation Test on Sample A-1**

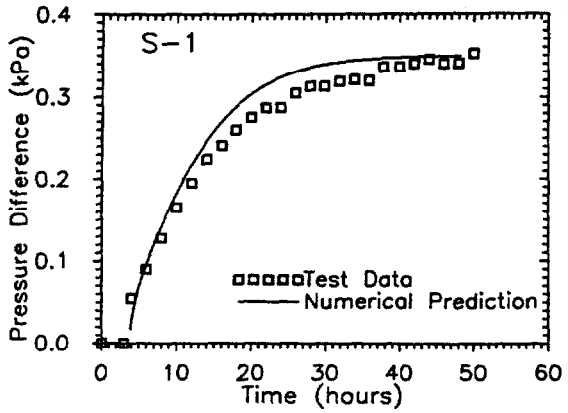


**FIG. 8. Measured and Predicted Data in Seepage Induced Consolidation Test on Sample S-1**

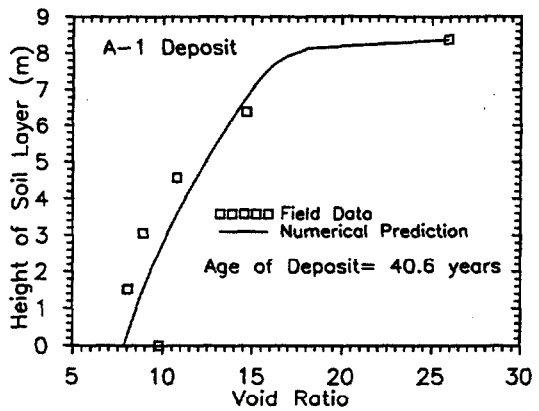


**FIG. 9. Field Measurements for Void Ratio Distribution in Settling Pond A-1 and Their Numerical Predictions**

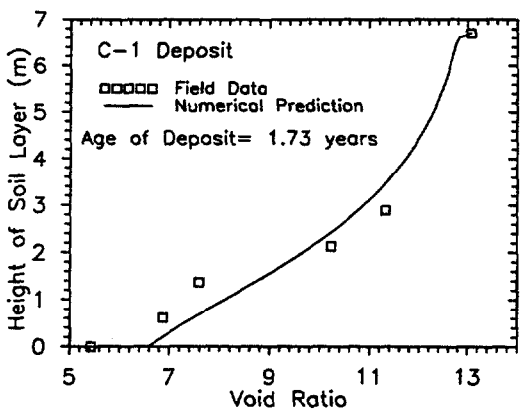


**FIG. 10. Field Measurements for Void Ratio Distribution in Settling Pond C-l and Their Numerical Predictlons**

presented void ratio profiles in Figs. 9-11. In addition, the $e_0$ value is used to represent the initial void ratio of the slurry phosphatic clays at the beginning of consolidation. For the stated boundary and initial conditions, the only source of the slurry phosphatic waste densification is the self-weight consolidation.

Since we could not obtain information on the slurry filling rates and periods, such information was either estimated or investigated with the available field data and the CADA program. The measured data of void ratio with depth were used to estimate the height of solids contained in each profile, $H_s$. Then, the uniform deposition rate, in terms of volume of deposited waste clay per unit area and per unit time, *DR*, during a filling period *F* is estimated as:

$$DR = H_s/F \tag{10}$$

The height of the unconsolidated slurry column, $H_0$, for each deposit can be calculated as $H_s(1 + e_0)$, and the corresponding filling rate is $H_0/F$. For example, the estimated values of $H_s$ and $H_0$ for deposit S-l are 0.516 m and 17.3 m, respectively. For each deposit, the self-weight consolidation of the unconsolidated slurry column with a total height of $H_0$ is modeled. The deposition conditions were simulated with the instantaneous tilling and with varying uniform filling rates. A sample of the obtained settlement response for deposit S-1 is shown in Fig. 12. The graphical results indicate that the soil layer height during the self-weight consolidation could be assumed independent of the filling rate, especially when the filling rate is high. A similar result was obtained by Carrier et al. (1983). Therefore, it is assumed that the phosphatic clay conditions at the time of sampling are independent of the filling rate history and are related only to the elapsed time **from** the beginning of the slurry deposition operations, $T_c$.

The consolidation analysis results for the instantaneous filling am used to predict the void ratio profiles in the phosphatic clay deposits. The value of $T_c$ corresponding to the sampling time, designated as the deposit age, was estimated with the measured soil layer height. For example, the age of deposit S-1 at the time of sampling is estimated as 13.13 years, since at that time the predicted soil layer height from Fig. 12 is 7.62 m, which is equal to the measured height of profile S-1 shown in Fig. 11. The void ratio profiles cotresponding to the sampling time for the three phosphatic deposits are then obtained, and

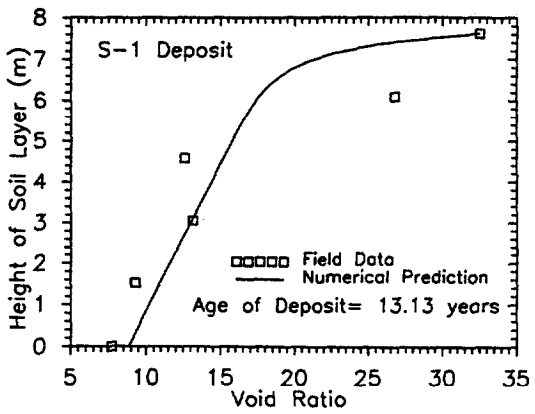


**FIG. 11. Field Measurements for Void Ratio Distribution in Settling Pond S-1 and Their Numerical Predictions**

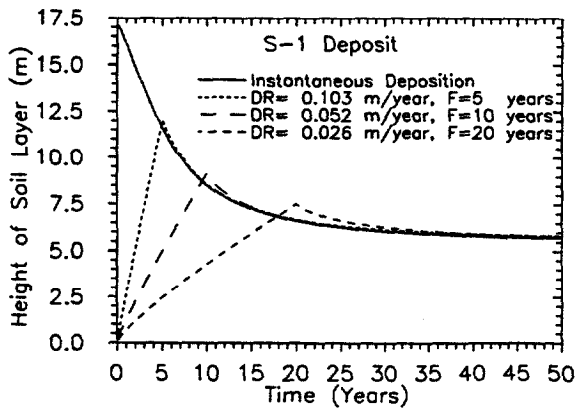


**FIG. 12. Predicted Settlement-Time Curves for the Waste Clay in Settling Pond S-1 under Different Deposition Conditions**

they are presented in Figs. 9- 11. The graphical results show a good agreement between the measured field data of void ratio with depth and their numerical predictions. 'Ibis represents further evidence of the reliability of the obtained consolidation characteristics from the seepage induced consolidation test and analysis, and supports the use of such results in the consolidation analysis of real field situations. Fig. 10 indicates that the upper portion of deposit C-1 is relatively unconsolidated, implying that this deposit was relatively young at time of sampling. This is not the case for deposits A-1 and S-1.

## CONCLUSIONS

The seepage induced consolidation test and analysis provide a rational method for the determination of the consolidation constitutive relations for soft phosphatic clays and other fine-grained materials. The analysis procedure is consistent with the finite strain consolidation theory that is routinely used in the analysis of field conditions in the settling ponds at phosphate mines. The presented methodology solves the difficult problem of material characteristics determination, usually the most critical aspect of any field prediction.

The advantages of the presented methodology include the precise control of the steady-state flow rate using the flow pump, the accurate measurements of the pressure difference across the sample with the sensitive differential pressure transducer, and an efficient analysis of the test results without any restrictive assumptions. The quality of the obtained results is verified by the comparison with three types of independent measurements including the field data.

## ACKNOWLEDGMENTS

The work presented in this paper was partially supported by the Florida Institute of Phosphate Research. This support as well as the permission to publish the data is gratefully acknowledged. Throughout the work reported in this paper, the last author was at BCI of Lakeland, Fla.

## APPENDIX I. REFERENCES

Abu-Hejleh, A. N., and Znidarčić, D. (1992). "User manual for computer program SICTA." *Rep. Prepared for FIPR*, Dept. of Civ. Engrg., Univ. of Colorado. Boulder. Colo.

Abu-Hejleh, A. N., Znidarčić, D., and Robertson, A. (1992). "Results of seepage induced consolidation tests on phosphatic clays." *Rep. Prepared for FIPR*, Dept. of Civ. Engrg., Univ. of Colorado, Boulder, Colo.

Abu-Hejleh, A. N. (1993). "Desiccation theory for soft soils," PhD dissertation, Dept. of Civ. Engrg., Univ. of Colorado, Boulder, Colo.

Abu-Hejleh, A. N., and Znidarčić, D. (1994). "Estimation of the consolidation constitutive relations." *8th Int. Conf. on Comp. Methods and Adv. in Geomech. (IACMAG94)*, H. J. Siriwardane and M. M. Zaman, eds., Morgantown, W.Va., 499–504.

Aiban, S. A., and Znidarčić, D. (1989). "Evaluation of the flow pump and constant head techniques for permeability measurements." *Géotechnique*, London, U.K., 39(4), 655–666.

Al-Tabbaa, A., and Wood, D. M. (1987). "Some measurements of the permeability of kaolin." *Géotechnique*, London, U.K., 37(4), 499–503.

Alva-Hurtado, J. E., and Selig, E. T. (1981). "Survey of laboratory devices for measuring soil volume change." ASTM *Geotech. Testing J.*, 4, 11–18.

Been, K., and Sills, G. C. (1981). "Self-weight consolidation of soft soils: an experimental and theoretical study." *Géotechnique*, London, U.K., 31(4), 519–535.

Cargill, K. W. (1986). "The large strain consolidation controlled rate of strain (LSCRS) device for consolidation testing of soft fine-grained soils." *Tech. Rep. GL-86-13*, U.S. Army Engineer Waterways Experiment Station, Vicksburg, Miss.

Carrier, W. D., Bromwell, L. G., and Somogyi, F. (1983). "Design capacity of slurried mineral waste ponds." *J. Geotech. Engrg. Div.*, ASCE, 109(5), 699–716.

Dennis, J. E., and Schnabel, R. B. (1983). "Numerical methods for unconstrained optimization." *Series in computational mathematics*, Prentice-Hall, Englewood Cliffs, N.J.

Gibson, R. E., England, G. L., and Hussey, M. H. L. (1967). "The theory of one-dimensional consolidation of saturated clays, I. finite nonlinear consolidation of thin homogeneous layers." *Géotechnique*, London, U.K., 17(3), 261–273.

Huerta, A., Kriegsmann, G. A., and Krizek, R. J. (1988). "Permeability and compressibility of slurries from seepage-induced consolidation." *J. Geotech. Engrg.*, ASCE, 114(5), 614–627.

Imai, G. (1979). "Development of a new consolidation test procedure using seepage force." *Soils and Found.*, Tokyo, Japan, 19(3), 45–60.

Liu, J. C. (1990). "Determination of soft soil characteristics," PhD dissertation, Dept. of Civ. Engrg., Univ. of Colorado, Boulder, Colo.

Liu, J. C., and Znidarčić, D. (1991). "Modelling one-dimensional compression characteristics of soils." *J. Geotech. Engrg.*, ASCE, 117(1), 162–169.

McVay, M., Townsend, F., and Bloomquist, D. (1986). "Quiescent consolidation of phosphatic waste clays." *J. Geotech. Engrg.*, ASCE, 112(11), 1033–1049.

Sills, G. C., Hoare, S. D. L., and Baker, N. (1984). "An experimental assessment of the restricted flow consolidation test." *Oxford Univ. Engrg. Rep. SM052/84*, Oxford Univ., Oxford, U.K.

Somogyi, F. (1979). "Analysis and prediction of phosphatic clay consolidation: implementation package." *Tech. Rep.*, Florida Phosphatic Clay Res. Proj., Lakeland, Fla.

You, Z. (1993). "Flow channeling in soft clay and its influence on consolidation," PhD dissertation, Dept. of Civ. Engrg., Univ. of Colorado, Boulder, Colo.

Znidarčić, D. (1982). "Laboratory determination of consolidation properties of cohesive soils," PhD dissertation, Dept. of Civ. Engrg., Univ of Colorado, Boulder, Colo.

Znidarčić, D., Schiffman, R. L., Pane, V., Croce, P., Ko, H. Y., and Olsen, H. W. (1986). "The theory of one-dimensional consolidation of saturated clays: V, constant rate of deformation testing and analysis." *Géotechnique*, London, U.K., 36(2), 227–237.

Znidarčić, D., and Liu, J. C. (1989). "Consolidation characteristics determination for dredged materials." *Proc., 22nd Annu. Dredging Seminar*, Ctr. for Dredging Studies, Texas A&M Univ., College Station, Tex., 45–65.

Znidarčić, D., Abu-Hejleh, A. N., Fairbanks, T., and Robertson, A. (1992). "Seepage induced consolidation test, equipment description and user's manual." *Rep. Prepared for FIPR*, Dept. of Civ. Engrg., Univ. of Colorado, Boulder, Colo.

## APPENDIX II. NOTATION

*The following symbols are used in this paper:*

$A, B, Z, C, D$ = consolidation constitutive parameters;
$A_s$ = sample area;
$DR$ = deposition rate of solid wastes;
$e$ = void ratio;
$e_c$ = measured void ratio in the loading test;
$e_0$ = zero effective stress void ratio;
$F$ = filling period;
$G_s$ = specific gravity of solids;
$H_f$ = measured height of the sample in steady-state seepage-induced consolidation test;
$H_{fn}$ = numerical prediction of $H_f$;
$H_s$ = height of solids in sample or soil layer;
$H_0$ = initial height of unconsolidated sample or soil layer;
$k$ = coefficient of permeability;
$k_c$ = measured coefficient of permeability in permeability test;
$Q$ = total normalized difference;
$T_c$ = age of waste deposit;
$v$ = applied water flux across sample;
$W_d$ = dry weight of sample;
$z$ = material coordinate;
$\gamma_w$ = unit weight of water;
$\Delta P_s$ = pressure difference across sample in steady-state seepage-induced consolidation test;
$\sigma'_b$ = measured bottom effective stress in steady-state seepage-induced consolidation test;
$\sigma'_{bn}$ = numerical prediction of $\sigma'_b$;
$\sigma'_c$ = measured vertical effective stress in loading test;
$\sigma'_v$ = vertical effective stress; and
$\sigma'_0$ = vertical effective stress on top of sample.

# DESICCATION THEORY FOR SOFT COHESIVE SOILS

By A. Naser Abu-Hejleh[1] and Dobroslav Znidarčić,[2] Associate Members, ASCE

**ABSTRACT:** A new desiccation theory is developed that provides a rational framework for the consolidation and desiccation analysis of soft fine-grained waste soils. The theory includes four consecutive segments that correspond chronologically to the phases that a soft soil layer undergoes in the field after deposition: consolidation under one-dimensional compression; desiccation under one-dimensional shrinkage: propagation of vertical cracks and tensile stress release; and desiccation under three-dimensional shrinkage. A general form of the finite strain governing equation of the overall consolidation and desiccation process is formulated. It includes the cracking function and the nonlinear constitutive relations. The experimentally obtained consolidation and desiccation characteristics for soft china clay. which are needed for the overall analysis of a given field problem, are presented. The predictions of this theory for the response of a hypothetical soft china clay layer undergoing self-weight consolidation, seepage consolidation, and desiccation due to lowering of the ground-water level or surface drying are presented and discussed.

## INTRODUCTION

Significant amounts of slurried fine-grained waste soils are produced in the mining and dredging operations and deposited hydraulically in large disposal facilities. For example, more than 50,000,000 t (dry weight) of highly plastic phosphatic clays are produced annually in Florida's phosphate industry (Carrier et al. 1983). Quantities of sediments, approaching 400,000,000 $m^3$ are dredged annually from the navigable waterways of the United States (Poindexter and Walker 1988). These and other soft wastes have unconventional consolidation properties such as high water content, high compressibility, and low strength and permeability. Hence, densification of the waste is required either at the time of deposition or later. The densification maximizes the disposal-site capacity, stabilizes the disposal-facility structure, and allows for the reclamation of the disposal site for subsequent land use by increasing the soil shear strength and reducing the long-term settlements. Out of several densification techniques reported (Johnson et al. 1977; Mitchell 1988), desiccation due to surface drying and lowering of the ground-water level is of interest in the present paper.

Due to desiccation, the surface of the soil layer settles, and cracks initiate and propagate downward forming cracked soil columns with a desiccated surface crust. According to Blight (1988), surface drying has the effect of considerably reducing the void ratio of the deposited slurry materials and increasing the solid storage capacity of the impoundments. East et al. (1987) argued that surface drying can fully consolidate the slurry soil during the subaerial deposition (i.e., when the surface water on the top of the soil layer is removed), thus reducing the long-term settlement to a minimum. Often, the reclamation operations for soft cohesive waste-disposal sites require the development of a desiccated surface crust with an adequate strength in order to support workers and equipment (Carrier and Bromwell 1983; Johnson et al. 1977). The depth of the surface crust depends on the climatic conditions (i.e., evaporation rate), the final ground-water level, and vegetation (Mitchell 1988).

There are many reasons why a rational method to predict the response and behavior of soft cohesive soils undergoing desiccation is needed. First, the available models in the literature for the analysis of desiccation of soft soils are empirical or semiempirical. For example. Swarbrick and Fell (1992) described a semiempirical one-dimensional model of sedimentation and desiccation that includes restrictive assumptions, such as a uniform distribution of water content with depth throughout the desiccation process. The U.S. Army Engineer Waterways Experiment Station (WES) model (Cargill 1985) is also empirically based and can be used only in a limited number of field situations. Second, only a few oversimplified models for the three-dimensional shrinkage are available. For example, the Bronswijk (1988) model might be applicable only for relatively stiff soils, where small strains occur and the changes in the total vertical stresses are negligible. These conditions are unjustified for modeling three-dimensional shrinkage of soft fine-grained soils. For example, McNeilan and Skaggs (1988) reported observations for a dried-out surface of a hydraulic landfill in Los Angeles. Orthogonal desiccation crack patterns with 0.3-m width and as much as 1.5-2.1m depth were noted, and the total settlement in the softest area of the landfill from spring 1983 to spring of 1987 was 1.8 m. Third, a complete study on desiccation cracking of soft soils or a model that incorporates the desiccation cracking analysis in the transition from one-dimensional to three-dimensional shrinkage is not described in the literature. Fourth. the constitutive and cracking relations for soft fine-grained soils undergoing desiccation are not reported in the literature. For all these reasons, many researchers stressed the need for more work in the area of desiccation of soft soils (Johnson et al. 1977).

A new theory for modeling the overall consolidation and desiccation process of soft fine-grained soils after deposition was developed (Abu-Hejleh 1993). It eliminates all the stated shortcomings of existing studies. The theory was implemented in a finite-element computer program, and laboratory tests were developed to provide all the necessary desiccation constitutive relations for soft cohesive soils. The present paper describes the main components of the theory and the experimentally obtained consolidation and desiccation characteristics for soft china clay that are needed for the overall analysis. The predictions for the response of a hypothetical soft china clay layer undergoing self-weight consolidation, seepage consolidation, and desiccation due to lowering of the ground-water level or surface drying are also included.

## THEORETICAL DEVELOPMENT

While the proposed desiccation theory overcomes most of the limitations of existing analyses reported in the literature. several assumptions were used in order to proceed with the

[1]Res. Assoc., Dept. of Civ., Envir. and Arch. Engrg., Univ. of Colorado, Boulder, CO 80309.

[2]Assoc. Prof., Dept. of Civ., Envir. and Arch. Engrg., Univ. of Colorado, Boulder, CO.

Note. Discussion open until November 1, 1995. To extend the closing date one month, a written request must be filed with the ASCE Manager of Journals. The manuscript for this paper was submitted for review and possible publication on July 2, 1993. This paper is part of the ***Journal of Geotechnical Engineering,*** Vol. 121. No. 6, June, 1995, ©ASCE, ISSN 0733-9410/95/00066-0493-0502/$2.00 + $.25 per page. Paper No. 6369.

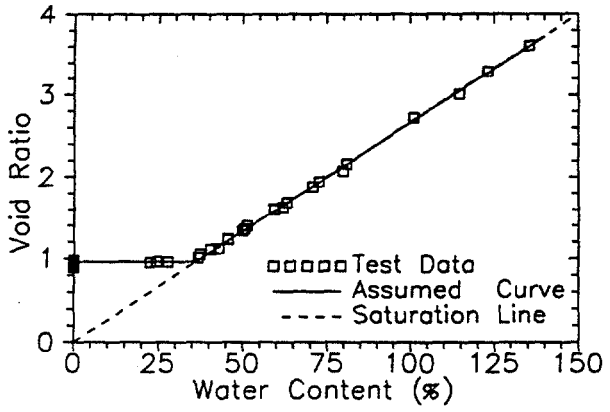


**FIG. 1. Shrinkage Curve for China Clay**

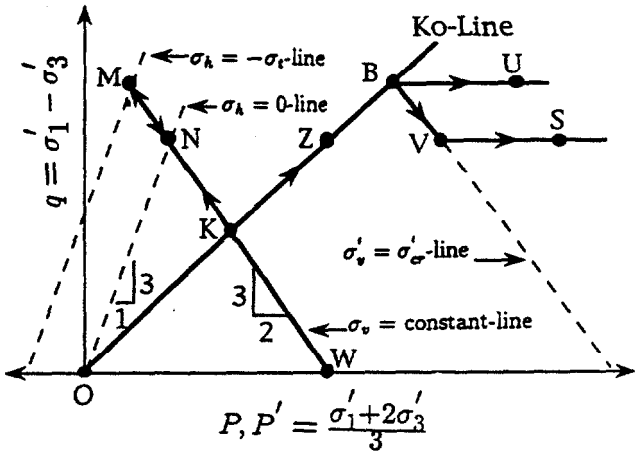


**FIG. 2. Total and Effective Stress Paths during Overall Consolidation and Desiccation Process**

analysis for solving this complex problem and to provide a practical approach for analyzing soft waste-disposal sites. First, the theory is based on the assumption that soft fine-grained soils undergoing desiccation remain saturated until the void ratio reaches the shrinkage limit void ratio, that is, the void ratio at which soil shrinkage is terminated. Thereafter, the desiccated soil becomes rigid and its response is not modeled in the present theory, The experimental results obtained by Bronswijk (1988) show that soils with high clay content (cohesive soils) remain staurated over a wide range of water contents during desiccation and low clay content soils show residual shrinkage; that is, the reduction in soil volume is smaller than the water volume lost during the desiccation process. Fox (1964) reported that air entered a desiccated clay sample at a suction of 1.000 kPa, whereas Yule and Ritchie (1980) gave a value of 1.500 kPa. The experimentally obtained shrinkage data, void ratio versus water content, for soft china clay are shown in Fig. 1. They suggest that soil shrinkage can be modeled with two stages: (1) normal shrinkage. where the soil remains saturated from the initial void ratio to the shrinkage limit void ratio, $e = 0.96$; and (2) zero shrinkage. where the soil does not show any volumetric change from the shrinkage limit void ratio to the end of the desiccation process. Consequently, this assumption can be justified for soft fine-grained soils, which are of primary interest in the present paper. since this type of material undergoes a large volume decrease when the moisture content is reduced (Johnson et al. 1977).

Second. the theory considers a homogeneous soil that does not vary in properties from point to point horizontally, which is a common assumption in many theories. This assumption allows for modeling a simultaneous development of desiccation cracks at different locations, which propagate vertically to the same crack depth forming cracked soil columns with equal crack spacing (Lachenbruch 1962).

Third, the soil skeleton exhibits no intrinsic time effects with incompressible water and solid phases, which is assumed in most classical small- and large-strain consolidation analyses (McVay et al. 1986). For soft soils undergoing desiccation, the presented assumptions allow for the application of the effective stress principle and allow the material constitutive relations to be a function of the void ratio only for a given stress path (Gibson et al. 1967).

Fourth, during the overall consolidation and desiccation process. the lateral and vertical planes through any point in the cracked and the uncracked soil columns are principal planes (Miller 1975). This assumption simplifies the analysis of three-dimensional shrinkage, as is discussed in subsequent sections of the present paper.

The overall consolidation and desiccation process of soft soils is modeled in the theory with four consecutive segments. which correspond chronologically to the phases that a soft soil layer undergoes in the field after deposition. These phases are consolidation under one-dimensional compression, one-dimensional shrinkage, propagation of desiccation vertical cracks with tensile stress release, and three-dimensional shrinkage. The total and effective stress paths during these four phases for a typical soil element are presented in Fig. 2. At the beginning of the consolidation process, when the effective stresses acting on the slurry soil element are zero, the element is at the effective stress state O and the total stress state W. The initial positive pore-water pressure acting on the soil element, equal to the total vertical stress, is the distance on the graph between the total stress state W and the effective stress state O. Due to consolidation and desiccation, this initial positive pore-water pressure decreases. While the stress paths are presented in the following for an element experiencing a constant total vertical stress. the theory is not restricted to this case and the analysis properly accounts for the change in the total vertical stresses throughout the consolidation-desiccation process.

In the development of this theory, it is convenient to consider the soil deformation as consisting of two components. One is associated with the change in the pore-water pressure. and the other results from the change in total stresses. The first is termed free strain, since it is the only strain component that occurs during desiccation of unconfined soil element, and the other is termed the mechanical strain, The sum of free and mechanical strains is the net strain, which arises due to change in effective stresses. Before the initiation of cracks, the net lateral strain for any soil element remains zero, and so the effective stress path during consolidation and desiccation must follow $K_0$ line where $K_0$ is the coefficient of lateral earth pressure at rest. Due to the reduction of pore-water pressure, the lateral total stress decreases, while, for illustration purposes only, the total vertical stress is assumed to remain constant. Therefore, the total stress path at this phase has a slope of -3/2 in the coordinate system shown in Fig. 2.

Along the total stress path WK and effective stress path OK, the pore-water pressure remains positive, and thus consolidation under one-dimensional compression takes place. Along the total stress path KM and the effective stress path KB, the pore-water pressure is negative while the soil undergoes one-dimensional shrinkage. For modeling the consolidation process, the compressibility and permeability relations are defined as

$$\sigma'_v = F_1(e);\ k = Q_1(e) \quad (1)$$

where $\sigma'_v$ = vertical effective stress; $e$ = void ratio; and $k$ = coefficient of permeability. The constitutive relations needed for modeling the one-dimensional shrinkage are

$$\sigma'_v = F_2(e);\ k = Q_2(e) \quad (2)$$

Soils start cracking during one-dimensional shrinkage when total lateral tensile stress at the crack tip reaches the soil tensile strength

$$-\sigma_h = \sigma_t \quad (3)$$

where $\sigma_h$ = total lateral stress; and $\sigma_t$ = tensile strength. The lateral mechanical tensile strain and the corresponding total lateral tensile stress are developed during one-dimensional shrinkage, since zero net lateral strain is maintained. This type of restraint causes the development of shrinkage cracks in concrete (Penev and Kawamura 1993) and in permafrost regions (Lachenbruch 1962). Corte and Higashi (1964) used (3) to predict the development of desiccation cracks in soft soil samples. Lambe and Whitman (1969) used (3) to predict the crack depth due to lowering of the ground-water level for a normally consolidated soil layer that has a zero tensile strength. In a soil having no tensile strength, vertical desiccation cracks can open only when the total lateral stress vanishes, that is, only atmospheric pressure acts on the face of an open crack. Thus, the total stress state for this case is at N, which is on the $\sigma_h = 0$ line (Fig. 2). However, the effective stress state is at Z, where the lateral effective stress is compressive and equal to the suction (negative pore-water pressure) at the moment the cracks open. If the soil possesses some tensile strength, a larger suction is needed to create cracks. In this case, the cracking criterion is reached at the total stress state M and the effective stress state B, as shown in Fig. 2. At that point, the soil element is at the cracking void ratio $e_{cr}$ and the cracking vertical effective stress $\sigma'_{cr} = F_2(e_{cr})$.

The lateral effective stress is equal to $K_0\sigma'_v$, and the pore-water pressure is equal to $\sigma_v - \sigma'_v$. The lateral tensile stress $-\sigma_h$ at any depth is thus related to the vertical effective stress and the total vertical stress by

$$\sigma_h = \sigma_v + (K_0 - 1)\sigma'_v \quad (4)$$

Hence, a crack at any depth, which is characterized by a total vertical stress $\sigma_v$, initiates once the void ratio at that depth is reduced enough to reach the cracking void ratio $e_{cr}$, which can then be related to the total vertical stress by a cracking function $G$

$$e_{cr} = G(\sigma_v) \quad (5)$$

The cracking function is determined from (3) and (4) and the $e$-$\sigma'_v$ relation during one-dimensional shrinkage.

Theoretically, the cracks should develop at the surface and propagate downward simultaneously and uniformly for a homogeneous soil layer. However, reported field observations indicate that a network of more or less regularly spaced cracks develops. Their spacing and pattern is influenced by small lateral variations in material characteristics (Lachenbruch 1962; Corte and Higashi 1964). Such variations should be expected in any natural soil deposit. At the beginning of crack opening, a fracture zone of small thickness develops in the weakest points of the soil layer, where the cracks later develop, and the soil is unloaded elastically from the lateral total tensile stresses outside the fracture zone (the unfractured zone), which later forms the cracked soil column. In the fracture zone, the total lateral tensile stress starts to decrease, and once this stress drops to zero (at point N in Fig. 2), the cracks fully develop or open, and the cracked soil columns separate completely (Abu-Hejieh 1993. Hillerborg et al. 1976). The total lateral tensile stresses in the fractured and unfractured zones drop uniformly. so that no lateral and vertical shear stresses arise in the soil mass during and after the development of cracks. Therefore, the drop of total lateral tensile stresses in any vertical plane during the development of cracks can be represented by the total stress path MN in Fig. 2. where the total stress state N indicates that the cracked soil columns are free from lateral stresses. Assuming that no suction changes occur during the development of cracks. the effective stress path during the tensile stress release can be represented by BV, which is parallel to the total stress path MN as shown in Fig. 2.

Along path MN or BV, the soil layer is unloaded, and any associated volumetric changes could be neglected. This is a realistic assumption for desiccation of soft soils, for which these unloading strains are much smaller than the large strains during loading. Furthermore, these strains are insignificant when compared to those caused by a change in suction during three-dimensional shrinkage along effective stress path VS. Neglecting the volumetric changes during the development of cracks implies that the desiccation cracks initiate and open at the same void ratio $e_{cr}$. Eq. (5) can be used to calculate the distribution of $e_{cr}$ along depth characterized by total vertical stress $\sigma_v$. With the known void ratio distribution e in the soil column (from the solution of the governing equation), the cracks propagate to a depth where $e = e_{cr}$. This depth defines the horizontal boundary between the cracked ($e < e_{cr}$) and uncracked ($e > e_{cr}$) soil columns.

Neglecting the volumetric changes during the development of cracks implies also that the three-dimensional shrinkage in the cracked soil columns can be represented with the incremental isoptropic effective stress path BU shown in Fig. 2. This "free" three-dimensional shrinkage is attributed to change in suction only under a constant total vertical stress. For soil elements under different total vertical stresses, consolidation and desiccation follow the $K_0$ line up to cracking, and then three-dimensional shrinkage starts at different values of $e_{cr}$ [determined by (5)] and $\sigma'_{cr}$ [determined as $F2(e_{cr})$], and continues along different incremental isotropic effective stress paths. Some difference in the constitutive relations for one-dimensional shrinkage along the $K_0$ line and three-dimensional shrinkage along the incremental isotropic effective stress paths could be expected. One-dimensional shrinkage should produce a more dispersed structure with the parallel orientation of the particles, while during the three-dimensional shrinkage a flocculated structure could be expected, since lower shear stresses should develop at the particle interfaces. Thus, unlike the unique void ratio-vertical effective stress relation used to represent the compressibility relation along the $K_0$ compression line, the void ratio-vertical effective stress relations along different incremental isotropic effective stress paths are expected to be a function of the void ratio at which the three-dimensional shrinkage starts

$$\sigma'_v = F_3(e, e_{cr}) \quad (6)$$

The compressibility functional predicts only the current void ratio during three-dimensional shrinkage. Another functional, $\alpha(e, e_{cr})$, is defined to characterize the proportion of vertical and lateral deformations along the incremental isotropic effective stress paths from the beginning of three-dimensional shrinkage where $e = e_{cr}$ to a current void ratio $e$ (e.g., from state B to state U in Fig. 2). For a soil element with a unit initial area and a unit solid volume, the three-dimensional free shrinkage reduces its volume from $1 + e_{cr}$ to $1 + e$ and the height from $1 + e_{cr}$ to $(1 + e_{cr})$ $[1 - \varepsilon_v(e, e_{cr})]$, where $\varepsilon_v(e, e_{cr})$ is the vertical strain from the beginning of three-dimensional shrinkage. Functional $\alpha(e, e_{cr})$ is defined

as the area of this element, or the volume of this element over its height

$$\alpha(e, e_{cr}) = \frac{1 + e}{(1 + e_{cr})[1 - \varepsilon_v(e, e_{cr})]} \tag{7}$$

Note that $\alpha$ is equal to unity (area) during consolidation and desiccation up to cracking. If $e_{cr}$ and $e$ can be determined at any depth during three-dimensional shrinkage and used to determine $\alpha(e, e_{cr})$, the specific area of cracks at that depth, defined as the area of cracks per unit area, can be predicted by

$$S_c(e, e_{cr}) = 1 - \alpha \tag{8}$$

## Formulation of Governing Equation

The derivation of the governing equation for the overall consolidation and desiccation process follows the lines of Gibson et al. (1967). The main difference is the treatment of the desiccation process under three-dimensional shrinkage. The soil column at the origin of time $t = 0$ and the deformed soil column at some subsequent time $t$ are shown in Figs. 3 (a and b). respectively. As shown in these figures, the vertical Lagrangian (initial) and current coordinates, designated as $a_1$ and $\xi_1$, respectively, are taken positive against the gravity from a reference datum plane, where the vertical deformations are zero; and the reference datum plane for the lateral (radial) Lagrangian and current coordinates, designated as $a_2$ and $\xi_2$, respectively, are taken from the centerline of the soil columns, where the lateral deformations are zero. The derivation is presented for an element WXYZ in the initial and deformed soil columns whose boundaries always encompass the same volume of soil solid particles. At $t = 0$, the soil element is located at the Lagrangian coordinate $a_1$, has a unit area, a thickness of $\delta a_1$ and a void ratio of $e_i$. The deformed soil element at time t is located at the current coordinate $\xi_1$, has an area equal to a (see the definition of a), a thickness of $\delta\xi_1$, and a current void ratio of $e$. Since the same volume of solids is encompassed by the element in the initial and current conditions

$$\frac{\delta a_1}{1 + e_i} = \frac{\alpha\delta\xi_1}{1 + e} \tag{9}$$

Thus, for an infinitesimal element, (9) is reduced to

$$\frac{\partial a_1}{\partial \xi_1} = \frac{\alpha(1 + e_i)}{(1 + e)} \tag{10}$$

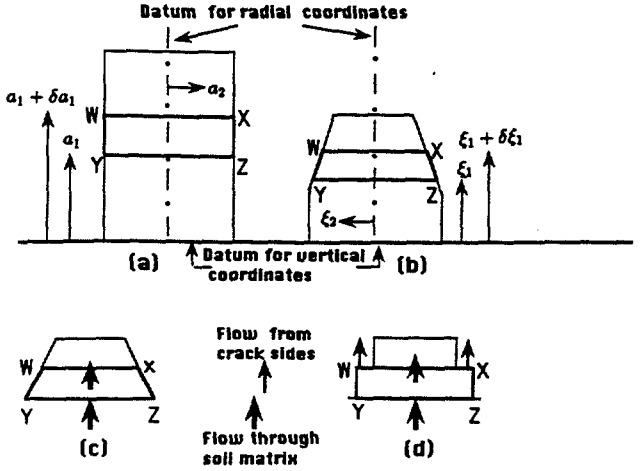


FIG. 3. Soil Element in Initial and Current Coordinate Systems

The equilibrium equation, the flow equation. the effective stress principle, and the continuity equation are used in the derivation of the governing equation.

Since no lateral shear stresses develop in the soil mass during three-dimensional shrinkage, the total vertical stresses are equal at all radii of the soil column. The vertical equilibrium equation is given as

$$\frac{\partial \sigma_v}{\partial \xi_1} = -\gamma = -\frac{\frac{\alpha\delta\xi_1}{1 + e}(\gamma_s + e\gamma_w)}{\alpha\delta\xi_1} = -\frac{e\gamma_w + \gamma_s}{1 + e} \tag{11}$$

where $\gamma$, $\gamma_w$ and $\gamma_s$ = unit weights of water-solid mixture, water phase, and solid phase, respectively. With (10), the equilibrium equation in Lagrangian coordinate system is obtained as

$$\frac{\partial \sigma_v}{\partial a_1} = -\frac{(e\gamma_w + \gamma_s)}{\alpha(1 + e_i)} \tag{12}$$

The principle of effective stress is

$$\sigma_v' = \sigma_v - u = \sigma_v - u_s - u_e \tag{13}$$

where $u$ = pore-water pressure, which is the sum of the static pore-water pressure, $u_s$ and the excess pore water $u_e$. Note that $\partial u_s/\partial\xi_1 = -\gamma_w$.

Using Darcy's Law in terms of the apparent relative velocity between the water and solid phases (Gibson et al. 1967), the flow equations in the vertical and lateral directions are given by

$$q_1 = n(v_{w1} - v_{s1}) = -\frac{k}{\gamma_w}\frac{\partial u_e}{\partial \xi_1};$$

$$q_2 = n(v_{w2} - v_{s2}) = -\frac{k}{\gamma_w}\frac{\partial u_e}{\partial \xi_2} \tag{14}$$

where $q_1, q_2$ = apparent relative velocities between the water and solid phases in the vertical and lateral directions, respectively; $n$ = porosity; $v_{w1}$ and $v_{s1}$ = velocities of the water and solid phases in the vertical direction; and $v_{w2}$ and $v_{s2}$ = velocities of the water and solid phases in the lateral direction. The $v_{s2}$ and $v_{w2}$ are zero during consolidation and desiccation up to cracking, and are assumed equal to each other during three-dimensional shrinkage, so that the relative flow velocity between the water and solid phases in the lateral direction $q_2$ is always zero. Consequently, the excess pore-water pressures as well as the vertical effective stresses are equal at all radii of the cracked and uncracked soil columns. The flow equation in the vertical Lagrangian coordinate system can be obtained from (14), (13), and (10) as

$$q_1 = -k - \frac{k}{\gamma_w}\frac{\alpha(1 + e_i)}{(1 + e)}\left(\frac{\partial \sigma_v}{\partial a_1} - \frac{\partial \sigma_v'}{\partial a_1}\right) \tag{15}$$

From (6)

$$\frac{\partial \sigma_v'}{\partial a_1} = \frac{\partial \sigma_v'}{\partial e}\frac{\partial e}{\partial a_1} + \frac{\partial \sigma_v'}{\partial e_{cr}}\frac{de_{cr}}{d\sigma_v}\frac{\partial \sigma_v}{\partial a_1} \tag{16}$$

By substituting (16) and (12) in (15), $q_1$ can be expressed as

$$q_1 = -k + \frac{k}{\gamma_w}\frac{(e\gamma_w + \gamma_s)}{1 + e}\left(1 - \frac{\partial \sigma_v'}{\partial e_{cr}}\frac{de_{cr}}{d\sigma_v}\right) + \frac{k}{\gamma_w}\frac{\alpha(1 + e_i)}{(1 + e)}\frac{\partial \sigma_v'}{\partial e}\frac{\partial e}{\partial a_1} \tag{17}$$

For any values of $e$ and $e_{cr}$, $\partial\sigma_v'/\partial e_{cr}$ and $\partial\sigma_v'/\partial e$ can be determined from (6). and $de_{cr}/d\sigma_v$ can be determined from (5). The $\partial\sigma_v'/\partial e_{cr}$ arises from the fact that the void ratio-effective stress relation is not a unique function for the material during

three-dimensional shrinkage but depends on the void ratio at which the three-dimensional shrinkage starts. Thus, in calculating the gradient of the effective stress, the chain rules of derivatives are observed.

Finally, the continuity equation of the mixture of water and solid phases is derived for element WXYZ. This element is deforming in the space with a speed of $\partial\xi_1/\partial t$ in the vertical direction and a speed of $\partial\xi_2/\partial t$ in the lateral direction. Since the volume of solids in this element does not change with time, that is, no solid flows into or out of the element in the vertical and lateral directions, it is required that $v_{s1} = \partial\xi_1/\partial t$ and $v_{s2} = \partial\xi_2/\partial t$. Also, since $v_{w2} = v_{s2}$, there is no flow of water into or out of element WXYZ in the lateral direction. The volume of water that flows into the element shown in Fig. 3(c) through section YZ in a period of $\delta t$ is

$$\alpha n(v_{w1} - v_{s1})\delta t = \alpha q_1 \delta t \tag{18}$$

and the volume of water that flows out of the element through section WX is

$$\alpha q_1 \delta t + \frac{\partial(\alpha q_1)}{\partial \xi_1}\delta\xi_1\delta t \tag{19}$$

The volume of water stored in the element over $\delta t$ must equal the net change in the volume of water in the element over $\delta t$, so that

$$-\frac{\partial(\alpha q_1)}{\partial \xi_1}\delta\xi_1\delta t = \frac{\alpha\delta\xi_1}{1+e}\frac{De}{Dt}\delta t \tag{20}$$

where $(\alpha\delta\xi_1 e)/(1+e)$ = volume of water in the element; $(\alpha\delta\xi_1)/(1+e)$ = constant volume of solids in the element; and $De/Dt$ = material derivative of the void ratio (McVay et al. 1986) that models properly the change of void ratio with time for moving soil elements

$$\frac{De}{Dt} = \frac{\partial e}{\partial t} + \frac{\partial e}{\partial \xi_1}v_{s1} + \frac{\partial e}{\partial \xi_2}v_{s2} = \frac{\partial e}{\partial t} + \frac{\partial e}{\partial a_1}\frac{\partial a_1}{\partial t} + \frac{\partial e}{\partial a_2}\frac{\partial a_2}{\partial t} \tag{21}$$

Considering (10) and that $\partial a_1/\partial t = 0$ and $\partial a_2/\partial t = 0$, the continuity equation for the water-solid mixture in the Lagrangian coordinate system can be obtained as

$$\frac{\partial(q_1\alpha)}{\partial a_1} + \frac{1}{(1+e_i)}\frac{\partial e}{\partial t} = 0 \tag{22}$$

Assuming that $\alpha$ is constant across $\delta\xi_1$, as shown in Fig. 3(d), the continuity equation can be simpfilied to

$$\frac{\partial q_1}{\partial a_1} + \frac{1}{\alpha(1+e_i)}\frac{\partial e}{\partial t} = 0 \tag{23}$$

It is considered in the derivation of (22) that there is no flow of water relative to the solid phase across the crack sides [see Fig. 3(c)]. This is not the case with (23) [see Fig. 3(d)], since a flow of $q_1\Delta\alpha$ is lost across the crack sides of the element, where $\Delta\alpha$ is the projected area of the element crack sides in the vertical direction. The condition represented by (22) is suitable for modeling desiccation due to lowering the ground-water level, where the downward water flow is limited to the soil matrix, and the crack sides can be considered impermeable. Since the water is lost through evaporation from both the soil layer surface as well as the crack sides, the condition represented by (23) should be reasonable for modeling desiccation due to surface drying, especially if the evaporation rate from the crack sides is close to the calculated water flux in the soil matrix near to the crack sides. For the former case, it is found that both continuity equations lead to almost identical results, and, therefore, (23) is adopted in the further analysis.

The governing nonlinear partial differential equation can be obtained by combining (17) and (23)

$$\frac{\partial}{\partial a_1}\left[k - \frac{k}{\gamma_w}\frac{(e\gamma_w + \gamma_s)}{1+e}\left(1 - \frac{\partial\sigma'_v}{\partial e_{cr}}\frac{de_{cr}}{d\sigma_v}\right)\right]$$
$$- \frac{\partial}{\partial a_1}\left[\frac{k}{\gamma_w}\frac{\alpha(1+e_i)}{(1+e)}\frac{\partial\sigma'_v}{\partial e}\frac{\partial e}{\partial a_1}\right] = \frac{1}{\alpha(1+e_i)}\frac{\partial e}{\partial t} \tag{24}$$

For the consolidation and desiccation up to cracking, $\alpha = 1$ and the void ratio–effective stress relation is a unique function for the material so that $\partial\sigma'_v/\partial e_{cr} = 0$. Applying these conditions to (24), the equation derived by Gibson et al. (1967) in the finite-strain consolidation theory is obtained

$$-\left(\frac{\gamma_s}{\gamma_w} - 1\right)\left[\frac{d}{de}\left(\frac{k}{1+e}\right)\right]\frac{\partial e}{\partial a_1}$$
$$- \frac{\partial}{\partial a}\left[\frac{k}{\gamma_w}\frac{1+e_i}{(1+e)}\frac{d\sigma'_v}{de}\frac{\partial e}{\partial a_1}\right] = \frac{1}{1+e_i}\frac{\partial e}{\partial t} \tag{25}$$

While (25) models the one-dimensional soil response during the consolidation and desiccation processes in the uncracked soil columns, (24) is the governing equation for the overall consolidation and desiccation process in the cracked and uncracked soil columns.

## EXPERIMENTAL RESULTS

As stated in the theoretical development and in the derivation of the governing equation, several material functions are required in the solution process of a certain field situation. These included three pairs of compressibility and permeability relations for consolidation, desiccation under one-dimensional shrinkage, and desiccation under three-dimensional shrinkage. In addition, the cracking function $G$ and the $\alpha$ functional are required. All of these constitutive and cracking functions are determined from laboratory tests that were developed earlier or from new experiments developed as a part of this research. The void ratio-effective stress and void ratio-permeability relations during the consolidation phase of the process are obtained from the seepage-induced consolidation testing and analysis (Znidarčić and Liu, 1989; Liu, 1990; Abu-Hejieh and Znidarčić, 1994).

The desiccation compressibility and permeability characteristics are obtained from a suction test in which the water is removed from the bottom of a sample in the oedometer using a flow pump to control precisely the outflow rate (Abu-Hejleh 1993). Capillary menisci develop at the sample top, creating an effective stress increase and the corresponding sample compression. Since the sample remains saturated in the test, the sample volume change is equal to the withdrawn volume of water, and this change is used to estimate the sample average void ratio at various testing times. The applied suction at the bottom of the sample is measured with a precision transducer and used to estimate the sample bottom effective stress at various testing times. For the slow withdrawal flow rate, the effective stress within the sample is uniform, and, therefore, the desiccation effective stress-void ratio relation is determined directly from the obtained test results. Desiccation compressibility characteristics along the $K_0$ line are obtained from samples that are laterally confined in order to produce one-dimensional shrinkage response only. Desiccation compressibility characteristics along the isotropic effective stress path (after cracking) are obtained from unconfined samples that are allowed to shrink freely in the lateral and vertical directions. To obtain material characteristics for varying cracking void ratios, several preconsolidated samples with different void ratios are prepared and then tested.

A suction test with a higher withdrawal flow rate is performed on the same material in order to produce a measureable pore pressure gradient within the sample. The generated gradient depends on the material permeability characteristics. With the known desiccation effective stress-void ratio relation, the obtained experimental results under the higher flow rate are used to evaluate indirectly the desiccation void ratio-permeability relationship. The test analysis follows the inverse problem solution algorithm equivalent to the one used in the analysis of the seepage induced consolidation test (Abu-Hejleh and Znidarčić 1994).

The obtained void ratio-effective stress relations for soft china clay during consolidation, one-dimensional shrinkage, and three-dimensional shrinkage are presented in Fig. 4. The graphical results indicate that these three relationships are very close to each other and could be assumed identical. The obtained permeability characteristics for soft china clay during consolidation and desiccation under one-dimensional shrinkage are presented in Fig. 5. Again, similar permeability characteristics during consolidation and desiccation can be noticed. While accepting that these two last conclusions lead to a simpler analysis, the obtained results for a single material should not be taken as a general rule. More tests on other soft cohesive materials should be made before general conclusions regarding their consolidation and desiccation behavior is made. The permeability during three-dimensional shrinkage is assumed to have the same permeability-void ratio relationship as during one-dimensional shrinkage. This assumption is justified by the similar compressibility characteristics for the two desiccation phases of the process.

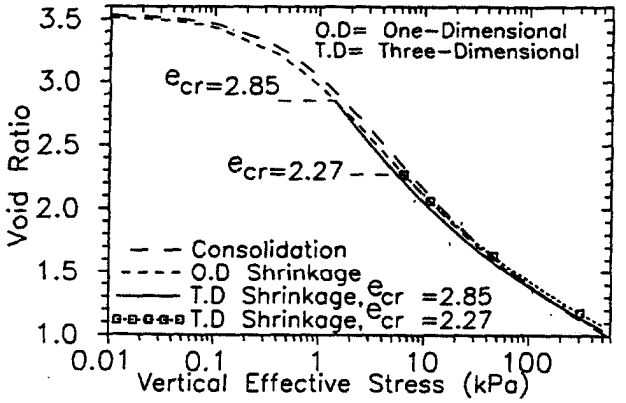


**FIG. 4. Consolidation and Desiccation Compressibility Characteristics for Soft China Clay**

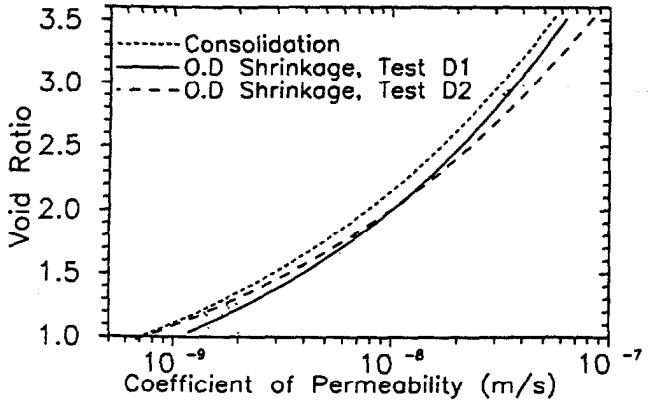


**FIG. 5. Consolidation and Desiccation Permeability Characteristics for Soft China Clay**

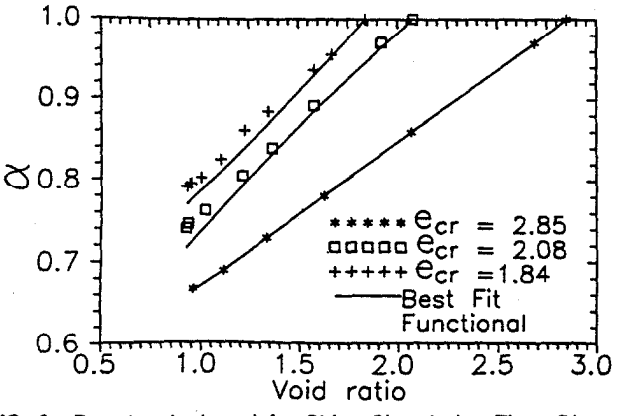


**FIG. 6. Functional $\alpha(e, e_c)$ for China Clay during Three-Dimensional Shrinkage**

To relate the development of the total lateral tensile stresses in china clay to the void ratio and the total vertical stress

The free shrinkage test provides the experimental data needed for the determination of functional a (Abu-Hejleh 1993). In this test, a soil sample is left to shrink vertically and laterally freely without the presence of any external constraint, and both vertical and lateral deformations are measured. Preconsolidated soil samples, with different void ratios, are prepared for this test. The experimentally obtained values of $\alpha(e, e_{cr})$ for three soft china clay samples, with three different initial void ratios, were fitted with an analytical function. Fig. 6 shows the data of a together with the fitted functional.

Finally, the evaluation of the tensile strength function and the corresponding cracking function $G$ are needed in the analysis. The tensile strength, like the shear strength, is a function of the vertical effective stress or void ratio. Its experimental determination is quite difficult and no routine tests exist for its measurement. Thus, the tensile strength is here related to the shear strength that could be determined from routine tests. The factor $F$ is defined as $F = \sigma_t/S_u$, where $S_u$ is the undrained shear strength. For example, the experimentally obtained undrained shear strength-void ratio relation for china clay by Znidarčić et al. (1992) was used to estimate the tensile strength-void ratio relation as

$$\sigma_t = F10^{(1.945 - e/0.435)} \tag{26}$$

The exponential relation between the tensile strength and void ratio in (26) confirms the published data (Williams and Sibley 1992; Farrel et al. 1967). While the lower limit for $F$ is zero, the range of unconfined compressive strength to tensile strength reported by Lau (1987) suggests that an appropriate upper limit value for $F$ is 0.5.

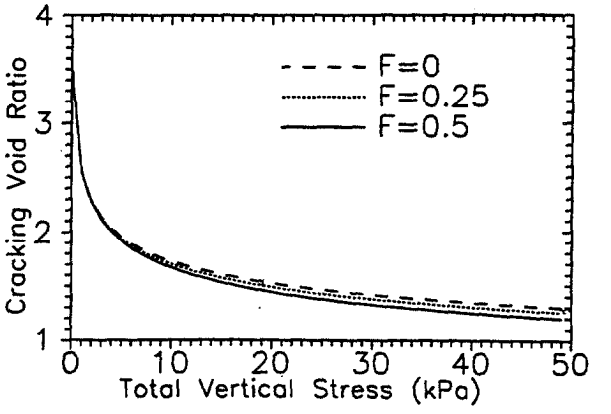


**FIG. 7. Cracking Function for Soft China Clay**

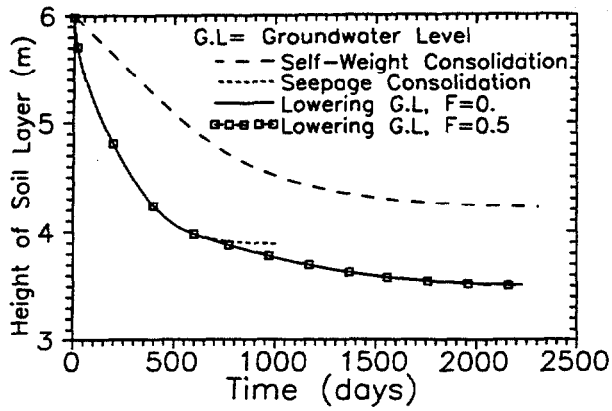


**FIG. 8. Progress of Settlement with Time during Self-Weight Consolidation, Seepage-Induced Consolidation, and Lowering Ground-Water Level**

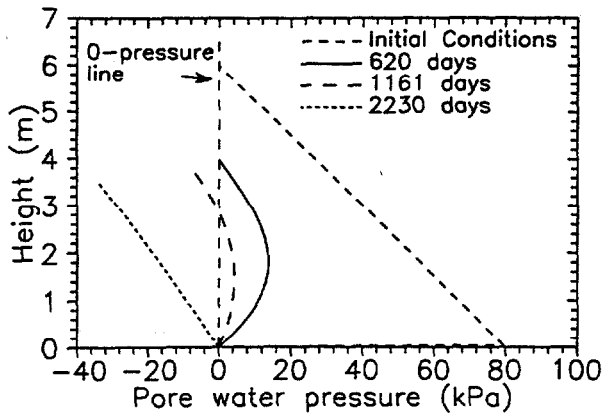


**FIG. 9. Profiles of Pore-Water Pressure during Lowering Ground-Water Level**

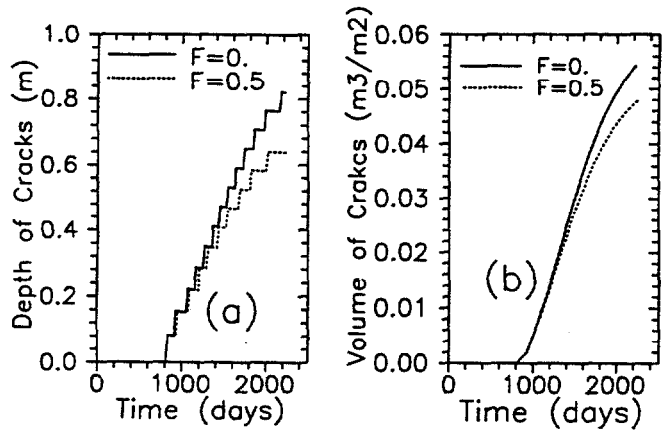


**FIG. 10. Progress of (a) Crack Depth and (b) Volume of Cracks per Unit Area with Time during Lowering Ground-Water Level**

only, the experimentally obtained $K_0$ value of 0.67 (Hutapea et al. 1992) and $e - \sigma'_v$ function during one-dimensional shrinkage are substituted in (4). Subsequently, the cracking function for china clay, $e_{cr} - \sigma_v$. relation, is obtained by substituting (26) and (4) in (3). Graphical forms of the obtained cracking functions for china clay with $F = 0$, $F = 0.25$, and $F = 0.5$ are shown in Fig. 7. Alternatively, the cracking function can be evaluated from desiccation experiments in which a soil sample is allowed to crack during the desiccation process. Since the cracking characteristics are dependent on the stress level, as (5) implies. a convenient way for obtaining these characteristics is to conduct the desiccation experiment in the geotechnical centrifuge under an increased gravity level that properly simulates the stress level in the field.

## EVALUATION OF THEORY

The theory has been implemented in an efficient nonlinear finite-element computer program. called CADA (Consolidation And Desiccation Analysis). The numerical solution predicts profiles of void ratio. cracking void ratio and total vertical stress along the vertical Lagrangian coordinate at each time step. By transforming the coordinates from Lagrangian to the current coordinates as expressed in (10). the settlement-time curve and profiles of effective stress. void ratio. pore-water pressure, and the specific area of cracks along the current depth are determined. The depth of vertical desiccation cracks is determined by the location of $e = e_{cr}$. The specific volume of cracks, defined as the volume of cracks per unit area, is evaluated by the numerical integration of the distribution of specific area of cracks along the crack depth.

A hypothetical soft china clay disposal site was used to demonstrate main features of the theory. The initial height of the soil layer is 6 m and the initial uniform distribution of void ratio corresponds to the zero effective stress void ratio for the soil, $e = 3.53$. The experimentally obtained consolidation and desiccation constitutive relations and cracking function for soft china clay are used in the analysis. Fig. 8 shows the time-settlement curves for the self-weight and seepage-induced consolidation of the layer. For the self-weight consolidation an undrained bottom boundary was assumed. and for the seepage induced consolidation a bottom drainage layer with zero pore pressure was considered. For both cases. zero effective stress void ratio, e = 3.53, is imposed at the top boundary throughout the process. since the soil layer surface should remain covered with water in these two scenarios. The beneficial effect of the bottom drainage layer in accelerating the rate of consolidation is evident in Fig. 8.

### Lowering Ground-Water Level

Fig. 8 also presents the time-settlement curve for the case in which the downward water flow causes the lowering of the ground-water table. Initially, the boundary conditions are equal to those in the seepage-induced consolidation case. Once the upward flow at the top boundary ceases. an impervious boundary is imposed. That reflects the absence of any evaporation from, or additional infiltration into, the soil layer. Capillary suction develops at the surface with time. and the ground-water table with zero pore pressure moves downward. Ultimately, the water table reaches the bottom boundary and the hydrostatic suction distribution is established within the layer. Pore-pressure profiles are presented in Fig. 9. while the development of crack depth and specific volume with time are presented in Figs. 10(a and b). The results show that the suction will develop at the surface after 620 days and that the tensile strength, as related to the $F$-value, has only a slight influence on the progress of settlement as well as on the crack depth and specific volume of cracks,

### Surface Drying

Surface drying is caused by the evaporation at a rate that depends on the climatic conditions at a given site. The evaporation has no effect as long as the upward surface-water flow, resulting from the self-weight consolidation of the soil layer, exceeds the evaporation rate. Once the flow rate drops below the evaporation rate, the desiccation process starts and continues until the top void ratio reaches the shrinkage limit.

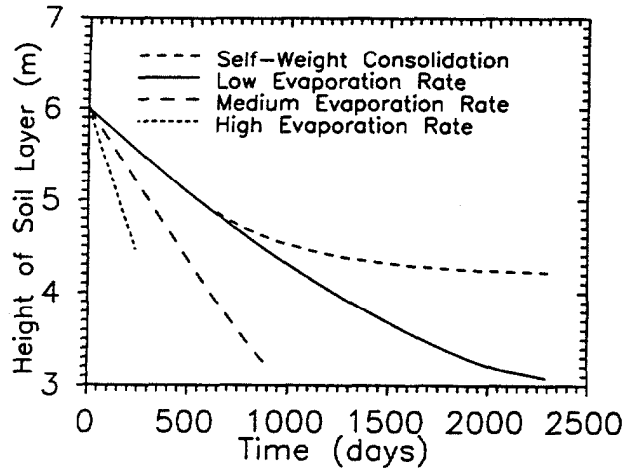


FIG. 11. Progress of Settlement with Time during Self-Weight Consolidation and Surface Drying

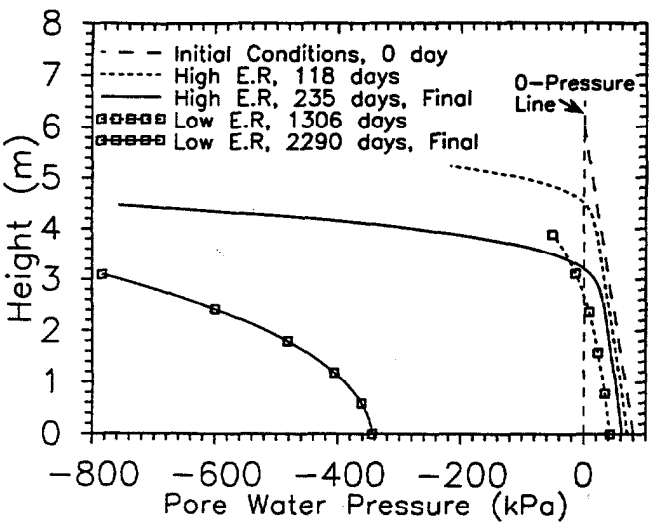


FIG. 12. Profiles of Pore-Water Pressure during Surface Drying

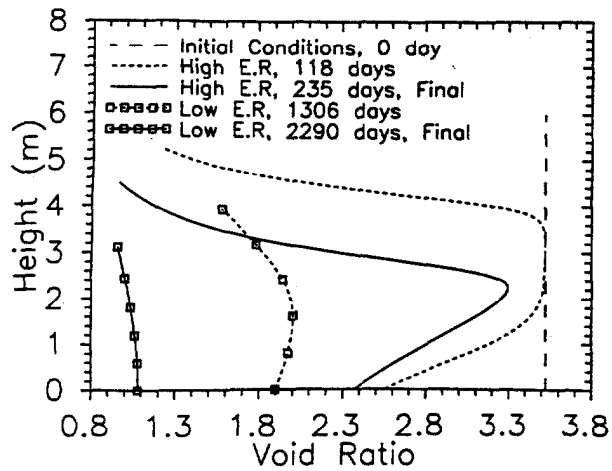


FIG. 13. Profiles of Void Ratio during Surface Drying

At that point, the soil starts to desaturate but without any associated volume change, as demonstrated in the shrinkage curve shown in Fig. 1. The present theory does not model this phase and the numerical analysis is terminated at that point. It should be noted that the actual physical process

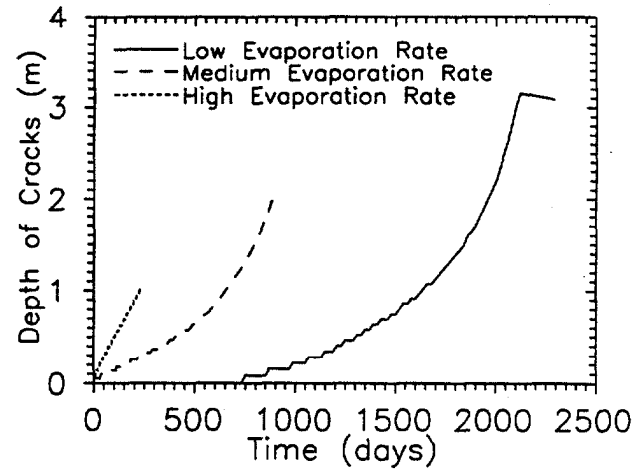


FIG. 14. Progress of Crack Depth with Time during Surface Drying

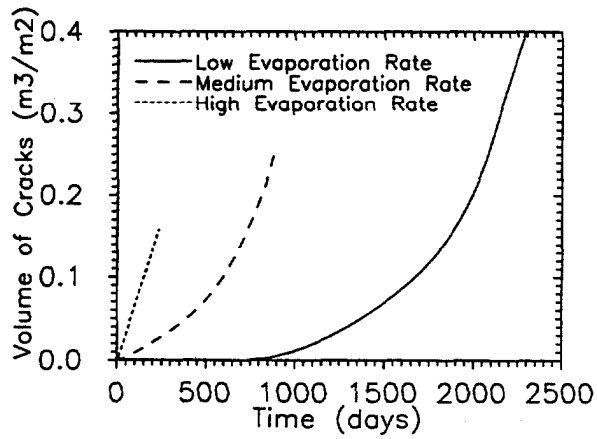


FIG. 15. Progress of Volume of Cracks with Time during Surface Drying

terminates as well, shortly after the shrinkage limit is reached, since the permeability of the desaturated soil at the surface is drastically reduced, creating an impervious crust that prevents further evaporation (Johnson et al. 1977).

The surface drying of the soft china clay layer is modeled with three surface evaporation rates: a low value of 1.87 x $10^{-8}$ m/s, a medium value of 4 x $10^{-8}$ m/s, and a high value of 8.5 x $10^{-8}$ m/s. The bottom boundary is assumed impervious while the top boundary has zero effective stress for the consolidation phase (as in the self-weight consolidation) and an imposed outflow rate equal to the evaporation rate in the desiccation phase. The results of the analyses are presented in Figs. 11-14. The void-ratio and pore-water pressure distributions clearly indicate the creation of a desiccated crust at the soil surface whose thickness and strength (void ratio) depend on the evaporation rate. The slower the evaporation rate, the thicker the crust. The time settlement and the crack-depth curves demonstrate that the shrinkage limit void ratio. $e$ = 0.96, is reached at the surface faster under the higher evaporation rates and that the desiccation process is terminated sooner. This might lead to the apparent paradox that the lower evaporation rate creates a larger overall compression. Again, this is easily explained by the sealing effect of the desiccated crust at the shrinkage limit. For example. as Figs. 11-13 indicate for the high evaporation rate, the desiccated crust can seal the soil surface even before the self-weight consolidation is completed, leaving a soft unconsolidated soil zone under a thin crust and preventing further dissipation of

the excess pore-water pressures. Thus, the higher evaporation rates can have a detrimental effect on the overall consolidation and desiccation process.

As demonstrated in Figs. 14 and 15, the higher evaporation rate creates more-shallow cracks with smaller volume than the lower rate. Since the crack spacing is related directly to the crack depth (Lachenbruch 1962), a thin and highly fractured crust should be expected for this case, and thicker crust with more widely spaced cracks should be expected under the lower evaporation rates. The volume of cracks resulting from surface drying increase with the decrease of the evaporation rate.

## CONCLUSIONS

The described desiccation theory provides a rational framework for the analysis of the overall consolidation and desiccation process of soft fine-grained soil in the field after deposition. The presented experimental results support the fundamental assumptions of the theory. The numerical analysis provides the rate of vertical and lateral deformations for a soil layer undergoing consolidation and desiccation, void-ratio and pore-water pressure distributions throughout the process, and the thickness and strength (from the void ratio) of the desiccated crust that forms at the soil surface.

The presented examples demonstrate that the theory is in qualitative agreement with the reported observation of the behavior of desiccating soil layers. The predicted relation between the evaporation rate and the thickness of the surface crust, as well as the depth and intensity of cracks are confirmed by many field observations (Mitchell 1988; Blight 1988; Johnson et al. 1977; Lachenbruch 1962; Corte and Higashi 1964). However, the quantitative verification of the theory requires additional experimental work in which a soft material is tested to obtain relevant material characteristics, and then the analysis results are compared to a well-controlled model experiment and ultimately to a field case. The centrifuge modeling technique provides an excellent tool for the confirmation, especially in terms of verifying the crack-formation mechanism. Short of an actual well-controlled field case, it is probably the only technique available to study crack development, since the field stress conditions that control crack propagation are properly simulated in the centrifuge models.

Several benefits are envisioned in applying the developed theory to analyzing various strategies in mine and dredging waste disposal. First, the theory can provide information on how to maximize simultaneously the benefits of the self-weight consolidation and desiccation for varying environmental evaporation conditions and slurry deposition rates. The second application is in predicting the strength and thickness of the desiccated crust for the final reclamation of the disposal site as well as in the intermediate stages in the staged filling operations. The third. and possibly the most beneficial, application is in providing a rational tool for evaluating possible aggressive disposal-management strategies prior to their trial implementation in the field. For example, the benefits of intermediate drainage layers sandwiched between the layers during the slurry deposition in accelerating the consolidation process and extending the influence of surface drying to larger depths inside the soil layer could be evaluated.

## APPENDIX I. REFERENCES


Abu-Hejleh, A. N. (1993). "Desiccation theory for soft soils," PhD thesis, University of Colorado, Boulder,Colo.

Abu-Hejleh, A. N., and Znidarčić, D. (1994). "Estimation of the consolidation constitutive relations." *Eighth Int. Conf. on Comp. Methods and Adv. in Geomech. (IACMAG94)*, H. J. Siriwardane and M. M. Zaman, eds., Balkema, Rotterdam, The Netherlands, 499–504.

Blight, G. E. (1988). "Some less familiar aspects of hydraulic fill structures." *Proc., Hydr. Fill Struct., Spec. Conf., Geotech. Spec. Publ. No. 21*, D. J. A. Van Zyl and S. G. Vick, eds., ASCE, New York, N.Y., 1000–1027.

Bronswijk, J. J. B. (1988). "Modelling of water balance, cracking and subsidence of clay soils." *J. Hydr.*, 97, 199–212.

Cargill, K. W. (1985). "Mathematical model of the consolidation desiccation process in the dredged material." *Tech. Rep. D-85-4*, U.S. Army Engineer Waterways Experiments Station, Vicksburg, Miss.

Carrier, W. D., and Bromwell, L. G. (1983). "Disposal and reclamation of mining and dredging wastes." *Proc., Seventh Panam. Conf. on Soil Mech. and Found. Engrg.*, Canadian Geotechnical Society, Lima, Peru, Vol. 2, 727–738.

Carrier, W. D., Bromwell, L. G., and Somogyi, F. (1983). "Design capacity of slurried mineral waste ponds." *J. Geotech. Engrg. Div.*, ASCE, 109(5), 699–716.

Corte, A., and Higashi, A. (1964). "Experimental research on desiccation cracks in soil." *Res. Rep. No. 66.*, U.S. Army Materiel Command, Cold Regions Research & Engineering Laboratory (CRREL), Hanover, N.H.

East, D. R., Haile, J. P., and Dew, H. P. (1987). "Sub-aerial deposition of phosphatic clay wastes." *Symp. on Consolidation and Disposal of Phosphatic and other Waste Clays, Prepared by Dept. of Civ. Engrg., Univ. of Florida*, sponsored by Florida Institute of Phosphate Research, Bartow, Fla.

Farrel, D. A., Greacen, E. L., and Larson, W. E. (1967). "The effect of water content on axial strain in a loam soil under tension and compression." *Soil Science Soc. of Am. Proc.*, 31, 445–450.

Fox, W. E. (1964). "A study of bulk density and water in a swelling soil." *Soil Sci.*, 98, 307–316.

Gibson, R. E., England, G. L., and Hussey, M. H. L. (1967). "The theory of one-dimensional consolidation of saturated clays, I. finite nonlinear consolidation of thin homogeneous layers." *Géotechnique*, 17(3), 261–273.

Hillerborg, A., Modeer, M., and Petersson, P. E. (1976). "Analysis of crack formation and crack growth in concrete by means of fracture mechanics and finite elements." *Cement and Concr. Res.*, 6, 773–782.

Hutapea, B., Znidarčić, D., Ko, H. Y., and Sture, S. (1992). "Drag anchor tests in clay, volume 1: soil property assessment." *Rep. Prepared for Exxon Production Res. Co.*, University of Colorado, Boulder, Colo.

Johnson, S. J., Gunny, R. W., Perry, E. B., and Devay, L. (1977). "State-of-the art applicability of conventional densification techniques to increase disposal area storage capacity." *Tech. Rep. D-77-4, Soils and Pavements Lab.*, U.S. Army Engineer Waterways Experiment Station, Vicksburg, Miss.

Lachenbruch, A. H. (1962). "Mechanics of thermal contraction cracks and ice-wedge polygons in permafrost." *Spec. Papers, No. 70*, Geological Survey of America, Lambe, T. W., and Whitman, R. V. (1969). *Soil mechanics*. John Wiley & Sons, Inc., New York, N.Y.

Lau, J. T. K. (1987). "Desiccation cracking of soils," MSc thesis, University of Saskatchewan, Saskatoon, Saskatchewan, Canada.

Liu, J. C. (1990). "Determination of soft soil characteristics," PhD thesis University of Colorado, Boulder, Colo.

McNeilan, T. W., and Skaggs, R. L. (1988). "In place properties of a hydraulic landfill." *Proc., Hydr. Fill Struct. Spec. Conf., Geotech. Spec. Publ. No. 21*, D. J. A. Van Zyl and S. G.Vick, eds., ASCE, New York, N.Y., 255–273.

McVay, M., Townsend, F., and Bloomquist, D. (1986). "Quiescent consolidation of phosphatic waste clays." *J. Geotech. Engrg.*, ASCE, 112(11), 1033–1049.

Miller, E. E. (1975). "Physics of swelling and cracking soils." *J. Colloid and Interface Sci.*, 52(3), 434–443.

Mitchell, J. K. (1988). "Densification and improvement of hydraulic fills." *Proc. Hydr. Fill Struct. Spec. Conf., Geotech. Spec. Publ. No. 21*, D. J. A.Van Zyl and S. G. Vick, eds., ASCE, New York, N.Y., 606–633.

Penev, D., and Kawamura, M. (1993). "Estimation of the spacing and the width of cracks caused by shrinkage in the cement-treated slab under restraint." *Cement and Concr. Res.*, 23, 925–932.

Poindexter, M. E., and Walker, J. E. (1988). "Dredged fill performance: South Blakeley Island." *Proc., Hydr. Fill Struct., Spec. Conf., Geotech. Spec. Publ. No. 21*, D. J. A. Van Zyl and S. G. Vick, eds., ASCE, New York, N.Y., 676–692.

Swarbrick, G. E., and Fell, R. (1992). "Modelling desiccation of mine tailings." *J. Geotech. Engrg.*, ASCE, 118(4), 540–557.

Williams, D. J., and Sibley, J. W. (1992). "The behavior at the shrinkage limit of clay undergoing drying." *Geotech.Testing J.*, 15(3), 217–222.

Yule, D. F., and Ritchie, J. T. (1980). "Soil shrinkage relationships of Texas vertisols: I. small cores." *Soil Sci. Soc. of Am. J.*, 44, 1285–1291.

Znidarčić, D., and Liu, J. C. (1989). "Consolidation characteristics determination for dredged materials." *Proc., 22nd Annu. Dredging Seminar, CDC Rep. No. 317*, Ctr. for Dredging Studies, Texas A&M University, College Station, TX., 45–65.
Znidarčić, D., et al. (1992). "Drag anchors tests in clay, volume 3: soil specimen preparation procedure." *Rep. Prepared for Exxon Production Res. Co.*, University of Colorado, Boulder, Colo.

## APPENDIX II. NOTATION

*The following symbols are used in this paper:*

$a_1$ and $a_2$ = Lagrangian coordinates in vertical and lateral directions, respectively;
$e$ = void ratio;
$e_{cr}$ = cracking void ratio, and void ratio at beginning of three-dimensional shrinkage;
$e_i$ = initial void ratio;
$F$ = ratio of tensile strength to undrained shear strength;
$F_1$, $F_2$ = compressibility functions;
$F_3$ = compressibility functional;
$G$ = cracking function;
$K_o$ = coefficient of lateral earth pressure at rest;
$k$ = coefficient of permeability;
$Q_1$ and $Q_2$ = permeability functions;
$q_1$ and $q_2$ = apparent relative velocity between waste and solid phases in vertical and lateral directions, respectively;
$S_c$ = specific area of cracks;
$t$ = time;
$u$ = pore-water pressure;
$u_e$ = excess pore-water pressure;
$u_s$ = static pore-water pressure;
$v_{w1}$ and $v_{w2}$ = velocities of water phase in vertical and lateral directions, respectively;
$v_{s1}$ and $v_{s2}$ = velocities of solid phase in vertical and lateral directions, respectively;
$\alpha$ = functional used to characterize proportion of vertical and lateral deformation during three-dimensional shrinkage;
$\gamma$, $\gamma_w$, and $\gamma_s$ = unit weight of water-solid mixture, water phase, and solid phase, respectively;
$\delta a_1$, $\delta \xi_1$ = thickness of small soil element in initial and current coordinates, respectively;
$\delta t$ = small time step;
$\varepsilon_v(e, e_{cr})$ = vertical free strain from beginning of three-dimensional shrinkage;
$\xi_1$ and $\xi_2$ = current coordinates in vertical and lateral directions, respectively;
$\sigma'_{cr}$ = cracking vertical effective stress, and vertical effective stress at beginning of three-dimensional shrinkage;
$\sigma_h$ = total lateral stress;
$\sigma_t$ = tensile strength;
$\sigma'_v$ = vertical effective stress; and
$\sigma_v$ = total vertical stress.